universität wien

DIPLOMARBEIT

Titel der Diplomarbeit

„Cellular Regulation of Skeletal Muscle Atrophy by microRNAs during Inflammatory Conditions“

Verfasserin

Laura Gryadunov-Masutti

angestrebter akademischer Grad

Magistra der Naturwissenschaften (Mag.rer.nat.)

Wien, August 2011

Studienkennzahl lt. Studienblatt:	A 441
Studienrichtung lt. Studienblatt:	Diplomstudium Genetik und Mikrobiologie
Betreuer:	Ao. Univ.-Prof. Mag. Dr. Georg Weitzer

Table of Contents

Preface

SKELETAL MUSCLE ATROPHY – the loss of muscle mass and function – is a growing problem in our over-aged and under-trained society.

Either through ageing, disease or immobility, muscle wasting is always accompanied by a reduced quality of life and can lead to serious health problems.

It was my personal interest to contribute to a possible solution of the problem of skeletal muscle atrophy, which has almost epidemical character since it is affecting every individual somehow throughout its life. With this master thesis my intention is to add a piece to the mosaic of knowledge which may in the end lead to a treatment of skeletal muscle loss.

1 ABSTRACT

Rationale: Skeletal muscle tissue is of essential importance for the human body and its deficiency can lead to severe health problems and a reduced quality of life. Its plasticity and sensitivity to the surrounding conditions may be a benefit in desirable conditions, but it also makes the skeletal muscle tissue attackable in critical situations. In case of muscle atrophy the balance between synthesis and degradation of proteins is destroyed. This results in a decrease in myofibre size leading to a decrease in total muscle mass. In critically ill patients, many chronic diseases (cancer, AIDS, etc.) as well as immobility and the physiological process of ageing an increased loss of skeletal muscle mass and strength was observed (Strasser et al., 2007). Interestingly, states of muscle loss are often accompanied by acute or chronic inflammation. Cell culture and animal models have shown that pro-inflammatory cytokines directly affect the insulin-like growth factor (IGF)-1 system, one of the major regulators of skeletal muscle growth (Frost et al., 2003; Frost et al., 2004). Recently, it has been discovered that miRNAs are also involved in 'fine-tuning' the expression of transcription factors and signalling mediators important for muscle biology, including the regulation of proliferation and the differentiation during myogenesis (Callis et al., 2008). Therefore, the aim of this study was to investigate to which extent the IGF-1 system, myogenic markers and miRNAs are directly influenced by inflammatory stimuli in skeletal muscle cells.

Methods: Mouse C2C12 skeletal muscle myoblasts were differentiated to myotubes in vitro. Differentiation lasted for 4 days and mRNA expression of IGF-1 splicing variants (IGF-1Ea, IGF-1Eb, MGF), myogenic differentiation markers (MyoD, Myogenin) and miRNAs (miR-1, -133a, -133b, -206, -499, -155) were analyzed by real-time qPCR at day 0 and day 4 for myoblasts as well as for myotubes. Myotubes were incubated with LPS (1µg/ml), TNF-α (10ng/ml), IL-6 (10ng/ml) or vehicle for 0, 1, 3, 6, 12, 24 and 48h. At the indicated time-points, mRNA expression of IGF-1 splicing variants (IGF-1Ea, IGF-1Eb, MGF), myogenic differentiation markers (MyoD, Myogenin) and miRNAs (miR-1, -133a, -133b, -206, -499, -155) were determined by real-time qPCR. IGF-1 and TNF-α protein concentration was measured in the supernatants after stimulation with LPS (1µg/ml), TNF-α (10ng/ml), or vehicle at the time-points 0, 1, 3, 6, 12, 24 and 48h, IL-6 protein concentration at the time-points 0, 12, 24 and 48h. Analyzes were performed via ELISA.

Results: During differentiation the myogenin expression increased 7-fold ($p < 0.05$) while MyoD was not affected. We observed a 36-fold ($p < 0.05$) up-regulation of IGF-1Ea and a 31-fold ($p < 0.05$) increase of MGF. IGF-1Eb expression level did not change. We detected a significant increase for miRNA-1 to 464-fold ($p<0.05$), for miR-206 to 14-fold ($p<0.001$), for miR-133a to 461-fold ($p<0.01$) and for miR-133b to 17-fold ($p<0.5$), whereas the levels of miR-499 and miR-155 did not change. Compared to 0h TNF-α stimulation leaded to a significant reduction of MyoD level to 61 ± 6% ($p<0.001$) 12h after incubation, whereas LPS-treatment revealed no effect. Myogenin drops significantly to 39 ± 15% ($p<0.01$) 12h after stimulation with TNF-α accompanied by a decrease of the control to 57 ± 12% ($p<0.01$). The expression level of IGF-1Ea decreased to 34 ± 11 % ($p<0.001$) and of MGF to 32 ± 11% ($p<0.001$) 12h after TNF-α treatment. At this time-point MGF dropped significant to 58 ± 13% ($p<0.05$) after LPS-treatment. IGF-1Eb levels decreased to 61 ±10% ($p<0.01$) after 12h of IL-6 stimulation. The chosen inflammatory stimuli did not affect the here analyzed miRNAs. After 48h the IGF-1 protein concentration control increased significantly 2.2-fold ($p<001$) in the control, 2.8-fold after LPS incubation ($p<0.01$) and 1.4-fold after IL-6 incubation ($p<0.05$). TNF-α stimulation showed no significant effect. TNF-α protein concentration increased only after TNF-α stimulation, IL-6 protein concentration only after IL-6 stimulation.

Conclusion: In our study we have shown that muscle regulatory genes, which are enhanced before and / or during differentiation, are directly influenced by TNF-α. Muscle-specific miRNAs as well as the immune-related miRNA-155 seem not to be involved in this interaction, although they are enhanced up to 400-fold during differentiation. The results from this study contribute to improve the knowledge about the mechanisms leading to skeletal muscle atrophy during inflammatory conditions.

1.1 Zusammenfassung

Rationale: Die Skelettmuskulatur ist von essentieller Bedeutung für den menschlichen Körper und ein Defizit kann zu ernstzunehmenden gesundheitlichen Schäden bzw. einer reduzierten Lebensqualität führen. Ihre Plastizität und Sensitivität der Umwelt gegenüber ist unter günstigen Bedingungen eine wünschenswerte Eigenschaft, macht das Gewebe aber auch gleichzeitig angreifbar in kritischen Situationen. Im Falle einer Muskelatrophie ist

die Balance zwischen Synthese und Abbau von Proteinen gestört. Das führt zu verringerter Muskelfasergröße und, daraus resultierend, zu einer verringerten totalen Muskelmasse. Bei kritisch kranken Patienten und vielen chronischen Erkrankungen wie Krebs, AIDS usw. sowie Immobilität und dem physiologischen Alterungsprozess kommt es zu einem gesteigertem Verlust der Muskelkraft und –masse (Strasser et al., 2007). Interessanterweise werden Zustände des Muskelverlustes oft begleitet vom Auftreten einer akuten oder chronischen Inflammation. Zellkultur und Tierversuchsmodelle haben gezeigt, dass proinflammatorische Zytokine direkt das Insulin-like growth factor (IGF)-1 system, einen der Hauptregulatoren des Skelettmuskelwachstums, beeinflussen (Frost et al., 2003; Frost et al., 2004). Kürzlich wurde gezeigt, das miRNAs ebenfalls involviert sind im 'Fine-Tuning' der Expression der Transkriptionsfaktoren und Signalmediatoren wichtig für die Muskelbiologie, eingeschlossen der Regulation der Proliferation und der Differenzierung während der Myogenese (Callis et al., 2008). Das Ziel dieser Studie ist es darum festzustellen, in welchem Umfang IGF-1 system, Muskelmarker und miRNAs direkt durch die Inflammation beeinflusst werden.

Methodik: Maus C2C12 Skelettmuskelmyoblasten wurden in vitro zu Myotubes differenziert. Die Differenzierung dauerte 4 Tage und die Expression der mRNA der IGF-1 Splicingvarianten (IGF-1Ea, IGF-1Eb, MGF), der Muskeldifferenzierungsmarker (MyoD, Myogenin) und der miRNAs (miR-1, -133a, -133b, -206, -499, -155) wurde mittels real-time qPCR an den Tagen 0 und 4 sowohl für Myoblasten als auch für Myotubes gemessen. Die Inkubation der Myotubes erfolgte mit LPS (1µg/ml), TNF-α (10ng/ml), IL-6 (10ng/ml) oder vehicle für 0, 1, 3, 6, 12, 24 und 48h. An den angegebenen Zeitpunkten wurde die Expression der mRNA der IGF-1 Splicingvarianten (IGF-1Ea, IGF-1Eb, MGF), der Muskeldifferenzierungsmarker (MyoD, Myogenin) und der miRNAs (miR-1, -133a, -133b, -206, -499, -155) mittels real-time qPCR gemessen. Die IGF-1 und TNF-α Proteinkonzentrationen im Überstand wurden nach Stimulation mit LPS (1µg/ml), TNF-α (10ng/ml), oder vehicle an den Zeitpunkten 0, 1, 3, 6, 12, 24 und 48h, die IL-6 Proteinkonzentration an den Zeitpunkten 0, 12, 24 und 48h via ELISA bestimmt

Resultate: Im Laufe der Differenzierung stieg die Expression von Myogenin um das 7-fache ($p < 0.05$) während MyoD nicht beeinflusst wurde. Wir konnten einen 36-fachen ($p < 0.05$) Anstieg von IGF-1Ea und einen 31-fachen ($p < 0.05$) Anstieg von MGF beobachten. Das Expressionslevel von IGF-1Eb blieb unverändert. Wir detektierten eine signifikante Zunahme der miRNA-1 auf das

464-fache ($p<0.05$), für miR-206 auf das 14-fache ($p<0.001$), für miR-133a auf das 461-fache ($p<0.01$) und für miR-133b auf das 17-fache ($p<0.5$), während die Level der miR-499 und miR-155 keine Veränderungen zeigten. TNF-α Stimulierung führte, verglichen mit 0h, zu einer signifikanten Reduktion des MyoD Levels zu 61 ± 6% ($p<0.001$) 12h nach der Inkubation, während die LPS Zugabe keinen Effekt zeigte. Die Myogeninexpression fiel signifikant auf 39 ± 15% ($p<0.01$) 12h nach der Stimulation mit TNF-α, was begleitet wurde von einem Abfall in der Kontrolle auf 57 ± 12% ($p<0.01$). IGF-1Ea sank auf 34 ±11% ($p<0.001$) und MGF auf 32 ± 11% ($p<0.001$) 12h nach TNF-α Zugabe. Zu diesem Zeitpunkt konnten wir auch eine signifikante Herabregulation von MGF auf 58 ± 13% ($p<0.05$) nach LPS Stimulation verzeichnen. Das IGF-1Eb Expressionslevel fiel ab auf 61 ± 10% ($p<0.01$) nach 12h IL-6 Stimulation. Die verwendeten inflammatorischen Stimuli hatten keinen Einfluss auf die hier analysierten miRNAs. Die IGF Proteinkonzentration stieg signifikant nach 48h 2.2-fach ($p<001$) in der Kontrolle, 2.8-fach nach LPS Inkubation ($p<0.01$) und 1.4-fach nach IL-6 Inkubation ($p<0.05$). Die TNF-α Stimulation zeigte keinen signifikanten Effekt. Eine TNF-α Proteinkonzentration war nur in den mit TNF-α stimulierten Proben messbar, eine IL-6 Proteinkonzentration nur in den mit IL-6 stimulierten.

Fazit: In unserer Studie haben wir gezeigt, dass Muskelregulatorgene, welche vor und / oder nach der Differenzierung erhöht sind, direkt durch TNF-α beeinflusst werden. Muskelspezifische miRNAs und die immunsystembezogene miRNA-155 scheinen bei dieser Interaktion, trotz ihres bis zu 400-fachen Anstiegs während der Differenzierung nicht involviert zu sein. Die Resultate dieser Studie tragen zu einer Erweiterung des Wissens über die Mechanismen, welche einer durch inflammatorische Bedingungen induzierten Skelettmuskelatrophie zu Grunde liegen bei.

2 INTRODUCTION

2.1 Skeletal muscle

Muscle tissue is one of the basic tissues in the human body. There are three types of muscle in the vertebrates: Skeletal muscle, cardiac muscle and smooth muscle. Skeletal muscle is one specialized form of muscle tissue. It shows similarities to the other muscle tissues in many fields, but it also differs in some main points to fulfil its unique functions.

Skeletal muscle tissue consists of long cells which have the ability to contract and it is primary required for locomotory functions and maintaining posture. Besides it is also needed for other essential physiological mechanisms, such as breathing. Skeletal muscles are normally under the control of the conscious which, beside structural differences, also distinguishes them from cardiac and smooth muscles. Beside these primary functions, the skeletal muscle tissue serves also as the biggest resource for amino acids and nitrogen in the body and the maintenance of muscle mass is therefore under strict metabolic control (Wolfe, 2006).

Skeletal muscles consist of muscle bundles which are composed of long multinuclear cells, called myofibres. Myofibres develop from fused mononuclear cells in the late embryonic period. Their nuclei are located peripherally just beneath the cell membrane (sarcolemma). Each of these myofibres itself consists of myofibrils containing two types of filaments, the thin actin filament and the thick myosin filament. These filaments are building the functional basis of the myofibril, the sarcomeres. The shortening of the sarcomeres allows the muscle to contract. Due to the sarcomeres, which let the muscle appear in dark and light bands, skeletal muscle is also called “striated”. Connective tissue supports the formation of the muscle: a muscle fibre is surrounded by the endomysium, a muscle fibre bundle (also known as fascicles) by the perimysium and the muscle itself by the epimysium (Campell, 2000) (Fig. 2-1).

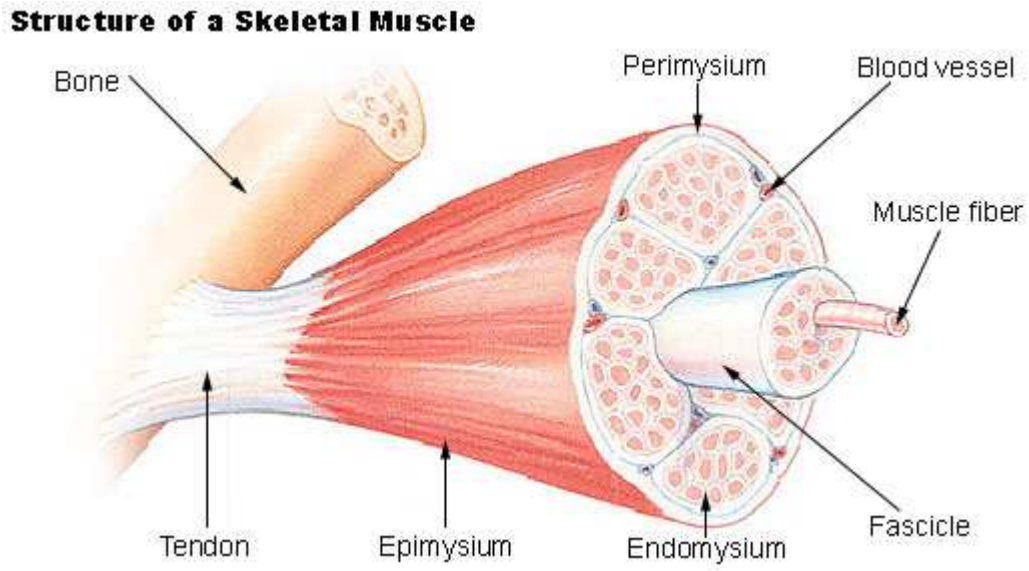

Figure 2-1: Muscle structure (National_Institutes_of_Health, 2000; National_Institutes_of_Health, 2010)

Muscle contraction is controlled by Calcium. If the Ca^{2+} level is low, the Troponin – Tropomyosin complex inhibits the interaction between Actin and Myosin. A high Ca^{2+} concentration effects the conformation of Troponin and activates the energy producing ATPase. Both is required to let Myosin interact with actin, leading to a contraction of the muscle (Campell, 2000).

2.1.1 Fibre types

Skeletal muscles can be divided in subtypes, each consisting of different fibre types. Due to its fibre type composition, a muscle develops different contractile characteristics. There are four fibre types known, which differ mainly in their myosin heavy chain (MHC) which itself is a part of the myosin filament. It was observed that the MHC protein expressed in a single muscle fibre is related to its maximum contraction velocity and that the MHC based fibre type composition of a muscle can be used to predict its contractile properties (Talmadge and Roy, 1993).

Type 1 MHC (β-MHC) can be found in the oxidative slow twitch type of muscle, which contracts slowly but can hold its contraction over a long period. These oxidative muscles possess characteristically a great amount of mitochondria.

The other three subtypes are fast twitch types, namely MHC type 2a, 2x and 2b. Fast type muscles are able to contract quickly and to create more force than the slow type, but they can hold the tensed state only for a short time. Type 2x and 2b are anaerobic muscles and develop the greatest amount of force (McCarthy et al., 2009).

Every human individual has a genetically predisposition for the amount of slow and fast type muscles. Nevertheless through a fibre type switch the muscle tissue is partly able to adapt to changed environmental conditions and requirements. This adaptation is also linked to the process of ageing and muscle atrophy. A fibre type transition from slow to fast for example is associated in humans with unloading and was observed in bed resting individuals as well as such in space flights (Trappe et al., 2009).

It was observed, that the Calcineurin - NFAT pathway is involved in fibre type specification and a slow motor neuron activity is supposed to activate this signalling transduction cascade which leads to the expression of slow oxidative muscle genes (Tothova et al., 2006). The authors describe NFAT as a nerve activity sensor in skeletal muscle fibres.

2.1.2 Development

During embryology muscle tissue develops from the paraxial mesodermal layer of embryonic germ cells. This mesoderm is divided into somites, which divide themselves into sclerotome, dermatome and myotome (muscle development). The myoblasts (muscle progenitor cells) can remain in the somits and form all muscles connected to the vertebral column or they move out into the body following chemical signals to build up all other muscles (Hirano et al., 1995).

2.1.2.1 Myogenic markers

Beside embryological development there is a life-long synthesis of new muscle cells. Myogenic markers are proteins specifically expressed in muscle cells. They play an essential role in the molecular regulation of muscle growth and their expression level depends on the developmental and differentiation state of the cell. MyoD family of myogenic transcription factors and MEF2 family of

MADS-box transcription factors play a central role in controlling myogenesis (Goldspink et al., 2008) (Fig. 2-2).

MyoD and its relatives are also called myogenic regulatory factors (MRFs). In the past few years, studies concentrated mainly on four of its members: MyoD, Myf5, myogenin and MRF4. MyoD belongs to a class of DNA binding proteins with a basic helix-loop-helix domain (bHLH). Promoters and enhancers of muscle specific genes contain a specific binding site for MRFs, the so called E boxes. The MRF necessary for a certain differentiation and developmental state binds to its consensus sequence to start transcription (Heidt et al., 2007).

The early Notch, Wnt and sonic hedgehog signalling in the embryo switches on the expression of Myf5 and MyoD in the somites (Buckingham, 2001). While these two MRFs are essential for the start of the myogenic lineage, myogenin can be seen as the “terminal differentiator”.

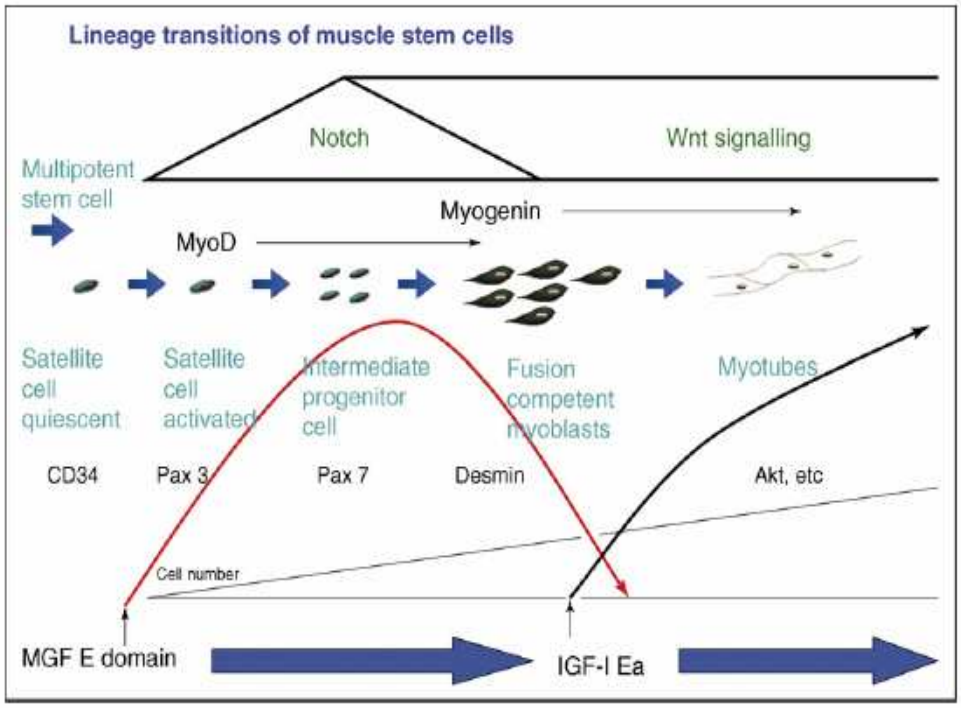

Figure 2-2: Muscle stem cell differentiation (Goldspink et al., 2008)

MyoD regulates the expression of myogenin and other genes important for muscle development, for example myosin heavy and light chains and M-cadherin. Another important regulatory effect of MyoD showing its relevance for differentiation is the up-regulation of cyclin-dependent kinase inhibitor p21, which causes an irreversible exit of the differentiating cells from the cell cycle (Halevy et al., 1995). Beside these activating effects, MyoD has also been shown to

suppress genes which expressions are related to a myogenic phenotype. It was demonstrated that MyoD induces miRNA-206, which as a result directly targets specific sequences and suppresses the expression of the genes Fstl1 and Utrn, both genes associated with the muscle precursor cell (Rosenberg et al., 2006).

Myogenin is located downstream of the early indicators Myf5 and MyoD. It seems that MyoD is unable to fulfil the terminal differentiation program because its functions are suppressed by in vivo signalling events. This might be the reason why myogenin, which shows no reaction on these suppressive signals, execute the terminal differentiation program instead of MyoD (Tapscott, 2005)

In contrast to the MyoD family, the Mef2 proteins belong to the MADS box-containing transcription factor family. Their spectrum of activity is broader than that of the MyoD family and also includes other developmental functions beside muscle development. Mef2 seems to assist MyoD and it has been found that E boxes and Mef2 binding sites are localized close to each other (Wasserman and Fickett, 1998). As the appearance of respective myogenic regulatory factors is tightly controlled during differentiation of muscle cells from myoblasts to myotubes, they can serve as “myogenic markers” to describe a certain differentiation state.

It has been shown that during cultivation of skeletal myoblasts there is no initiation of differentiation as long as proliferation continues. After leaving the cell cycle, myoblasts start to express muscle specific proteins like actine, myosin, tropomyosin and muscle specific enzymes. Although myoblasts are already expressing MyoD and Myf-5, they continue to proliferate in the presence of growth promoting proteins. It needs at least one other stimulus to make the cells leaving the cell cycle. Here the crucial factors are a decrease of the cell cycle activators (e.g. cyclins and cdks) and an increase of inhibitors of the cell cycle (e.g. p21, Rb, p57 and p27). This process seems to be partly under the control of MyoD. Interestingly the level of MyoD changes during cell cycle phases. The relevant step in muscle cell differentiation, the exit of the cell cycle, takes place in the G1 phase, when MyoD is maximally expressed. In contrast Myf5 is down regulated at this time. During non-differentiation phases (G0, G1 to S-phase transition) MyoD is down- and Myf5 is upregulated (Kitzmann and Fernandez, 2001) (Fig. 2-3).

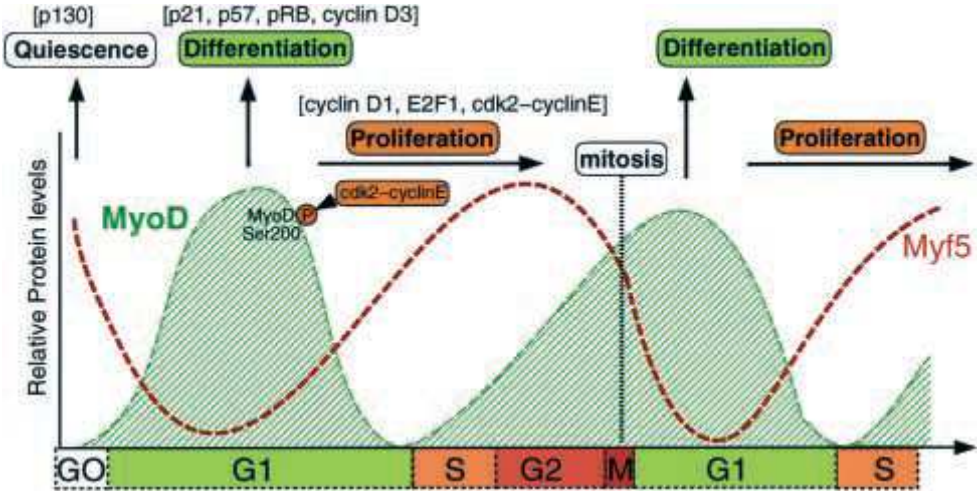

Figure 2-3: MyoD and Myf5 levels during the cell cycle (Kitzmann and Fernandez, 2001)

An importent actor during muscle differentiation is the Retinoblastoma Protein (Rb) (see Fig. 2-4). Entrance into the S Phase is achieved through phosphorylation of Rb catalysed by cyclin dependent kinases. This phosphorylation activates the E2F1-3 transcription factors which are responsible for gene expression of cell cycle progression associated genes. In a non phosphorylated state the Rb protein blocks the cell cycle (Coller, 2007).

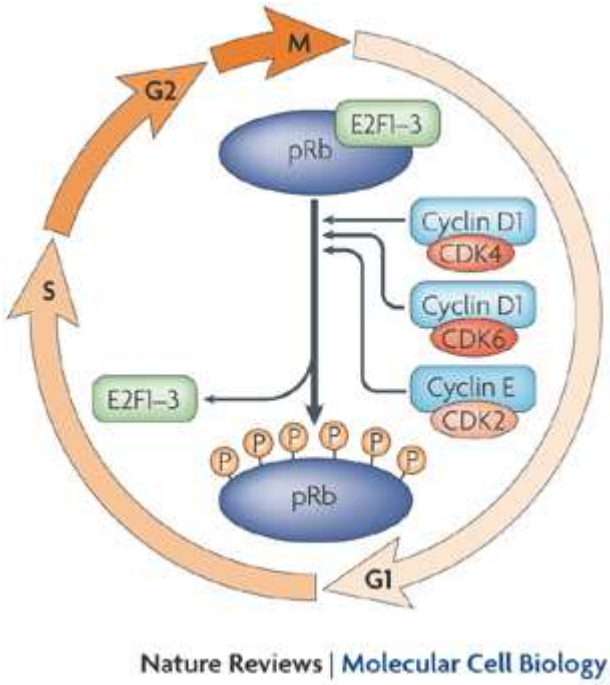

Figure 2-4: Acting of retinoblastoma protein in muscle cell differentiation (Coller, 2007)

After leaving the cell cycle, the myoblasts are able to differentiate and to fuse to form the multinucleate myotubes. Although it is known that muscle cell differentiation is controlled by external signals and interactions between various transcribtion factors, the detailed molecular mechanisms leading to terminal differentiation are still under investigation.

2.2 Skeletal muscle plasticity

The ability of the skeletal muscle tissue to adapt to special needs and to changed conditions is a result of its ability to react on environmental stimuli. In addition to environmental causes, every individual is influenced by its special characteristics as genetic predisposition, age, health and gender.

To adapt to the various conditions, muscle gene expression during synthesis and degradation is regulated at the transcriptional and translational level. A change in gene expression is caused by a variety of factors influencing different pathways responsible for muscle atrophy and hypertrophy, respectively.

2.2.1 Muscle hypertrophy

Both, external and internal anabolic stimuli are influencing skeletal muscle growth. The two most common external factors, playing together in regulating skeletal muscle mass, are the mechanical load (training) on the one hand and the nutrition on the other hand. The unique genetic predisposition of every individual enhances or constrains - same as the internal components - the reactivity of the muscle on growth related stimulation.

2.2.1.1 Insulin-like growth factor (IGF) signalling pathway

The body uses so called growth factors, to give positive signals for cell division, maturation, differentiation and other processes necessary for growth.

One of the most important growth factors which play a crucial role in the development of the organism is the insulin like growth factor (IGF) family. IGF as other hormones are part of a complex system cells use to communicate with the

surrounding. While IGF-2 is important for the prenatal growth, IGF-1 influences prenatal as well as postnatal growth. Although IGF-1 is primary produced in the liver mainly after stimulation with the growth hormone Somatotropin (systemic IGF-1), it can also be built extra hepatic in a variety of tissues (autocrine IGF-1) and is as well of essential importance for muscle development. The insulin-like-growth factor signalling pathway is known for regulating protein synthesis and the activation of this pathway by IGF-1 or related molecules leads to skeletal muscle fibre growth and hypertrophy (Goldspink, 2004). Besides it was described that an increase in muscle load correlates with an increase of IGF-1 expression (Jacinto and Hall, 2003).

The IGF-1 gene itself includes six exons and was found to be expressed through alternative splicing. The liver IGF-1 starts its transcription normally at exon two, whereas IGF-1 expression in other tissues is initiated at exon 1 (Harridge, 2003).

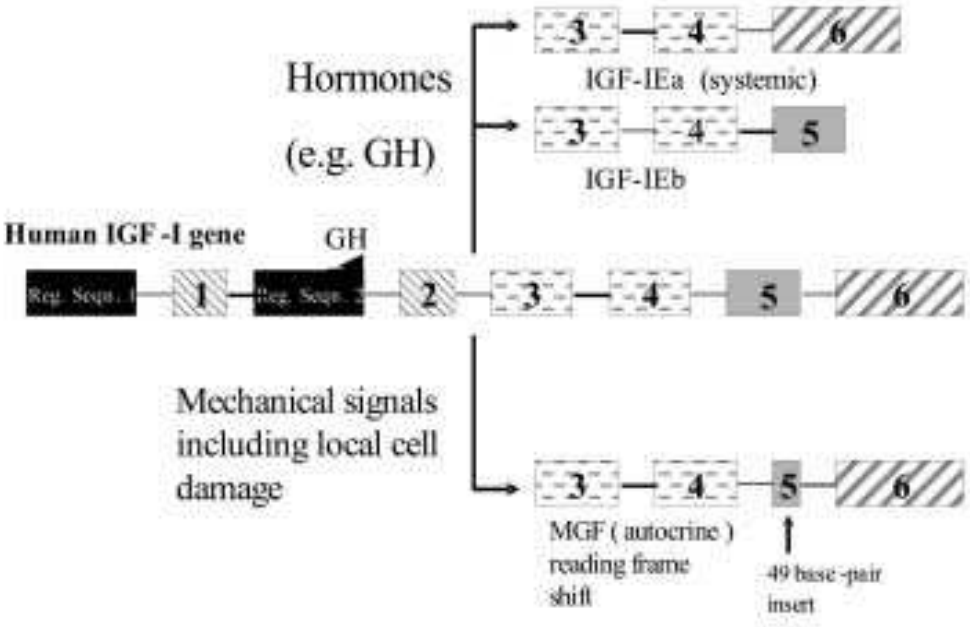

Figure 2-5: The IGF-1 splicing variants (Goldspink, 2004)

Depending on external signals (mechanical, hormonal) the IGF-1 gene is alternatively spliced to IGF-1Ea, IGF-1Eb and MGF (IGF-1Ec) (Fig. 2-5). In the resting muscle only IGF-1Ea is expressed. After exercise or muscle damage the muscle reacts over alternative splicing (reading frame shift) with the expression of the mechanical growth factor (MGF) which is sensitive to mechanical signals. In

case of damage, MGF is involved in the activation of muscle satellite cells which are essential in the regeneration process (Goldspink, 2003).

The IGF1-Eb splicing variant is mentioned in literature (Philippou et al., 2009), but its special modes of acting are not known up to date. However, in contrast to MGF, which is thought to play a role in activation and proliferation, IGF-1Eb was proven to be up-regulated together with IGF-1Ea in relation to differentiation (McKay et al., 2008).

A decrease of circulating levels of GH and IGF-1 was proven with increasing age and elderly individuals show a reduced up-regulation of MGF in response to exercise (Goldspink, 2004). If there is a closer connection of the age-related change in the expression level of IGF-1Ea and MGF to sarcopenia, remains to be discovered.

2.2.1.2 IGF-1 and mTOR

IGF-1 is an anabolic agent with many functions like insulin. It regulates for example the glucose uptake and the DNA / RNA synthesis and stimulates the AS uptake (Binoux, 1995). As mentioned above, IGF1 is important for muscle metabolism by increasing protein synthesis and inhibition of protein proteolysis. IGF1 was shown to act mainly over the PI3K / protein kinase B (AKT) / mammalian target of Rapamycin (mTOR) pathway which is thought to sense and integrate environmental signals to control protein translation (Fig. 2-6). The mTOR pathway is of great importance for muscle development, but it also plays a role in cancer and metabolic diseases. mTOR is part of two different complexes, the mTORC1 and the mTORC2. mTORC1 contains the regulatory associated protein of mTOR (raptor), which is sensitive to rapamycin. Instead of this protein mTORC2 contains the rapamycin-insensitive companion of mTOR (rictor). The two complexes carry out different functions.

mTORC1 acts primary over inhibition of 4E-BP1, leading to activation of the translation factor eIF4E and the formation of the eIF4E complex needed for ribosomal assembly. mTORC1 also acts over activation of p70S6k, which then phosphorylates rpS6. Through these major targets mTORC1 is able to regulate muscle mass development by controlling the initiation of protein translation.

The major function of mTORC2 in the mTOR pathway is the activation of PKB/Akt. Akt itself was already described in literature to increase the cross

sectional area of skeletal muscle fibres by further signalling transduction (Glass, 2005).

Akt1 is responsible for the phosphorylation status of the Foxo family of transcription factors. If Foxo is phosphorylated by Akt1, it leaves the nucleus and becomes inactive, thereby preventing the induction of atrophy. It was shown that not only mTOR, but also the Calcineurin / NFAT pathway is induced by IGF-1 and it was suggested that Calcium is able to couple a mechanical stimulus to the IGF-1 pathway (Jacinto and Hall, 2003) (Fig. 2-6). As mentioned above, NFAT was already described as a nerve activity sensor in skeletal muscle and therefore an activation of this pathway by IGF-1 seems to be also interesting in the context of fibre-type switch.

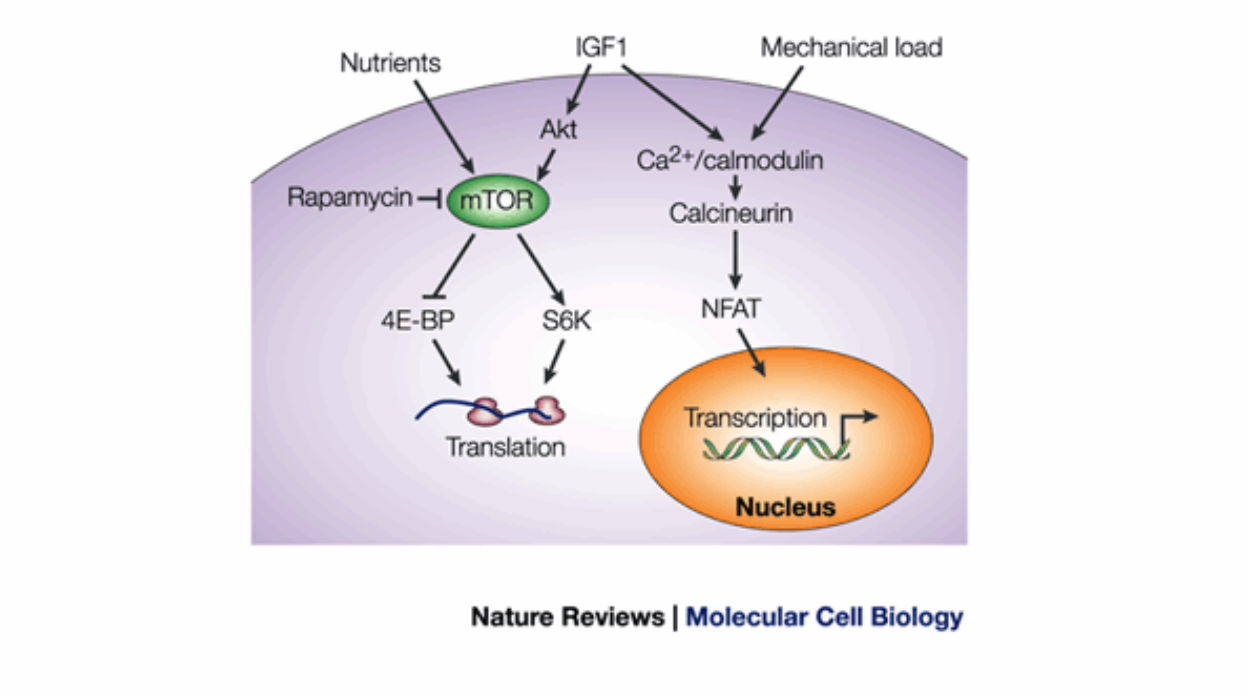

Figure 2-6: IGF-1 induced skeletal muscle hypertrophy (Jacinto and Hall, 2003)

2.2.1.3 IGF-1 and satellite cells

Satellite cells are proliferating skeletal muscle cells responsible for regenerating muscle tissue in response to injury or after increased loading conditions.

These small mononucleated skeletal muscle stem cells are located between the basal lamina of the muscle and the sarcolemma of myofibres. After their

activation, the satellite cells differentiate into myoblast-like cells, which are able to fuse with each other to form new myofibres. It is also possible that these myoblasts become incorporated into existing myofibres in case of damage (Bischoff, 1989).

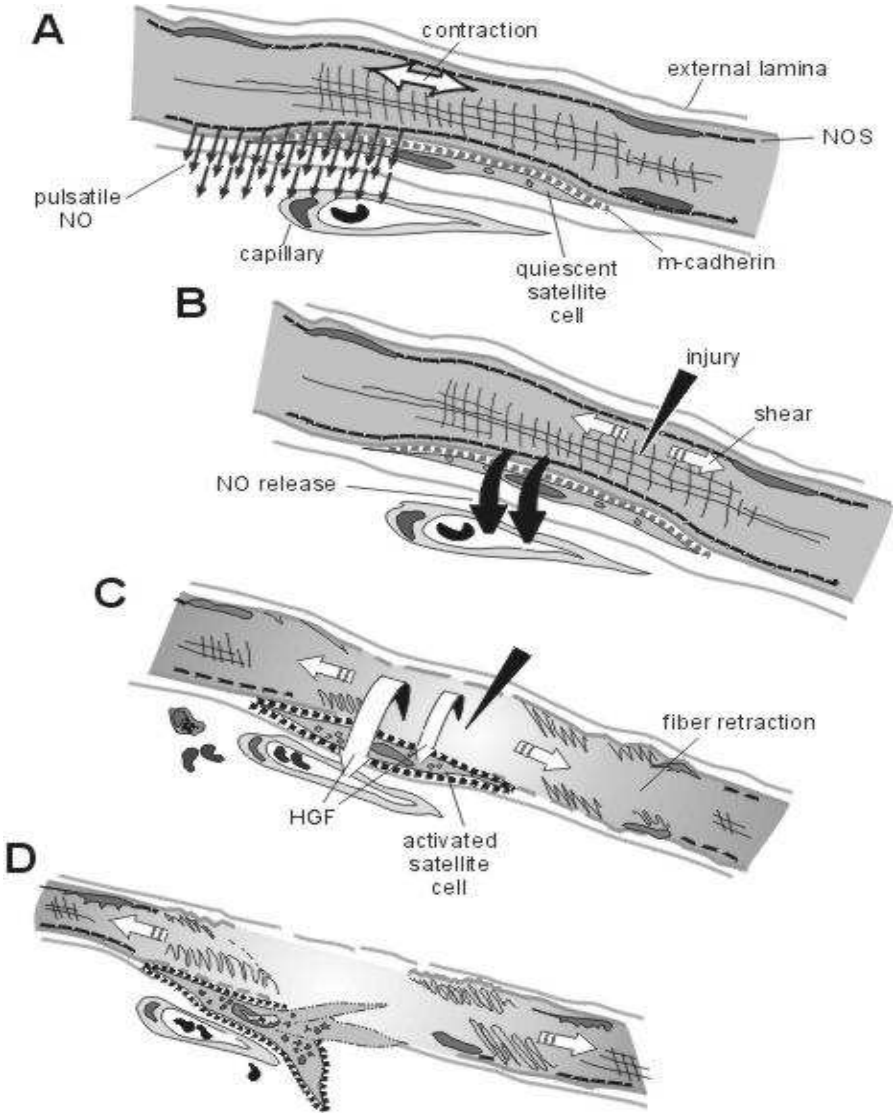

Figure 2-7: Activation of satellite cells (Anderson, 2000)

According to Anderson et al, in a damaged muscle which is normally accompanied by a damage of the sarcolemma, the depolarization during muscle contraction goes not hand in hand with a repolarisation afterwards (Anderson, 2000). This results in an immense shear, which causes increased synthesis of reactive nitrogen species (such as NO) which leads in cooperation with the hematopoietic growth factor (HGF) to an activation of quiescent satellite cells.

Another important factor for satellite cell development is the insulin-like growth factor 1, which has been shown to promote the proliferation, differentiation and fusion of satellite cells in primary cultures (Chambers and McDermott, 1996). IGF-1 therefore is thought to contribute to a hypertrophy response through stimulation of the proliferation of satellite cells.

2.2.2 Muscle atrophy

The maintenance of muscle mass involves a multitude of signalling mechanisms keeping protein synthesis and degradation in balance. Atrophy is caused by a disturbed balance in which protein degradation takes overhand.

Therefore, atrophy can be a result from reduced protein synthesis, increased degradation, or both. Generally muscle atrophy is characterised by a decrease in myofibre size leading to a decrease in total muscle mass. It can be distinguished between physiological and pathological occurrences.

2.2.2.1 Physiological forms of muscle atrophy

The physiological form of muscle atrophy is also known as sarcopenia. It occurs in elderly and is characterized by a loss of muscle mass and strength. Seventy to 80 years old people lose an average of 20-30% of their total muscle mass and this decrease continues at the rate of 1 % - 2 % a year. The loss of muscle mass is accompanied by a reduced strength, which falls to a level of 30 – 40 % of that from young individuals (Porter et al., 1995).

The detailed mechanisms leading to this form of atrophy remain to be discovered. However, recent examinations suggest a close connection between loss of muscle mass in elderly individuals and a reduced number and activation of satellite cells, a decreased muscle protein synthesis, increased oxidative stress and changes in the glucose metabolism (Bruunsgaard and Pedersen, 2003).

Also a change in fibre type composition from slow to fast was described to be associated with age-related muscle loss, as well as hormonal changes, or the replacement of muscle by connective and adipose tissue (Lee et al., 2007).

Also the genetic influence in age related muscle-loss becomes more and more a focus in research. One of the best studied genes for sarcopenia is the vitamin D receptor (VDR) which plays a key regulatory role in calcium homeostasis and skeletal muscle function. Endo et al. found out that the muscle fibres of VDR null knock-out mice were smaller and the expression level of early markers of myogenic differentiation was significantly higher compared with the controls (Endo et al., 2003). In addition to these findings a specific genotype of the Vitamin D receptor (VDR), the FokI genotype, was reported to be associated with a decreased muscle mass and strength. Individuals with this gene polymorphism showed a 2-fold higher risk to develop sarcopenia (Roth et al., 2004).

2.2.2.2 Pathological forms of muscle atrophy

The pathological form of muscle atrophy accompanies a lot of diseases, e.g. cancer, AIDS, cachexia, sepsis, chronical diseases and burn injury. Loss of skeletal muscle mass is also a common feature in conditions associated with immobility as for example in critically ill patients. The percentage of total muscle loss can be at a very high level (e.g. 13% for immobility, 30% in cancer). Muscle atrophy can cause post surgical complications and is often responsible for a prolonged recovery phase and hospitalization.

Cachexia is one form of pathological muscle loss, which occurs during sepsis, AIDS, trauma as well as in cancer patients. It can be described as a wasting syndrome of skeletal muscle tissue and adipose tissue in connection with severe injury, chronic or end-stage malignant or infectious diseases (Jespersen et al., 2006). As inflammatory cytokines influence cachexia, it was suggested, that a possible change in myogenic expression level caused by TNF-α may contribute to cachexia-related muscle wasting (Larsen et al., 2008).

Both, the pathological and the physiological form of skeletal muscle atrophy are suggested to be regulated partly by components of the immune system as they are associated with inflammatory processes in the body (Frost et al., 2003).

2.2.2.3 Protein degradation

Muscle atrophy caused by protein degradation involves at least three degradation systems which help the muscle to adapt to various conditions and provide amino acids and nitrogen in case of higher needs (e.g. diseases).

One of the degradation pathways being proven to take part in causing proteolysis in case of activation is the evolutionary well conserved ubiquitin-proteasome pathway (Fig. 2-8). The most important enzymes leading to proteasome mediated protein degradation are the E1 ubiquitin-activating enzyme, the E2 ubiquitin-conjugating enzyme and the E3 ubiquitin-ligating enzyme. These three enzymes work together to attach ubiquitins to the target protein. Now the 26S proteasome is able to recognize and to degrade the ubiquitin marked protein (Diao et al., 2008).

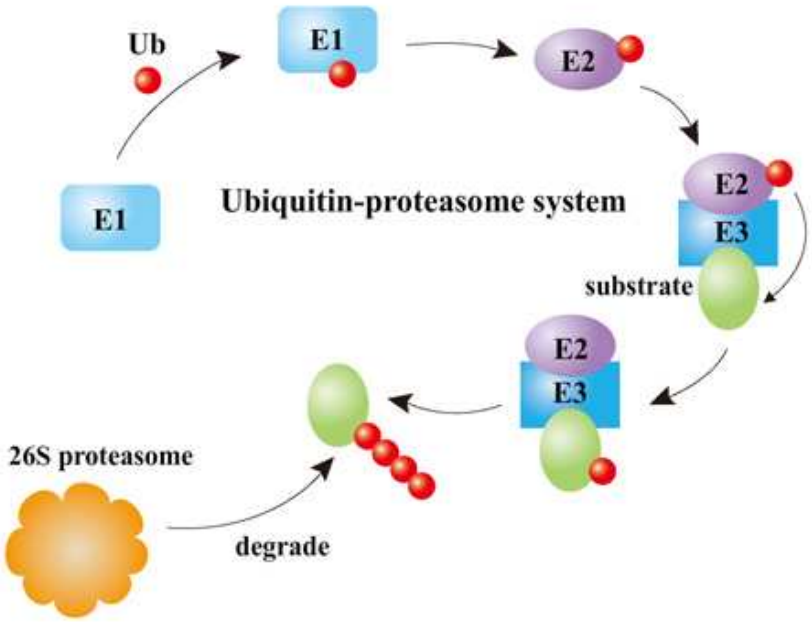

Figure 2-8: Ubiquitin proteasome protein degradation system (Diao et al., 2008)

E3 was shown to possess substrate specificity. In case of muscle protein degradation two genes were identified to encode E3 ubiquitin ligases: the muscle ring finger 1 (MuRF1) and the muscle atrophy F-box (MAFbx). The expression of both genes increased significantly in experimental models of skeletal muscle

atrophy. MuRF1 and MAFbx are expressed in response to NfkB activation (Bodine et al., 2001).

The ubiqitin-proteasome pathway seems to be the most important protein degrading system in skeletal muscle atrophy. However, its actions are limited to abnormal muscle fibres. Muscle fibres which are intact cannot be accepted for degradation without the help of two other degradation systems, the lysosomal proteases and the calpains (Jackman and Kandarian, 2004).

2.2.3 Skeletal muscle energy metabolism

2.2.3.1 Calcium signalling pathway

Skeletal muscle fibre type switch seems to be regulated by a calcium signalling pathway, involving calcineurin and the peroxisome proliferators-activated receptor-gamma coactivator 1alpha (PGC-1alpha) (Fig. 2-10). One key fat burning molecule mediating long-chain fatty-acid beta-oxidation is the peroxisome proliferators-activated receptor (PPAR)delta, which was also proven to play an essential role in fibre type switch. PPAR, which was suggested as a possible downstream transcription factor of the calcineurin pathway, is activated primarily by fatty acids and their metabolites. Activation of PPARdelta enhances the expression of type 1 fibre contractile proteins and increases the mitochondrial biogenesis and the number of oxidation enzymes (Wang et al., 2004).

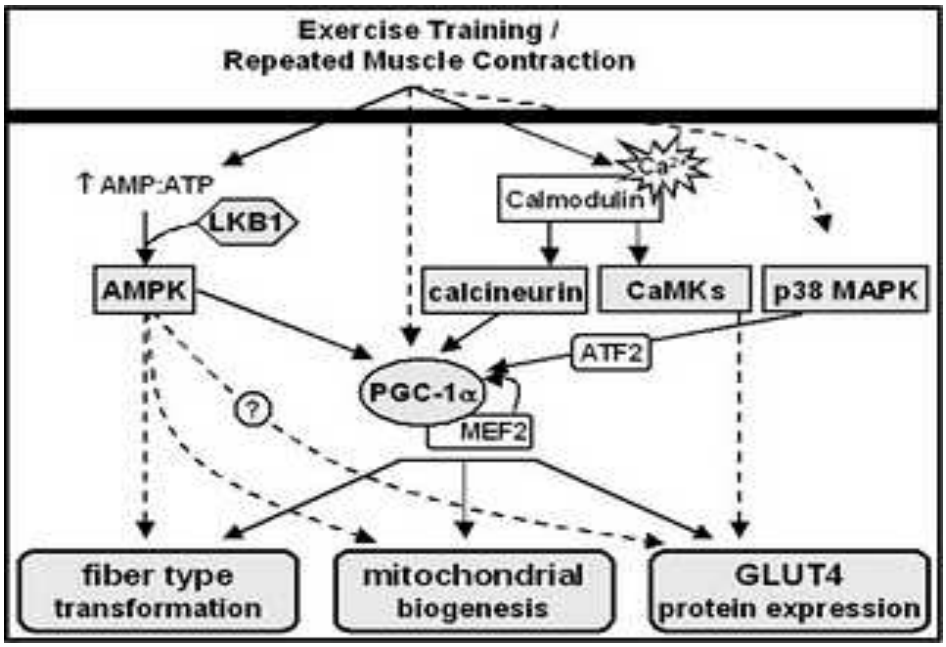

Figure 2-9: Effect of exercise training on skeletal muscle metabolism (Rockl et al., 2008)

PPARdelta is also associated with high levels of UCP3 expression, which goes confirm with the discovery of a PPAR response element on the UCP3 gene promoter (Riquet et al., 2003).

2.2.3.2 Uncoupling proteins

The uncoupling proteins (UCPs) 1, 2 and 3 play an important role in energy metabolism. As mitochondrial inner membrane transporters they can act over uncoupling the ATP synthesis by dissipating the proton gradient. This leads to thermogenesis and to a decrease in ATP synthesis (Fig. 2-11). UPCs have been described in a variety of species, from animals to plants. Recent findings showed also an involvement in myogenesis. Chen et al. examined the expression of UPC2 in C2C12 cells on the transcriptional and the translational level. Although they detected UPC2 mRNA they were not able to measure any protein, which let them suspect a post-transcriptional regulatory mechanism. In their studies they observed a connection of the presents of MyoD and the expression of skeletal muscle specific UCP3 as well as UCP2. During myogenesis MyoD seems to up-regulate UCP3 together with miRNA-133a. UCP2 translation is inhibited by miRNA-133a (Chen et al., 2009).

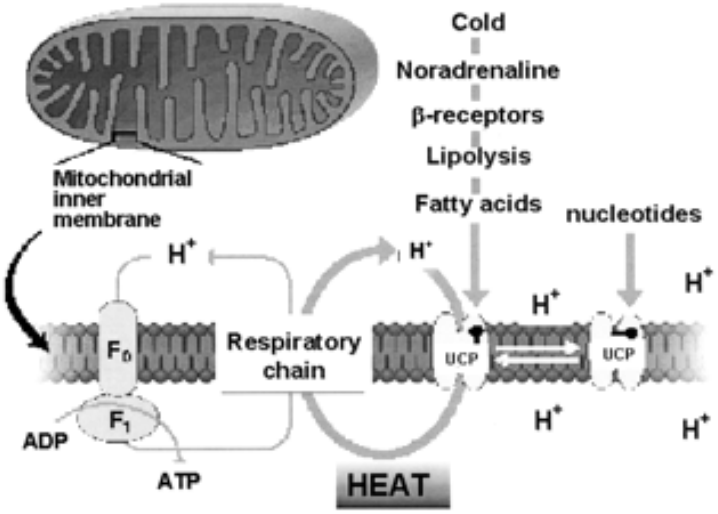

Figure 2-10: Uncoupling the ATP synthesis over uncoupling proteins in the mitochondrial membrane (Collins et al., 2001)

2.2.3.3 AMPK

AMP-activated protein kinase is a kinase with a key role in energy metabolism which reacts on a change in the AMP/ATP ratio. Its function is conserved in all eukaryotes. Low ATP levels, occuring during exercise, induce the activation of AMPK, which then up-regulates the oxidative metabolism. As recently discovered, AMPK and PPARdelta, which are both up-regulated during exercise, collaborate in reprogramming skeletal muscle transcription and endurance (Narkar et al., 2008) (Fig 2-10).

2.2.3.4 Starvation

Starvation condition is a stress situation for the body and has a serious impact on the skeletal muscle tissue metabolism. Pyruvate dehydrogenase kinase (PDK) 4 protein plays a key role during starvation. It is regulated by insulin and is involved in regulating the level of blood glucose. High levels of PDK4 were shown to decrease the activity of the pyruvate dehydrogenase and that this would down-regulate the consumption of carbohydrates in skeletal muscle during starvation (Majer et al., 1998).

As recently discovered, FOXO gene expression plays a regulatory role during nutrition depletion (Furuyama et al., 2003). According to the authors, especially FOXO1 showed in connection with PDK4 a remarkable increase during starvation. They also described a possible enhancing effect on the metabolic shift from glucose to fatty acid metabolism in skeletal muscle via FOXO1.

2.2.3.5 Nutrition

Nutritional supplements showing to regulate skeletal muscle mass are for example essential amino acids and carbohydrates. A broad spectrum of literature describes an influence of amino acids on muscle protein synthesis.

As mechanical signals, nutrients can act over the mTOR pathway, but they are also able to activate transcription and initiate protein synthesis directly via an mTOR independent pathway (Kimball and Jefferson, 2004).

Recently research concentrates also on the branched-chain amino acids, as leucine, valine or isoleucine. Leucine was found to act as a signal for accelerating protein synthesis (Matsakas and Patel, 2009).

The activation of mTOR over nutrition supplements, as amino acids, seems to contribute to signalling transduction and to optimized protein syntheses. Amino acids are suggested to activate mTORC1 over the inhibition of TSC1-TSC2 or the stimulation of Rheb. It was proposed that amino acids lead to a conformational change within the mTORC1 so that the complex is able to interact with its targets. At the end of this pathway the phosphorylation of the p70S6k and rpS6 stimulates protein synthesis (Wullschleger et al., 2006).

Another interesting finding points out a possible difference between nutritional and growth factor signalling transduction after mTOR activation. It was observed that amino acid-induced rapamycin signalling seems to act only over mTORC1 and is therefore completely independent of PKB and PI3K activation (Hornberger and Chien, 2006) (Fig. 2-6).

2.3 Crosstalk between skeletal muscle tissue and immune system

In physical activity, muscle damage, pathological conditions as well as ageing the muscle corresponds to actions of the immune system. Cells of the immune system, as leukocytes, and pro- and anti-inflammatory cytokines are players of the immune system often mentioned in association with muscle atrophy. Especially proinflammatory cytokines, as TNF-α and IL-6 are closely linked to age-related muscle loss and they were shown to contribute to sepsis-induced atrophy (Callahan and Supinski, 2009).

It was proven that skeletal muscle cells are sensitive to these immunological signals. Skeletal muscle cells can react on systemic inflammatory stimuli, but they are also able to express various cytokines themselves.

Cell culture experiments have shown that bacterial lipopolysaccharide directly up-regulates pro-inflammatory cytokines in skeletal muscle cells via toll like receptors 2 and 4 and an experimental animal model revealed that LPS causes a drop of insulin-like growth factor (IGF)-1 which may contribute to muscle loss (Frost et al., 2003; Frost et al., 2004).

2.3.1 LPS recognition by Toll-like receptors (TLRs)

Lipopolysaccharide (LPS) is a cell wall component of gram negative bacteria, often used in trials to simulate an infection with this type of bacteria. It is recognized by Toll-like receptor 4 (TLR4), which then induces the immune response. TLRs are one type of cell-associated pattern recognition receptors specialized to recognize pathogen-associated molecular patterns (PAMPs). Over PAMPS the body is able to react on a pathological invasion by activation of the immune system and stimulation of cytokine release. TLRs are localized in the plasma (TLR1,-2,-4,-5,-6) or endosomal (TLR3,-7,-8,-9) membranes of various cell types. The different TLRs recognize specific molecules. TLR2 appears often in combination with either TLR1 or TLR6 and is known to react on molecules of gram positive bacteria. TLR7 and 8 are both sensitive for viral single stranded RNA. TLR9 is specialized on viral and bacterial unmethylated CpG DNA. Molecules of gram negative bacteria, as LPS, are recognized by TLR4. A muscle cell is able to react on LPS stimulation as TLRs are also expressed on the

surface of skeletal muscle cells. An expression of TLR1-7, but not TLR8 and TLR9 was observed in mouse skeletal muscle as well as in C2C12 cells (Frost et al., 2006).

2.3.1.1 NF-kB signalling pathway

Experiments with C2C12 myocytes showed that LPS activates the NF-kB signalling transduction which results in increased expression of proinflammatory cytokines (Frost et al., 2006).

NF-kB is an important signalling pathway in protein degradation and is followed by the activation of the mitogen-activated protein kinase (MAPK) pathways leading to skeletal muscle atrophy. NF-kB can be activated by a great spectrum of stimuli, such as growth factors, cytokines, viral and bacterial infections, oxidative and biomechanical stresses and others. In skeletal muscle, NF-kB activation occurs mainly as a response to a disease situation. It leads to muscle atrophy through different mechanisms: first of all it is able to induce the expression of proteins related to the ubiquitin- proteasome systems, as MAFbx (also known as Atrogin1) or MuRF1 (=muscle ring finger protein). Secondly, the expression of inflammatory molecules such as pro-inflammatory cytokines, chemokines, cell adhesion molecules and tissue degrading enzymes are regulated by NF-kB (Kumar et al., 2004).

NF-kB belongs to a family of eukaryotic transcription factors, the Rel family. It is localized in the cytoplasma. In an inactive state, the NF-kB dimere binds to the NF-kB-inhibitors (IkBs). Activation occurs over degradation of IkB, so that the free NF-kB is able to enter the nucleus (Fig. 2-9).

NF-kB may also be a potential actor in muscle development and differentiation. It is suggested that it plays an essential role in keeping the myoblasts in a proliferating state by stimulating cyclin D1 accumulation and cell cycle progression (Guttridge et al., 1999).

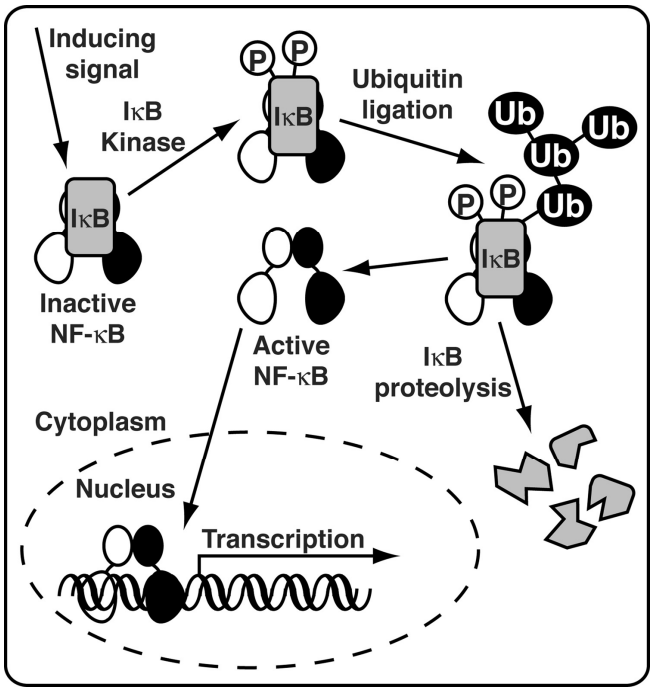

Figure 2-11: Activation of Nf-kB by inducing signals (SanDiego_State_University, 2005)

2.3.2 Influence of TNF-α and IL-6 on skeletal muscle metabolism

2.3.2.1 TNF-α

The proinflammatory cytokine tumor necrosis factor (TNF)-α plays an essential role in pathological and age-related skeletal muscle atrophy. Skeletal muscle cells are able to respond to TNF-α over the two TNF-α receptor isoforms (TNFR1 and TNFR2) which are both expressed in C2C12 myotubes. In sarcopenia, systemic inflammation strongly contributes to muscle atrophy. Particularly TNF-α negatively regulates the regeneration capacity over inducing apoptosis of satellite cells in the elderly. The effect of TNF-α seems to be threshold and time dependent (Degens, 2011). However, not only age-related muscle loss, but also muscle wasting, accompanying a lot of disease, is also partly influenced by acute and / or chronic inflammation. COPD patients suffering from muscle wasting and with no weight increase after nutritional support, were proven to posses high circulating levels of TNF-α (Rabinovich and Vilaro, 2011).

A broad spectrum of literature describes a TNF-α dependent up-regulation of atrogin (MAFbx) mRNA in vitro and in vivo. It was shown that this inflammation

induced increase of the expression of protein degrading genes, occurs mainly over the activation of Foxo4 expression and do not effect Foxo1/3 mRNA levels (Moylan et al., 2008) (Fig. 2-12).

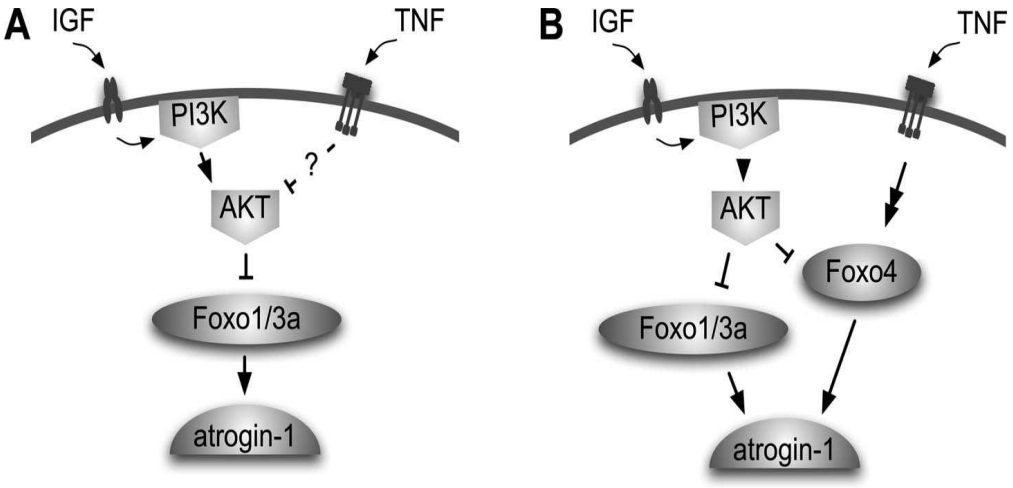

Figure 2-12: Increase of protein degrading genes by TNF-α (Moylan et al., 2008)

On the other hand, TNF-α was shown to down-regulate PGC-1 (see 2.2.3.1) and enhance this way the expression of its alpha target genes atrogin-1 and MuRF1 (Tang et al., 2010). This correlates with the finding that PPAR-γ activation inhibits inflammation induced NF-kB activity in skeletal muscle (Remels et al., 2009). In addition, in cachectic COPD patients lower levels of PPAR-γ were measured (Rabinovich and Vilaro, 2011).

TNF-α is not only a key factor in degradation and metabolic pathways, it also effects muscle cell differentiation over inhibition of the expression of genes involved in myogenic differentiation, as cyclin-dependent kinase inhibitor 1A, p21, marker genes as MyoD and others (Chandran et al., 2007).

TNF-α seems to act mainly over the NF-kB pathway. Although it was proven that NF-kB is activated by TNF-α in myotubes, there might exist additional signalling for the decreasing effect of TNF-α on IGF1 because no direct influence of NF-kB activation on the IGF1 expression level could be measured (Fernandez-Celemin et al., 2002). The detailed molecular mechanisms between TNF-α expression, the expression of muscle markers and growth-related genes and muscle wasting therefore remain to be discovered.

2.3.2.2 IL-6

IL-6 is a proinflammatory cytokine and involved in acute-phase response in case of infection or injury. In skeletal muscle studies it is often mentioned in connection with muscle atrophy. It is associated with protein breakdown, decreased physical decline and muscle wasting. It was already shown that its expression level, especially the level of plasma IL-6, increases with age and therefore it is a potential candidate for increasing sarcopenia (Roubenoff, 2003).

Besides, this cytokine is also upregulated after training as well as after muscle damage. IL-6 mRNA expression was shown to be up regulated immediately after exercise 10 to 20-fold (Keller et al., 2001).

Another interesting finding describes that an overexpression of IL-6 in transgenic mice leads to muscle atrophy and to an increased level of cathepsins. This suggests a role for IL-6 in the activation of the protein degradation machinery (Tsujinaka et al., 1995).

IL-6 expression also seems to be connected to growth factor expression. There are more and more evidences that IL-6 and IGF1 levels influence one another. High IL-6 was shown to down regulate IGF1 in a broad spectrum of literature, and on the other hand it was suggested that a low IGF1 level may stimulate IL-6 expression (Sesmilo et al., 2001).

2.3.2.3 Other cytokines

A TNF-α mediated significant up-regulation of different cytokine levels in C2C12 skeletal muscles including IFN-γ, IL-6 and the anti-inflammatory cytokines IL-9 and IL-10. (Alvarez et al., 2002).

The modulation in their expression levels in the context of muscle mass maintenance let them appear as interesting research targets beside TNF-α and IL-6. Proinflammatory cytokines as IL-1β or interferon (IFN)-γ on the one hand and anti-inflammatory cytokines as IL-10 on the other hand, may both be involved in the crosstalk of skeletal muscle tissue with the environment.

Like TNF-α, IL-1β also activates the NFkB pathway, but in contrast to TNF-α, IGF1 expression seems to be not affected. It was suggested that IL-1β as well as IL-1α act via an AKT / Foxo-independent mechanism. They mediate the

activation of p38 MAPK, stimulate NF-kB signaling, increase the expression of atrogin1 / MAFbx and MuRF1 and reduce the myofibrillar protein content in differentiated myotubes (Li et al., 2009).

2.4 miRNAs

2.4.1 Fine tuning of gene expression

miRNAs were discovered recently and are a class of short noncoding 18-22 nt long RNA molecules involved in the posttranscriptional regulation of gene expression. They are building an additional step of regulation after e.g. alternative splicing.

miRNA mediated gene expression can be found in human, animal and even plant genes. It occurs in about 30% of all human genes (Ambros, 2004). The exact number of miRNAs is not known but up to date more than 500 human miRNA genes have been observed, many of them are evolutionarily conserved.

The interest in miRNAs is growing, as it is known that they play a role not only during differentiation but also in cell proliferation, apoptosis tumorigenesis and several diseases.

2.4.2 Processing and acting of miRNAs

miRNAs belong to the so called ncRNA (non coding RNA), a part of the RNA not coding for proteins. They are transcribed in the nucleus where the primary miRNA (pri-miRNA) transcript is encoded in the DNA. The further procession of the pri-miRNA is mediated by an enzyme called Drosha which catalyses the transport from the nucleus into the cytoplasm (Fig. 2-13).

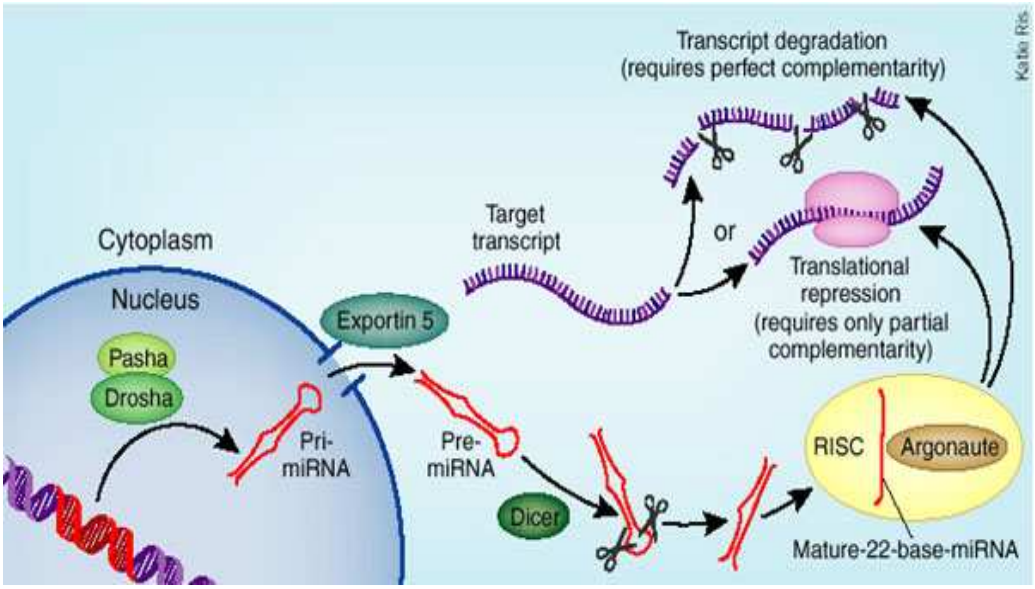

Figure 2-13: Processing and acting of miRNAs (Mack, 2007)

The mature miRNAs become part of the RNA-induced scilencing complex (RISC) and negatively regulate gene expression over repressing of protein synthesis by blocking translation or causing transcript degradation (Mack, 2007).

MiRNAs act through complementary base-pairing between the miRNA and the 3'untranslated region (UTR) of the targeted mRNA (Pillai et al., 2004).

2.4.3 Muscle specific miRNAs

Interestingly, many miRNAs are expressed in a tissue-specific manner, suggesting they may play important roles in the regulation of tissue-specific genes (Wang, 2006). A miRNAs is called specific if it is expressed only in a specific tissue or if its expression level in this tissue is significantly above their expression level in other tissues. Recently, it has been discovered that miRNAs are also involved in 'fine-tuning' the expression of transcription factors and signalling mediators important for muscle biology, including the regulation of proliferation and the differentiation during myogenesis (Callis et al., 2008). Beside these developmentally important processes miRNA influence has been observed during muscle diseases such as cardiac hypertrophy or muscular dystrophy.

miRNA-1, miRNA-206 and miRNA-133a/b were discovered to be specific for muscle tissue (McCarthy and Esser, 2007). Whereas miRNA-1 and miRNA-133 can be found in cardiac and skeletal muscle, miRNA-206 is expressed only in

skeletal muscle. MiRNA-1 and miRNA-133 are situated on the same gene locus and are therefore transcribed together. In skeletal muscle there expression seems to be controlled by MyoD. Interestingly, although the two miRNAs are located on the same gene locus miR-1 enhances myogenesis while miRNA-133 represses it (Chen et al., 2006), (Zhao et al., 2005). As recently discovered, miRNA-206 expression causes down regulation of cyclin D1 and phospho-retinobasma protein and up-regulation of p21 and myogenin (Taulli et al., 2009).

Other miRNAs found to be expressed in muscle tissue and predicted to play important roles in skeletal muscle metabolism are miRNA-499, miRNA-208b and miRNA-23a. For miRNA-499 and miRNA-208b a possible role in regulating the myostatin gene was described (Drummond et al). For miRNA-23a they indicated to act over its predicted targed MEF2C, which it also known to promote a slower muscle phenotype. Also miRNA-499, miRNA-208 and miRNA-208b (encoded by the intron of Myh7b, alphaMHC and betaMHC, respectively) were proven to be involved in fibre type twitch promoting the slow myofibre gene programs (McCarthy et al., 2009) (Fig. 2-14).

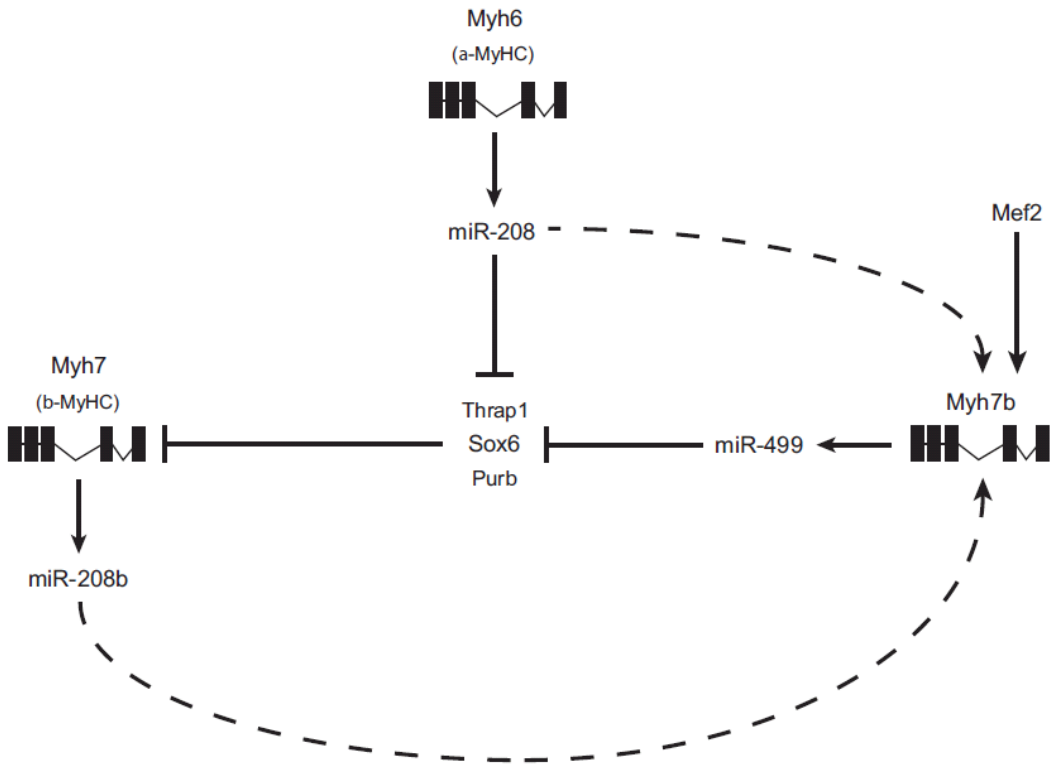

Figure 2-14: miRNA-499 / miRNA-208 mediated regulation of gene expression (McCarthy et al., 2009)

Sox6, Pur-beta and Thrap1 were proven by the authors mentioned above to be important target-genes of miRNA-499 as well as of miRNA-208 and their up-regulation during muscle atrophy represses the beta-MHC gene expression and by this way down-regulates the slow-twitch MHC isoform expression.

2.4.4 Immuno-related miRNA-155

As the specialized tissues in the body, also the immune system possesses its translational regulators. It was proven that some miRNAs react specifically on inflammatory stimuli or in association with changed immunological conditions. One of the miRNAs related to the immune system is miRNA-155. It was reported that miRNA-155 plays a role in the innate immune response as it is up-regulated in response to LPS (Tili et al., 2007).

Inflammatory cytokines, as TNF-α, IL-1 or IFN-γ were shown to increase miRNA-155 expression via activation of the JAK/STAT signalling pathway (Kutty et al., 2011). As skeletal muscle atrophy is accompanied by inflammatory conditions and due to the fact that down-regulation of IGF-1 after TNF-a treatment was proven to be JNK-dependent (Frost and Lang, 2007), there might be also a role for the immune-related miRNA-155 in connection with muscle wasting.

3 METHODS

3.1 Cell culture

3.1.1 Specifities of the cell line

To mimic common muscle tissue, we used C2C12 cells, which is a murine myoblast cell line (German collection of Microorganisms and Cell Cultures DSMZ, Deutsche Sammlung von Mikroorganismen und Zellkulturen GmbH, Braunschweig, Germany). These cells grow as an adherent monolayer with a doubling rate of approximately 20 hours in optimum proliferating conditions. C2C12 cells are mesenchymal progenitor cells with a stem cell like character which are often used for experiments in muscle biology due to their specifity to differentiate rapidly under changed culture conditions. The differentiation process lasts for 3-4 days where the myoblasts stop proliferating, they lose their stem cell like character and start to fuse to build the long multinucleated myotubes (protocol C2C12 cells, DSMZ).

3.1.2 Growing conditions

For normal proliferation, the cells were cultivated in growth medium (GM). This medium consisted of mixture of Dulbecco's Modified Eagle Medium (D-MEM) (4500 mg/L D-Glucose, Sodium Pyruvate, without L-Glutamine (Gibco, Paisley, Scotland) with 2 mM Glutamine (Gibco, Paisley, Scotland) and 10% fetal calf serum (FCS; Linaris, Wertheim-Bettingen, Germany). A 0.22 µm filter cartridge (SteriCup®- GP Express Plus Filter Unit; Millipore GmbH, Billerica, MA) was used to filter the complete medium.

In this medium the cells were grown to sub confluence, as tight confluent layers of cells would lead to a stress situation, abnormal growing and uncontrolled differentiation. The cells were incubated under standard conditions (37℃, 5% CO_2 and 95% humidity) in a CO_2 incubator (MCO-20AIC CO_2 Cell Culture Incubator with SafeCell™ UV; Sanyo E&E Europe BV Medical Division, Etten Leur, Netherlands) and the medium had to be changed every third day.

When the cells reached the right density (70% to 80% confluence), they were washed with $PBS^{-/-}$ (Gibco, Paisley, Scotland) and differentiation was induced using differentiation medium (DM) consisting of D-MEM (4500 mg/L D-Glucose, Sodium Pyruvate, Gibco, Paisley, Scotland) supplemented with 2 mM Glutamine and 2% Horse serum (Gibco, Paisley, Scotland). For full differentiation, cells were incubated in DM under standard conditions (see above) for four days. The medium was changed after two days.

The pictures were taken under an inverse microscope with a digital camera with 10 fold magnification.

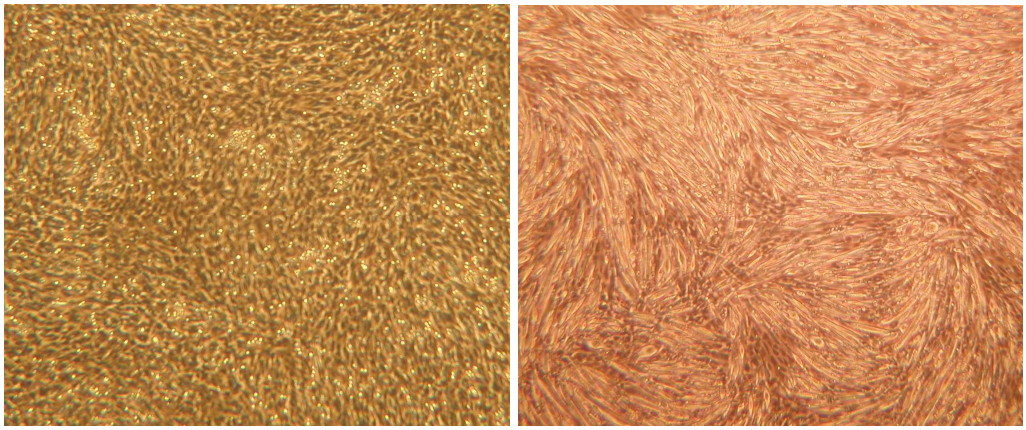

Figure 3-1: First picture: C2C12 myoblasts grown in growth media (proliferating cells). Second picture: C2C12 myotubes after serum deprivation (differentiated cells)

3.1.3 Subculturing

At a confluence of maximum 80%, cells were washed with PBS -/- and Trypsin/EDTA was used to detach the cells. This Trypsin/EDTA incubation lasted for 2 minutes and was stopped afterwards with GM. Flasks with pre-warmed GM were prepared and the cells were transferred directly with the correct volume of suspension to achieve the desired dilution (1:200, 1:100, 1:50 or 1:25).

If the cell number was determined via cell counting, the entire suspension was centrifuged (1,300xg, room temperature, 6minutes). The supernatant was discarded and the sample for counting was taken from the pellet resuspended in 1ml GM.

3.1.4 Cell counting

A haemocytometer of the Bürker-Türk type was used (Hecht-Assistant, Sondheim, Germany) to count the cells. The counting sample (10µl of cell suspension in GM) was diluted 1:2 with 0.4 % trypan blue (Sigma- Aldrich Handels GmbH, Vienna, Austria). This treatment helped to determine the number of living cells and the number of dead cells. The dead ones appeared blue coloured under the microscope in contrast to the colourless living ones. Counting took place under a light microscope (Olympus CK2, Olympus, Tokyo, Japan).

The grid of this type of haemocytometer was divided into 9 big squares. Each of these was subdivided into 16 smaller squares with an area of 0.04 mm^2 each. The depth was fixed to 0.1 mm.

Five small squares had to be counted.

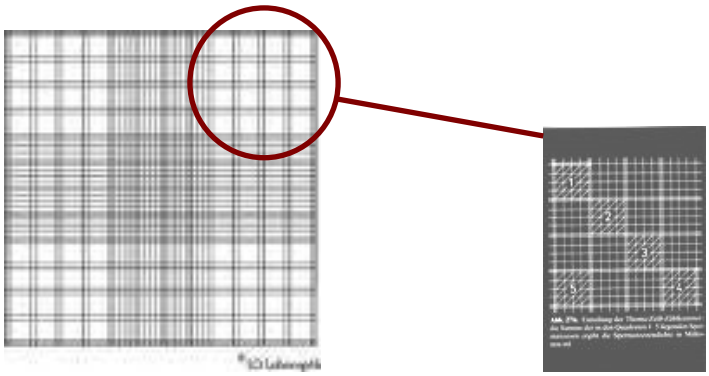

Figure 3-2: Bürker-Türk counting chamber. The picture illustrates the five squares counted (LO-Laboroptik, 1999)

The final cell number (x 10^5) was determined using the following formula:

$$Number\ of\ cells/ml = \frac{counted\ cells \cdot 0.1}{Number\ of\ counted\ big\ sqares}$$

3.1.5 Storage

Subculturing cannot be carried on endlessly. It depends on the life span of the cells and their reaction on toxic components like Trypsin as well as to the stress they experience during treatment. When using the cells more than a certain number of passages, they showed a reduced growing rate and a higher percentage of dead cells. To avoid faults and to get statistically more exact results, cells were cultivated up to a maximum passage of 14.

To store C2C12 cells over a longer period of time, they were frozen in liquid nitrogen. Therefore cells were grown in GM. When they reached approximately the desired number, they were washed 2 times with PBS-/-, detached with 1x Trypsin / EDTA (10x stock solution, Invitrogen, Carlsbad, CA), resuspended in GM, centrifuged (1,300xg, room temperature, 6min) and the supernatant was discarded. Freezing medium (80% GM + 20% FCS) was added to suspend the cells. After counting on a haemocytometer, cells were diluted to 3 x 10^6 cells / ml with freezing medium. 1ml aliquots were added to cryo vials and then cooled on ice for 5 minutes.

100 µl DMSO (Sigma-Aldrich Handels GmbH, Vienna, Austria) per vial was added. The cells were first frozen at -80°C for 24 hours before they were finally transferred to liquid nitrogen for long term storage.

For thawing the cells, the cryo vial with the cell suspension was quickly delivered into a water bath (37°C, 2min). After thawing, the vial was cleaned with 70% ethanol and then transferred into a cell culture flask (75 cm^2, Corning Costar, Bodenheim, Germany) with 14 ml pre-warmed GM. Incubation was carried out at standard conditions followed by the subculturing process.

3.1.6 Differentiation and stimulation with LPS / TNF-α / IL-6

For differentiation, C2C12 cells were seeded in 6 well plates (Corning Costar, Bodenheim, Germany) at a density of 0.05 x 10^5 cells / cm^2. After 3 days of standard incubation in GM where cells were allowed to settle down, the medium was switched to DM. Differentiation lasted for 4 days and medium switch to fresh

DM took place after the second day. Samples were taken directly before the medium switch and after 4 days of differentiation.

For time kinetics C2C12 cells were seeded in 6 well plates (Corning Costar, Bodenheim, Germany) at a density of 0.05 x 10^5 cells / cm^2. After 3 days of standard incubation in GM, the medium was switched to DM (day0). Differentiation lasted for 4 days and medium switch to fresh DM took place after the second and after the fourth day (day4). Day 4 was the starting point for LPS / TNF-α and IL-6 stimulation. For time kinetics concentrations of 1µg / ml LPS (E.coli 0111:B4, L4391 Sigma), 10ng / ml TNF-α (mouse recombinant ex. in E.coli, T7539, Sigma) and 10ng/ml IL-6 (mouse recombinant ex. In E.coli, I9646, Sigma) respectively were used. Samples were taken after differentiation (day 4) and after 1, 3, 6, 12, 24 and 48 hours of incubation (Fig. 3-3).

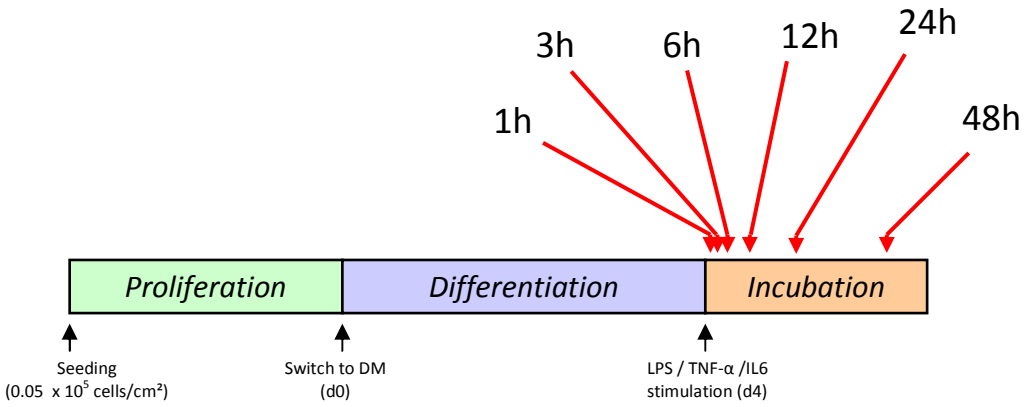

Figure 3-3: Time-kinetics overview, 3 days of proliferation followed by 4 days of differentiation. Analyzes were performed at 6 different time points during incubation

A washing step with PBS-/- was performed before cells were harvested using 650µl Lysis Binding buffer per well (mirVanaTM miRNA Isolation Kit (Ambion Inc., Austin, TX). For all time points the supernatant was taken, centrifuged (14,000xg, 6min, 4℃) and frozen at -80℃ for further analyzes .

3.2 Gene expression analyzes

3.2.1 RNA and miRNA isolation

For isolation of total RNA, including miRNAs, the mirVANA™ miRNA isolation kit (Ambion, Austin, TX) was used, which allows simultaneous RNA and miRNA isolation. The frozen samples were thawed on ice, vortexed and 550µl of each was transferred into new sample tubes to ensure equal starting volumes for all samples. Then the isolation procedure was performed according to the manufacturer's instructions.

Fifty five µl of miRNA homogenate additive (1/10 of the volume) was added to each sample, followed by a vortexing step. After 10min incubation on ice, 400µl Acid-Phenol:Chloroform solution was added and samples were mixed by intense vortexing. Centrifugation (5 min., 14,000xg) was used to separate the liquid into a lower organic and an upper aqueous phase which contains the RNA. Four hundred fifty µl of this upper phase was transferred into a fresh sample tube and mixed with 563µl of absolute ethanol (1.25 x volume) through vortexing. To isolate total RNA, the mixture was transferred into a filter cartridge and centrifuged (20s, 10,000xg, room temperature). As the maximum volume of the filter cartridge was 700µl, the flow through was removed and the collection tube was used again for centrifugation of the rest of the sample. Afterwards the filter was washed 1 time with 700µl miRNA wash solution 1 and 2 times with 500µl wash solution 2/3. Centrifugation between these steps was performed at room temperature for 15s at 10,000xg. The flow through was removed and the tubes were re-used. To dry the filter, it was centrifuged once more after washing (1 min., 10,000xg). Then the filter cartridge was transferred into a fresh collection tube, 30µl 95°C hot distilled water was added and the RNA was eluted by centrifugation (30s, room temperature, 18,000xg). The eluats of all samples were aliquoted, (2µl of each sample was taken for photometric quality and quantity control) and stored at -80°C.

Spectrophotometric measurement of absorbances at 230, 260, 280 and 320 nm was used to determine the amount of total RNA. The absorbance at 260nm shows the concentration of the RNA. This detection method also provides information about the quality of the isolated RNA, using the 260 / 280 nm and the 260 / 230 nm ratios. The ratio of 260 and 280 nm of absorbance is the main indicator of the quality of the RNA. If this ratio is lower than 1.6, it is a sign that

the sample is contaminated with proteins. The ratio of 260 and 230 nm absorbance provides additional information about RNA purity. A higher ratio than 0.2 indicates a possible contamination with organic solvents, salts or proteins (Gallagher, 2001).

mRNA and miRNA are extracted by the same procedure, but the amount was calculated differently. For total RNA, 1 unit at 260nm means 40µg of RNA per ml. Therefore the content of RNA was calculated following the formula below:

$$RNA\ concentration\ [\mu g / ml] = \frac{4000 \cdot Abs_{260} \cdot Dilution\ factor}{100}$$

In contrast to the total RNA measurement, 1 unit at 260nm for miRNA corresponds to only 33µg per ml. Therefore the formula for the determination of the miRNA content includes the factor 3,300 instead of 4,000:

$$RNA\ concentration\ [\mu g / ml] = \frac{3300 \cdot Abs_{260} \cdot Dilution\ factor}{100}$$

For photometric measurement, 198µl TE buffer pH 8 (preparation see Annexes) and 2µl RNA sample were mixed (1:100 dilution) and measured on the spectraphotometer using disposable UVetten (Eppendorf, Hamburg, Germany). 200µl TE buffer were used as a blank.

3.2.2 mRNA expression analyzes

3.2.2.1 cDNA synthesis

For cDNA synthesis SuperScript® III First Strand Synthesis System for RT-PCR (Invitrogen, Carlsbad, CA) was used according to the manufacturer's instructions. Three µg of total RNA in a volume of 8µl were reverse transcribed using a blend of Oligo(dT) and random hexamers (1:1) as primer. The samples

were thawn on ice and diluted to the desired concentration with dH2O. The annealing mix consisting of 8 µl RNA sample, 1µl dNTP and 1µl blend was prepared for every sample, heated for 5 min. at 65°C and then placed on ice for 1 min. Ten µl of a mixture of 2µl 10x RT buffer, 4µl $MgCl_2$, 2µl DTT, 1µl RNase OUT and 1µl Super Script RT per sample, called synthesis mix, were added to each prepared annealing mix. After a short centrifugation the samples are transferred to a Biometra thermocycler (Biometra, Göttingen, Germany). Cycling conditions for reverse transcription were chosen according to the manufacturer's instructions

TIME [min]	℃
25	10
50	50
5	85
∞	4

After spinning down, 1 µl of RNase H was added to each sample and digestion of the RNA template occurred for 20min. at 37℃. Samples were stored at -80℃.

3.2.2.2 Real-time qPCR

The influence of the inflammatory stimuli used in this study on muscle cell development is measured by analysing the mRNA expression levels of the myogenic marker genes MyoD and Myogenin and the insulin-like growth factor 1 splicing variants IGF1-Ea, IGF1-Eb and MGF. The mRNA expression levels of the chosen parameters in the samples were measured using the real-time PCR system.

For the analyzes performed in this study, the Taqman PCR was used, for this is a well-established and reliable method in our laboratory. A 7500 Real Time PCR System (Applied Biosystems, Foster City, CA) was taken for measurements.

The Taqman system uses fluorogenic-labeled probes which use the 5´ nuclease activity of the Taq DNA polymerase, therefore it is also called 5-prime nuclease assay. One of the benefits of the TaqMan® system is its increased specificity for a certain sequence. This is gained over a probe, an oligonucleotide able to anneal to the template between forward and reverse primer. The probe is also necessary for detection, as it includes beside the oligonucleotide also the reporter and quencher dye. The reporter dyes can be excited by light sources and emit fluorescence light. This process is suppressed by the quencher, when it is located near the reporter. Therefore there is no emission light present for intact annealed probes. The polymerase possesses exonuclease activity and cleaves the probe during each extension cycle, separating the quencher from the reporter which then starts to emit light (Applied_Biosystems, 2008) (Fig. 3-4).

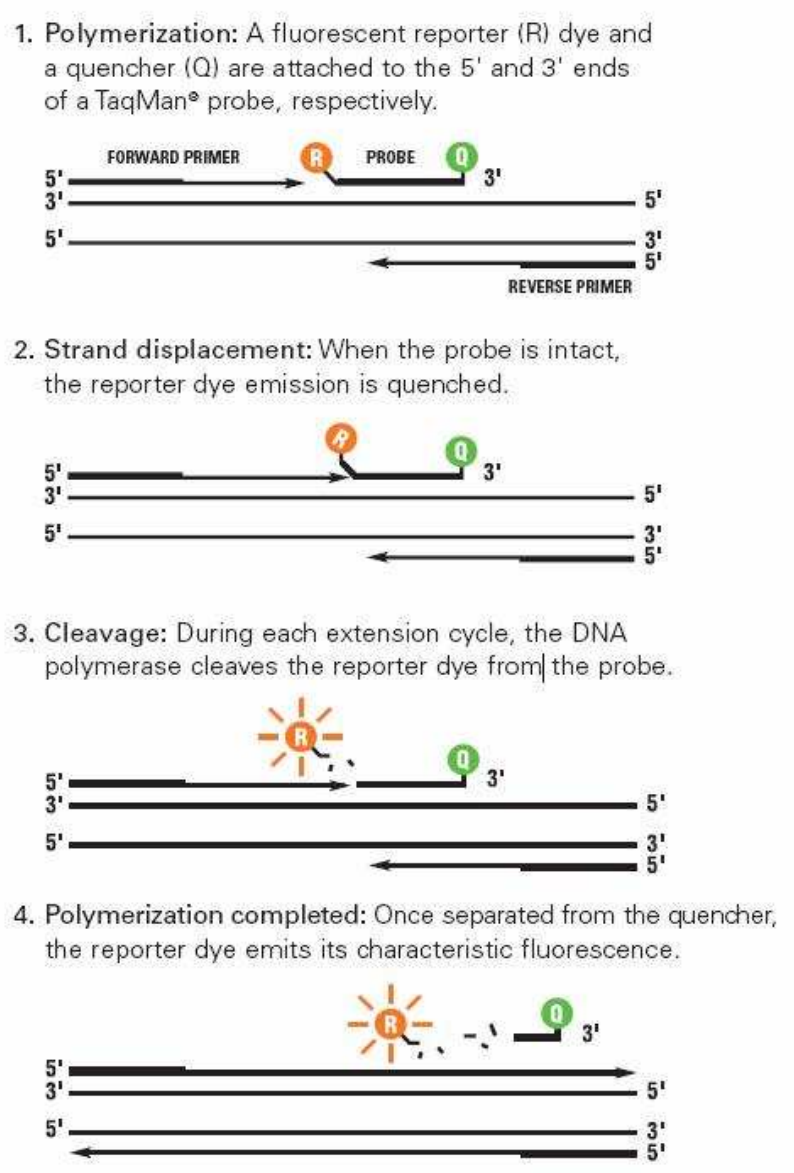

Figure 3-4: TaqMan PCR schematic (Applied_Biosystems, 2008)

Measuring the fluorescence, the amount of target gene RNA is determined. Data analyzes were performed with the 7500 System SDS v1.4 software (Applied Biosystems. Foster City, CA). For analyzes a threshold line has to be set. This line marks the cycle in the exponential phase of amplification, where the measured fluorescence exceeds background fluorescence (Ct = cycle threshold). The amount of target DNA in the sample determines when fluorescence reaches the Ct.

3.2.2.3 MyoD / Myogenin mRNA expression

The cDNA of the samples was diluted to 6,125ng / µl with ddH2O. For analysis of MyoD and myogenin TaqMan® Gene Expression Assays 20x primer and MGB probe (Applied Biosystems, Foster City, CA) and FAM™ dye-labeled mix for MyoD (Assay ID Mm00440387_m1) or myogenin (Assay ID Mm00446194_m1) was used. The housekeeping gene GAPDH (Mouse GAPDH 20x, Pre Developed TaqMan Assay Reagents 4352932 E, Applied Biosystems) was used as endogenous control, which is described in literature as a reliable control according to its equally expression in muscle tissue and C2C12 cell culture (Barber et al., 2005).

The standard was prepared by using pooled samples, which were diluted four times in 1:10 steps. The concentration ranges therefore from 250ng to 0.025ng RNA / well. Real-time PCRs were performed using PCR plates (96 well Optical plate with barcode, Foster City, CA). For one well, 16µl Master Mix, consisting of 10µl TaqMan® Gene Expression Master Mix (Applied Biosystems), 1µl Primer and 5µl dH2O were combined with 4µl of diluted sample. Per well, a total of 25ng of RNA was used. Analyzes were performed in duplets with dH2O instead of sample as a negative control (NTC). Cycling conditions shown below (table 3.1).

Times and Temperatures			
Initial steps		Each of 45 Cycles	
		Melt	A/E
HOLD	HOLD	CYCLE	
2 min 50°C	10 min 95°C	15 sec 95°C	1 min 60°C

Table 3.1: Real-time PCR cycling conditions; A/E = Anneal/Extend

3.2.2.4 IGF1-Ea, IGF1-Eb and MGF mRNA expression

For specific amplification of the splicing variants of the IGF1 gene, primers suitable for real-time PCR were designed.

The mRNA sequences of the target genes were gained from DNA data bases (NCBI / Celera) and the quality of the mRNA was then proofed according to the protocol for Bioinformatic Evaluation of a Sequence for Custom TaqMan Gene Expression Assays (Applied Biosystems).

Primer and probe design was performed using primer express software. IGF1-Ea, IGF1-Eb and MGF differ in the combination of their exons and therefore primers were placed over the various exon borders, which allow a specific recognition and therefore amplification of all three genes:

IGF-1Ea: Exon 5 (forward primer), Exon 5/6 (probe), Exon 6 (reverse primer)

IGF-1Eb: Exon 4/5 (forward primer), Exon 5 (probe), Exon 5 small (reverse primer)

MGF: Exon 5/6 (forward primer), Exon 6 (probe), Exon 6 (reverse primer)

The different splicing variants of the mus musculus IGF1 gene:

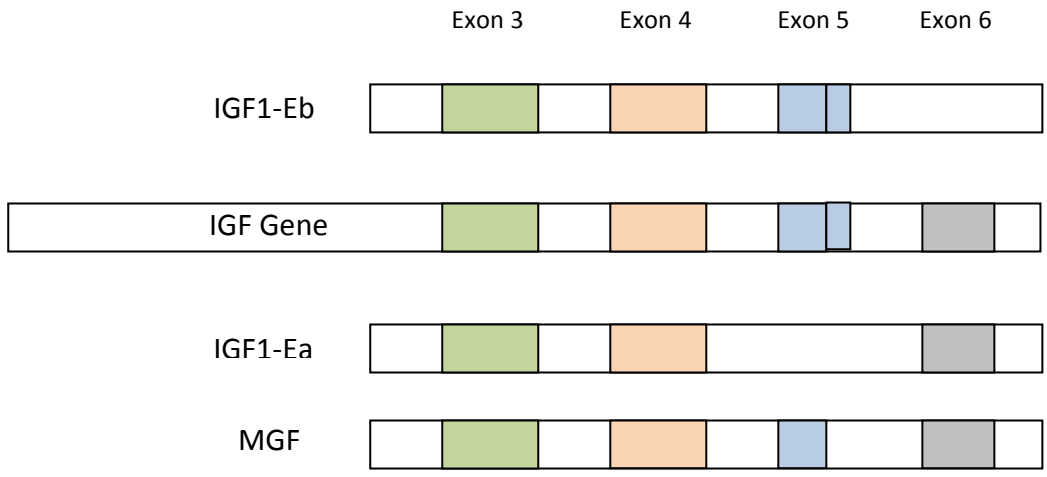

Primer / Probe sequences of the three target genes (table 3-2):

mmuIGF1-Ea	forward	5'-CTTCCGGAGCTGTGATCTG-3'
	reverse	5'-TCTTGTTTCCTGCACTTCCTC-3'
	probe	5'-TGACATGCCCAAGACTCAGAAG→GAAGT-3'
mmuIGF1-Eb	forward	5'-TCAGAAG→TCCCCGTCCCTAT-3'
	reverse	5'-AGTTGCCTCCGTTACCTCCT-3'
	probe	5'-AGAAGGAAAGGTGAGCCAAAGACACA-3'
mmuMGF	forward	5'-GCAAAGGAGAAGGAAAG→GAAGTA-3'
	reverse	5'-TGTTTTGCAGGTTGCTCAAG-3'
	probe	5'-6FAM-GGAGCCTCCCACGGAGCAGA-TAMRA-3'

Table 3-2: Primer and probe sequences; → = Exon border

As for myogenin and MyoD PCRs, the cDNA of the samples was diluted to 25ng / well with ddH2O. The pre-tested primers for IGF1-Ea, IGF1-Eb and MGF were used in a concentration of 300nmol, the probe in a concentration of 250nmol, all diluted in dH2O. As before, GAPDH was used as an endogenous control and dH2O as a negative control. For standard, the same sample pool and the same concentrations were taken as for MyoD / Myogenin.

Real-time PCRs with designed primers were performed using 16µl Master Mix per well, consisting of 10µl TaqMan® Gene Expression Master Mix (Applied Biosystems), 2µl of forward and 2µl of reverse Primer, 2µl probe and 5µl of dH2O. This was combined with 4µl of diluted sample.

3.2.3 miRNA expression analyzes

The transcription and amplification through real-time PCR of miRNAs slightly differs from that of mRNAs. A main problem when analyzing miRNAs is their

shortness. The normally used mRNA transcription procedure with a random primed reverse transcription step is not possible for a length of 18-22 nucleotides. Therefore a primer containing a target-specific stem loop structure was designed. Beside the so gained specificity for mature miRNAs, these target-specific RT primers fulfil another function: the resulting product of the transcription step is a combination of the mature miRNA and the primer, longer as the originally mature miRNA and therefore a suitable template for RT-PCR.

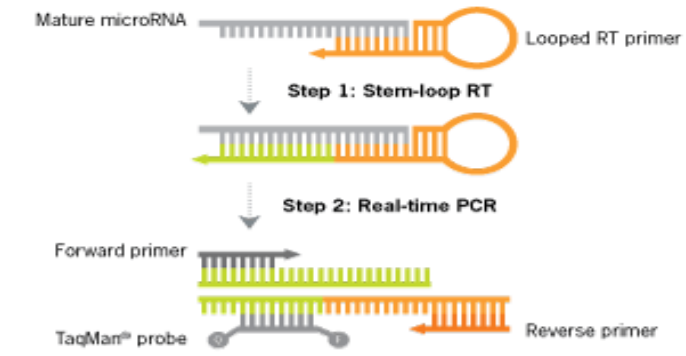

Panel A. TaqMan® MicroRNA Assay

Panel B. Precursor and Mature miRNA

Figure 3-5: TaqMan® miRNA Assay Mechanism (Ambion, 2010)

These stem-loop primers are better than conventional ones in terms of PCR efficiency and specificity and they are not affected by genomic DNA contamination (Chen et al., 2005). According to the authors the better specificity

and sensitivity could be a result of base stacking, which may improve the thermal stability of the primer/RNA duplex. The spatial constraint of the stem-loop structure could prevent it from binding to double-strand genomic DNA.

3.2.3.1 cDNA synthesis

For cDNA synthesis, the TaqMan® miRNA Reverse Transcription Kit (Applied Biosystems, Foster City, CA) was used, which allows TaqMan® RT-PCR amplification afterwards. Specific transcription of miRNAs into cDNA was performed according to the protocol (TaqMan® miRNA Reverse Transcription Kit protocol).

Reverse transcription was performed with the TaqMan® miRNA assays (Applied Biosystems, Foster City, CA, hsa-miR-206, hsa-miR-1, hsa-miR-133a, hsa-miR-133b, has-miR-499, has-miR-208 and hsa-miR-155) and TaqMan® Gene Expression Master Mix (Applied Biosystems, Foster City, CA). MiRNAs are conserved throughout species which allows for our trials the use of human primers for murine miRNAs.

An amount of 10ng RNA / 5µl was reverse transcribed. This calculation is based on the miRNA content and assumes a complete transcription of miRNA into cDNA. The Master Mix, containing 0,15µl 100mM dNTPs, 1,5µl 10 x reverse transcription buffer, 1µl MultiScribe ™ RT, 0,19µl RNase Inhibitor (20 U / µl) and 4,16µl ddH2O was prepared. After dilution of the miRNA to the right concentration, 5µl of the sample was mixed with 3µl primer mix and with 7µl of the Master Mix.

The Reference Panel (mirVana 4388891, Applied Biosystems), which serves as a standard for PCR, was diluted in 1:10 steps and each dilution was reverse transcribed, using 5µl of standard dilution, 7µl Master Mix and 3µl primer mix.

A Biometra thermocycler (Biometra, Göttingen, Germany) was used for converting miRNA into cDNA (cycling conditions see table 3-3) and samples were stored at -80℃.

TIME [min]	℃
30	16
30	42
5	85
∞	4

Table 3-3: MiRNA specific reverse transcription conditions

3.2.3.2 miRNA expression

For miRNA RT-PCR 96-well PCR plates (optical plate with barcode, Applied Biosystems, Foster City, CA) were used. The PCRs were all carried out due to the manufacturer's instructions. A Reference Panel, already diluted in 1:10 steps before the reverse transcription, was used as a standard, with the highest concentration of 1 fmol and the lowest of 0,0001 fmol. This Reference Panel consists of a mix of different miRNAs and allows absolute quantification. ddH2O was used as a negative control.

The samples were analyzed in duplets. For each well 10 µl of TaqMan® Gene Expression Master Mix (Applied Biosystems, Foster City, CA), 8 µl ddH2O and 1 µl of miRNA assay (20x, miR-1, -206, -133a, -133b, -155) was used. To this mix 1 µl of the reverse transcription product was added.

Cycling conditions are shown below (table 3-4)

Step	AmpliTaq Gold® Enzyme Activation	PCR	
	HOLD	CYCLE (40 cycles)	
		Denature	Anneal/ Extend
Time	10 min	15 sec	60 sec
Temp (°C)	95	95	60

Table 3-4: miRNA real-time PCR cycling conditions

3.2.4 Protein determination

ELISAs were used to determine the concentration of our proteins of interest from cell culture supernatants.

The ELISAs (enzyme-linked immunosorbent assay) is a biochemical technique, which is used to recognize a specific antigen in a sample. There are several types of ELISAs, as the indirect or the competitive ELISA, which are all using the antibody-antigen recognition, but in different combinations.

The ELISA used here is a sandwich-type ELISA (antibody-antigen-antibody).

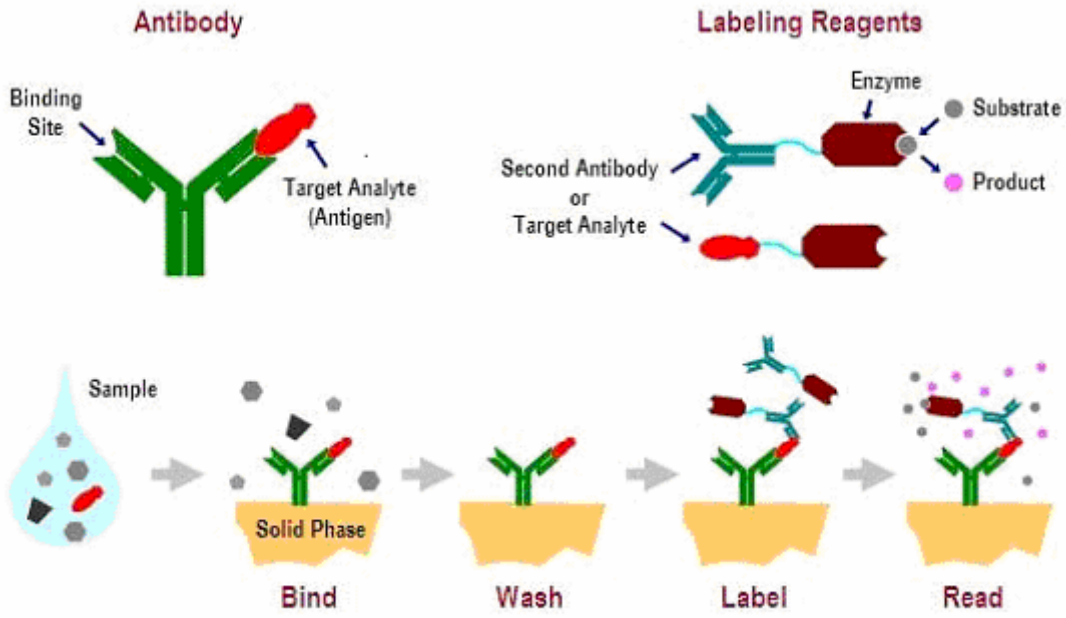

Figure 3-6: Sandwich ELISA schematic (Biosystemdevelopment, 2006)

A sandwich ELISA is carried out on a solid surface on which capture antibodies, with a specific binding site for the antigen, are immobilized. When the samples are added, the antigens are able to bind the antibodies while the rest of the sample is removed by several washing steps. For labelling, a second antibody, which is able to recognize the same antigen, is used. This second antibody is coupled to an enzyme. During incubation, this enzyme catalyzes a reaction so that its substrate becomes detectable over an observable color change or a fluorogenic signal. The measurement of the enzymatic activity corresponds to the concentration of the captured antigens.

This way the analyzes of the detectable signal determines the presents of the antigen of interest and its quantity.

3.2.4.1 IGF-1

To measure the concentration of IGF-1 protein in the cell culture supernatants, a mouse IGF-1 Immunoassay (Quantikine, R&D Systems, Minneapolis, US) was used. This assay is a solid phase ELISA, containing recombinant mouse IGF-1 and antibodies against it. With this kit it is possible to measure the concentration of natural mouse IGF-1.

Supernatants were taken 4 days after differentiation and 1, 3, 6, 12, 24 and 48 hours after stimulation with TNF-α, LPS or IL-6. Before freezing, they were centrifuged (14,000xg, 10min, 4℃) to eliminate eve ntually disturbing components. After centrifugation, supernatants were split up and transferred into sterile sample tubes. Samples were stored at -80℃ until further analyzes.

The assay was used according to the manufacturer's instructions. Samples were thawn at room temperature, centrifuged (10,000xg, 3min) and diluted 1:3 with Calibrator Diluent RD5-38.

All reagents were prepared due to the kit protocol. Recombinant mouse IGF-1 was prepared at a concentration of 2000pg / ml and then diluted in 1:2 steps down to 31,2pg / ml with Calibrator Diluent RD5-38, was used as a standard.

Analyzes were performed on a 96well mouse IGF-1 microplate, coated with the monoclonal antibody specific for mouse IGF-1. Fifty µl Calibrator Diluent were added to each well, followed by 50µl of the diluted sample, standard or control. Then the plate was covered and incubated (2h on the shaker, room temperature). Thereafter, the solution was discarded and each well was washed five times with wash buffer. The liquid was removed completely, and 100µl of mouse IGF-1 conjugate (mixture of stabilized hydrogen peroxide and the stabilized chromogen tetramethylbenzidine) which was used as substrate solution, was added to each well followed by 30min of incubation in the dark. After that, the washing step with wash buffer was repeated and the enzymatic substrate reaction was stopped by adding 100µl of stop solution to each well.

The optical density was measured on a ELISA reader (Victor 3, Perkin Elmer) at 450nm with a correction wavelength at 555nm.

3.2.4.2 TNF-α

The concentration of TNF-α in the cell culture supernatants was measured using a mouse TNF-α Immunoassay (Quantikine, R&D Systems, Minneapolis, US). This assay uses the same principles as the IGF-1 ELISA (see above).

Supernatants were taken 4 days after differentiation and 1, 3, 6, 12, 24 and 48 hours after stimulation with TNF-α, LPS or IL-6. Before freezing, they were centrifuged (14,000xg, 10min, 4℃) to eliminate eve ntually disturbing components. After centrifugation, supernatants were aliquoted and transferred into sterile sample tubes. Samples were stored at -80℃ until further analyzes. The assay was used according to the manufacturer's instructions.

Supernatants were thawn at room temperature and centrifuged (10,000xg; 3min). The TNF- α ones had to be diluted 1:10 with Calibrator Diluent RD5-38 due to their original high concentration of TNF-α. All other samples were used directly without dilution. Recombinant mouse TNF-α was prepared at a concentration of 1,500pg / ml and further diluted in 1:2 steps down to 23.4pg / ml. Calibrator Diluent RD5-38 was used as a standard.

Analyzes were carried out as mentioned above (see chapter 3.2.4.1).

3.2.4.3 IL-6

The concentration of IL-6 in the cell culture supernatants was measured by using a mouse IL-6 Immunoassay (Quantikine, R&D Systems, Minneapolis, US). Supernatants were taken 4 days after differentiation and 12, 24 and 48 hours after stimulation with TNF-α, LPS or IL-6. For protocol, sample preparation and analyzes see above (Chapter 3.2.4.2).

3.3 Statistical Analysis

Statistical evaluation was performed using SPSS software (SPSS software package for Windows, Version 8.0.0, Chicago, IL). Group comparisons during differentiation test were performed using independent t-tests. Levene tests were used to test for equality of variances. For time kinetic measurements a repeated measured ANOVA was performed to calculate time (0, 1, 3, 6, 12, 24, 48h), group (control, LPS, TNFα, IL-6) and time x group interactions. Post hoc Dunnett T-Tests were performed to describe differences between groups and/or time points.

Data are shown as mean ± SD (mean values ± standard deviation) and a p value < 0.05 was considered as being statistically significant.

4 RESULTS

4.1 Myoblast differentiation

In all trials cells were seeded at a density of 0.05 x 10^5 cells / cm^2 and allowed to adhere for three days before changing either to new GM or starting differentiation by adding DM instead of GM. Cells were counted on day 0, day 1, day 2, day 3 and day 4 using Bürker-Türk haemocytometer in order to determine the proliferative capacity of the cells during the different growth conditions. Data are shown as mean (normalized to day 0) ± SD (* p<0.05 and *** p<0.001 vs. day 0; Fig. 4-1).

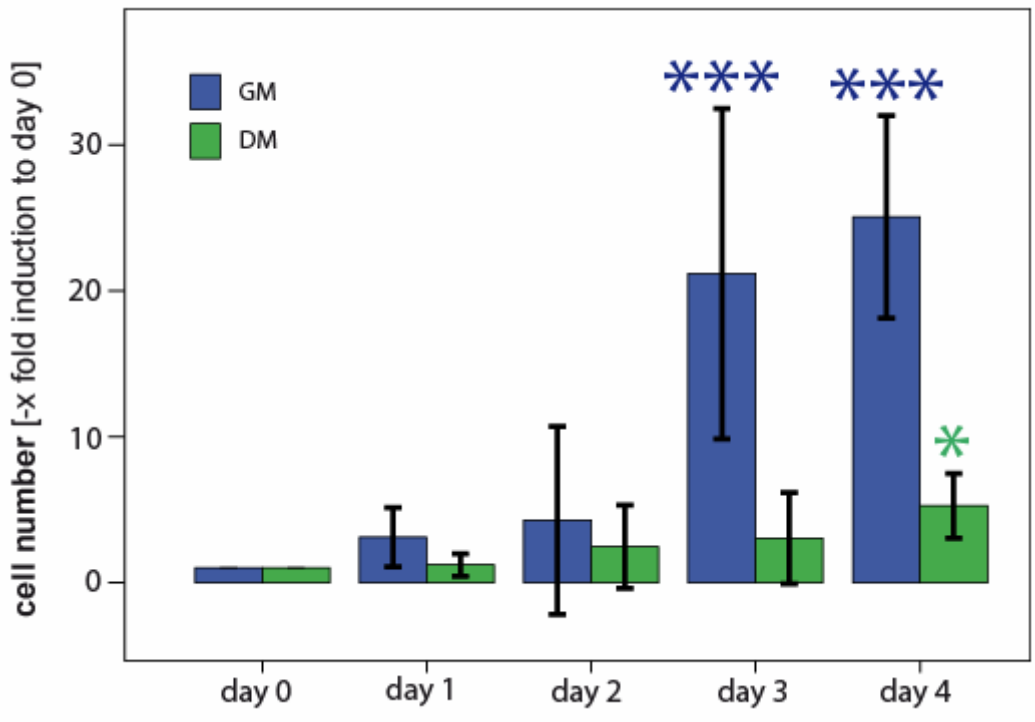

Figure 4-1: Cell number of C2C12 cells grown in GM and cells grown in DM

Statistical analysis of cell number revealed a significant time effect (p=0.000), time x group interaction (p=0.000) and group effect (p=0.000).

While the cells in GM proliferated, the differentiating cells nearly stopped growing and fused to form myotubes. The number of cells grown in GM increased significantly on day 3 and day 4 to the 21.2-fold (p<0.001) and the 25.1- fold (p<0.001) level, respectively, when compared to the number of cells at day 0. From day 0 to day 4 the number of cells grown in DM increased 5.3-fold (p<0.05) but to a lesser extent then cells grown in GM.

4.1.1 Myogenic marker gene expression

The expression of the myogenic marker genes MyoD and Myogenin was analyzed in order to determine the differentiation state of C2C12 cells. While MyoD should be expressed already in myoblasts, myogenin should be induced during differentiation of myoblasts to myotubes.

After cells were settled, GM was switched to DM. Incubation lasted for 4 days in differentiation media. For the myogenic markers MyoD and Myogenin measurements took place on day 0, before adding the DM (myoblasts), and after 4 days of differentiation (myotubes). For relative quantification the house keeping gene GAPDH was used and mRNA was analyzed via real-time PCR.

4.1.1.1 MyoD

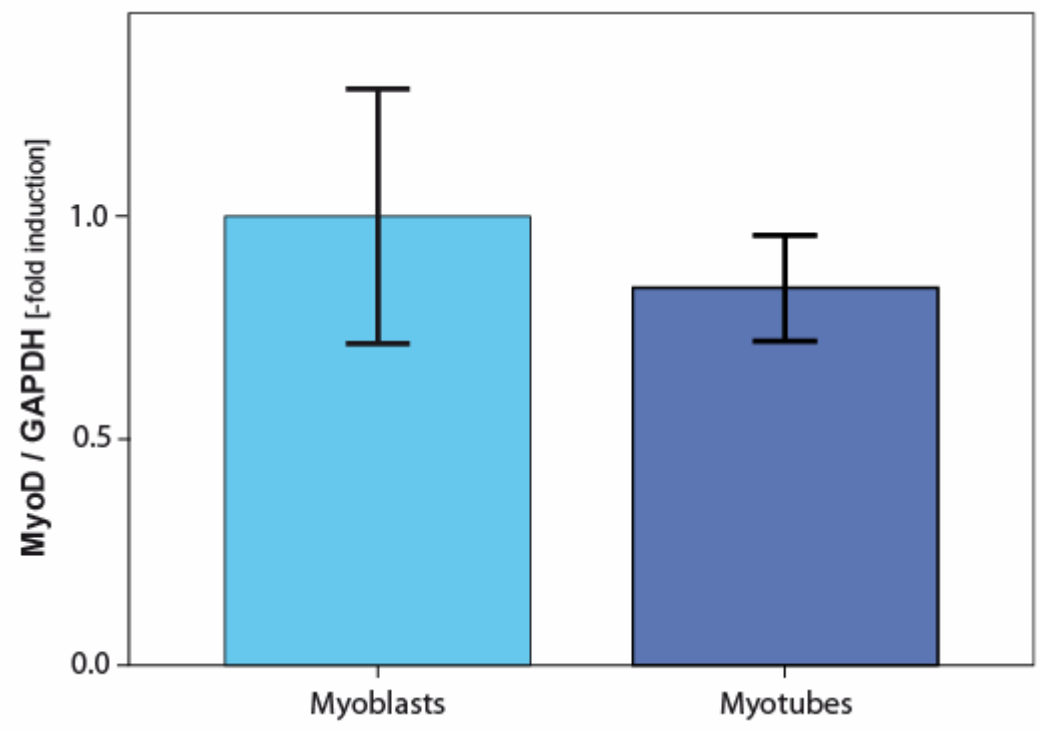

Figure 4-2: Expression of MyoD / GAPDH.

Data are shown as mean ± SD, n=3. Expression levels of MyoD did not change during differentiation (Fig. 4-2).

4.1.1.2 Myogenin

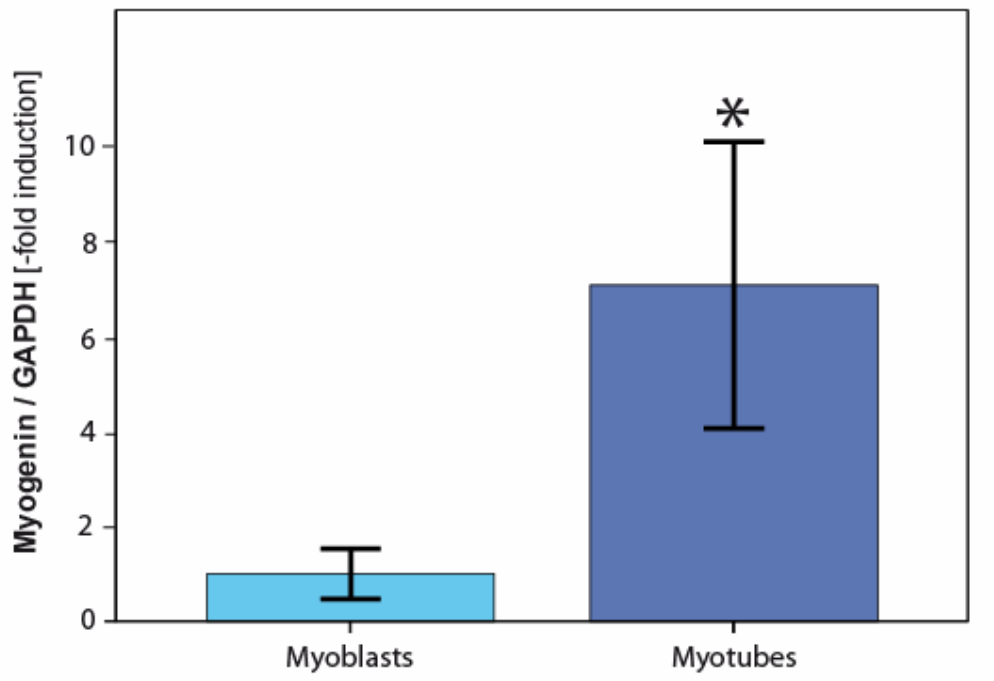

Figure 4-3: Expression of Myogenin / GAPDH.

Data are shown as mean ± SD (* $p<0.05$, n=3). Myogenin levels increased 7.1-fold during differentiation from myoblasts to myotubes (Fig. 4-3).

4.1.2 IGF-1 splicing variants

IGF-1Ea, MGF and IGF-1Eb comprise important growth factors for muscle cells and are therefore interesting parameters in the context of muscle atrophy.

As for the myogenic markers, IGF-1 splicing variant mRNA expression was measured on day 0, before adding the DM, and after 4 days of incubation. For relative quantification the house keeping gene GAPDH was used and mRNA was analyzed via real-time PCR.

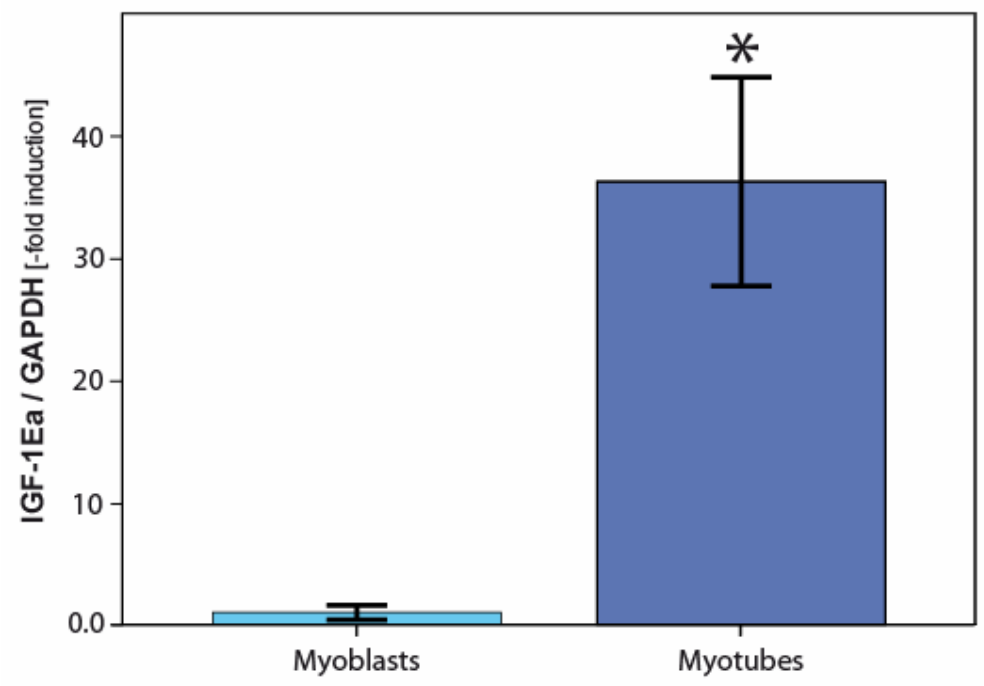

Figure 4-4: Expression of IGF-1Ea / GAPDH.

Data are shown as mean ± SD (* $p<0.05$, n=3) IGF-1Ea mRNA was up-regulated 36.1-fold during differentiation (Fig. 4-4).

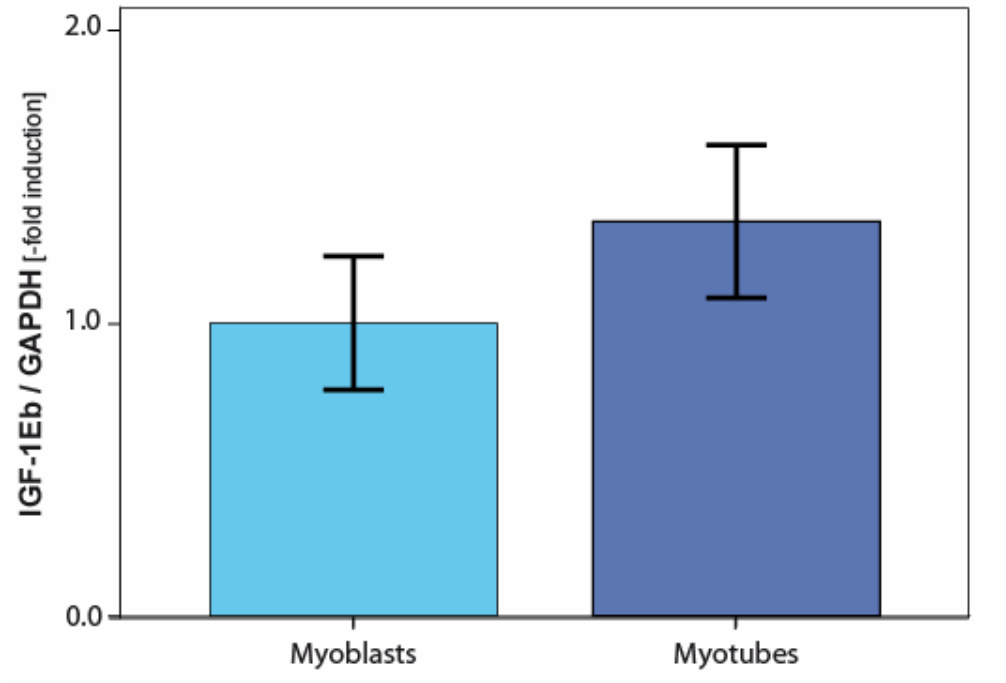

Figure 4-5: Expression of IGF-1Eb / GAPDH.

Data are shown as mean ± SD (n=3). In contrast to IGF-1Ea, IGF-1Eb expression did not significantly change during differentiation (Fig. 4-5).

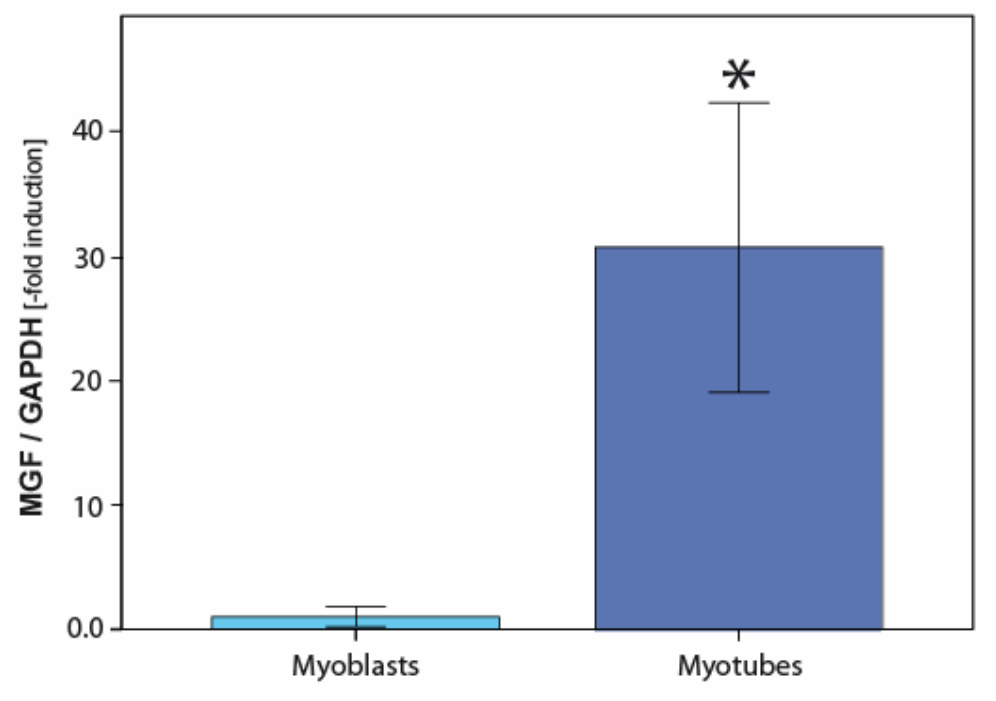

Figure 4-6: Expression of MGF / GAPDH.

Data are shown as mean ± SD (* $p<0.05$, $n=3$) MGF mRNA was increased 30.9-fold during differentiation (Fig. 4-6).

4.1.3 miRNA expression

In order to determine the influence of differentiation on muscle-specific miRNAs, their expression level were analyzed on day 0, before adding the differentiation media, and after 4 days of incubation. Additionally, an immuno-related miRNA (miRNA-155) was included as control. miRNAs were measured by absolute quantification using a reference panel with known equimolar concentrations of different miRNAs as a standard. miRNAs were analyzed via mi-RNA-specific real time PCR .

4.1.3.1 Muscle specific miRNAs

The expression levels of miRNA-1, -206, -133a, -133b and -499 were measured, as these miRNAs comprise important regulatory factors for muscle cell differentiation.

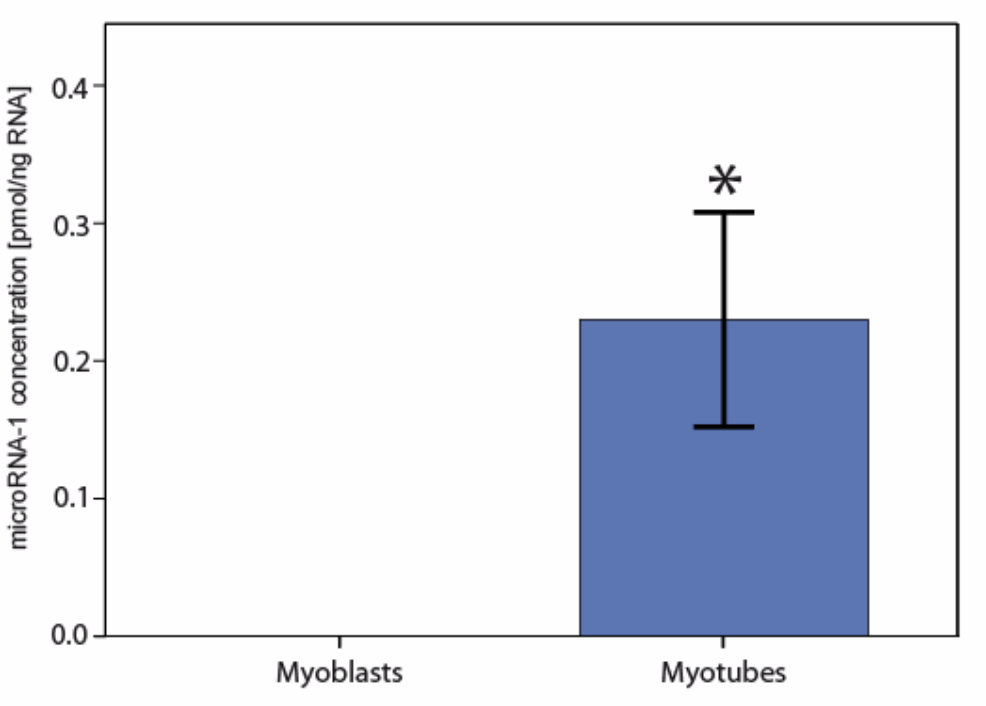

Figure 4-7: Expression of miRNA-1.

Fig. 4-7 shows the absolute amount of miRNA in the concentration of pmol / ng. Data are shown as mean ± SD (* $p<0.05$, $n=3$). The expression level of

miRNA-1 increased 464-fold in comparison to undifferentiated myoblasts. Interestingly, the initial values of miRNA-1 were very low.

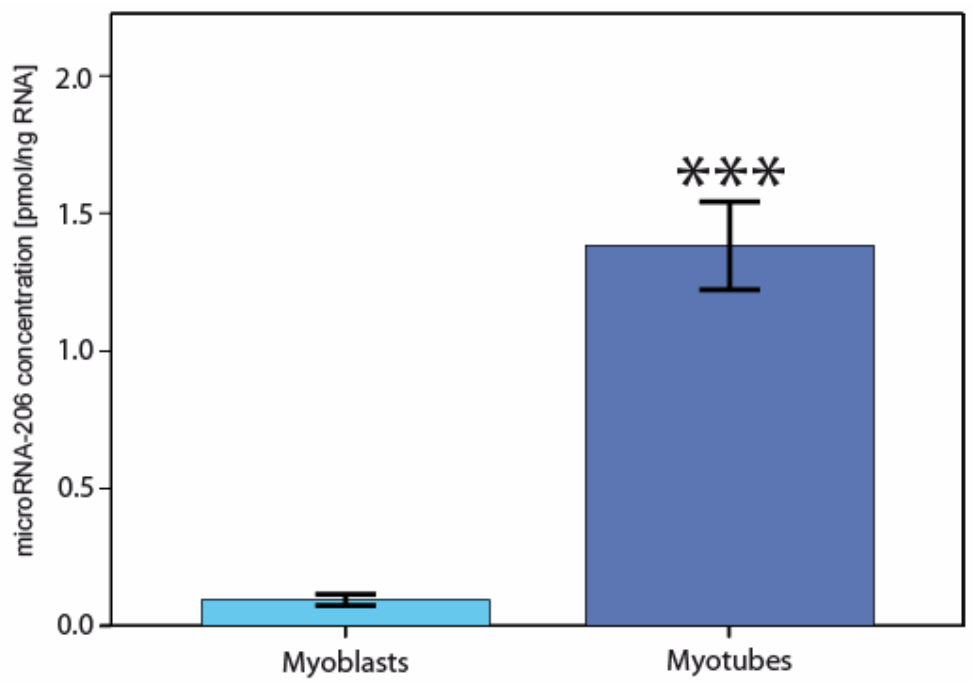

Figure 4-8: Expression of miRNA-206.

The absolute amount of miRNA-206 in the concentration of pmol / ng is shown in Fig. 4-8. Data are shown as mean ± SD (*** $p<0.001$, $n=3$). For miRNA-206 a significant increase after incubation with DM was detected. The expression level of miRNA-206 was enhanced to 14.3-fold in comparison to the initial level before differentiation.

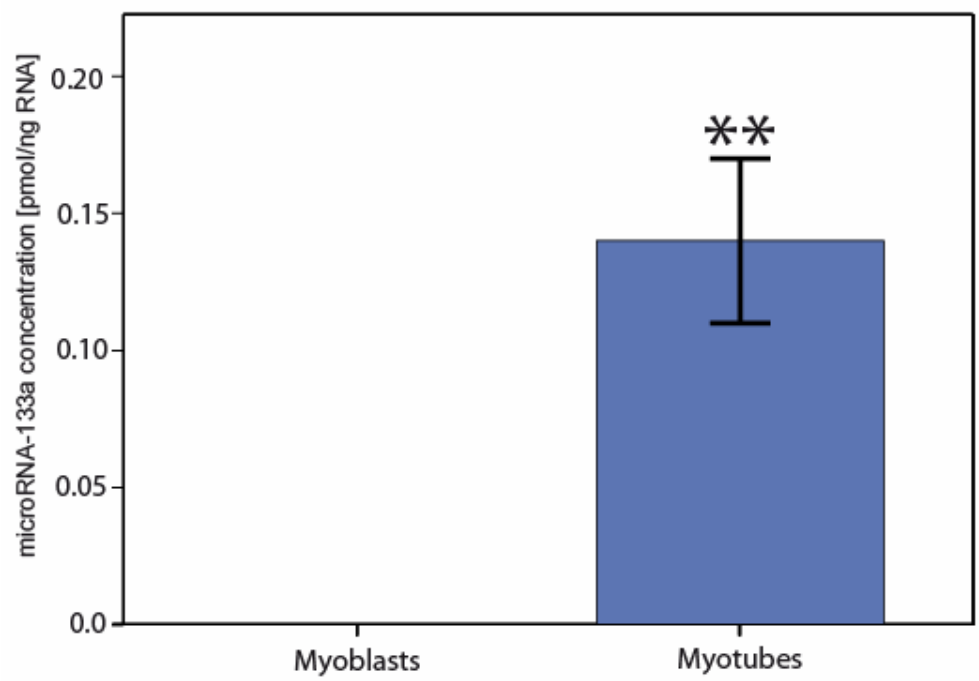

Figure 4-9: Expression of miRNA-133a.

Fig. 4-9 depicts the absolute amount of miRNA-133a in the concentration of pmol / ng. Data are shown as mean ± SD (** p<0.01, n=3). miRNA-133 increased 461-fold during differentiation.

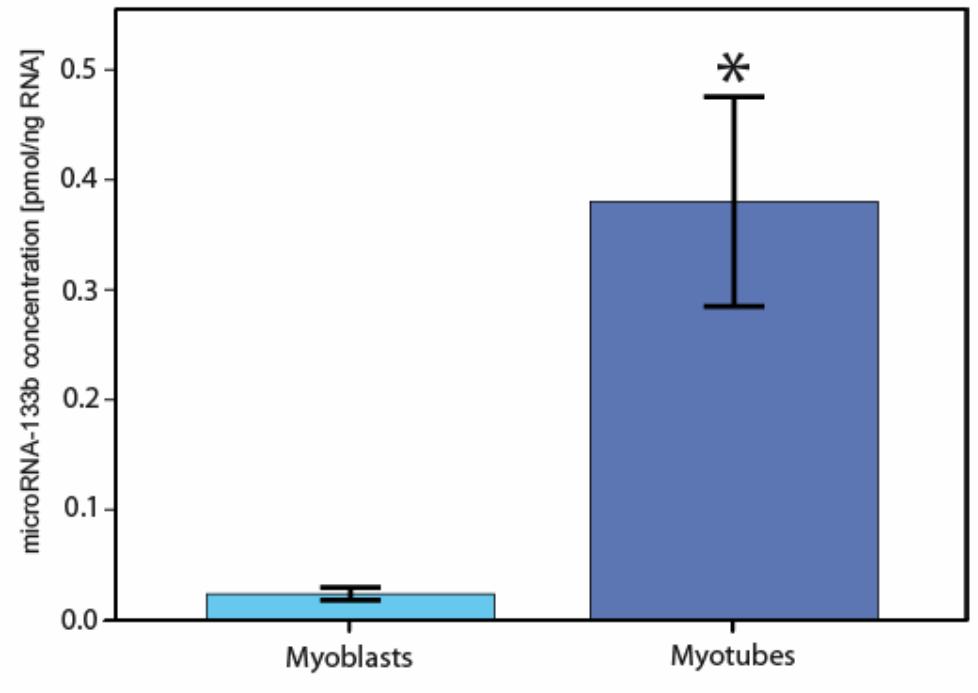

Figure 4-10: Expression of miRNA-133b.

Fig. 4-10 shows the absolute amount of miRNA-133b in the concentration of pmol / ng. Data are shown as mean ± SD (* p<0.5, n=3). We detected a 16.5-fold increase of miRNA-133b during differentiation.

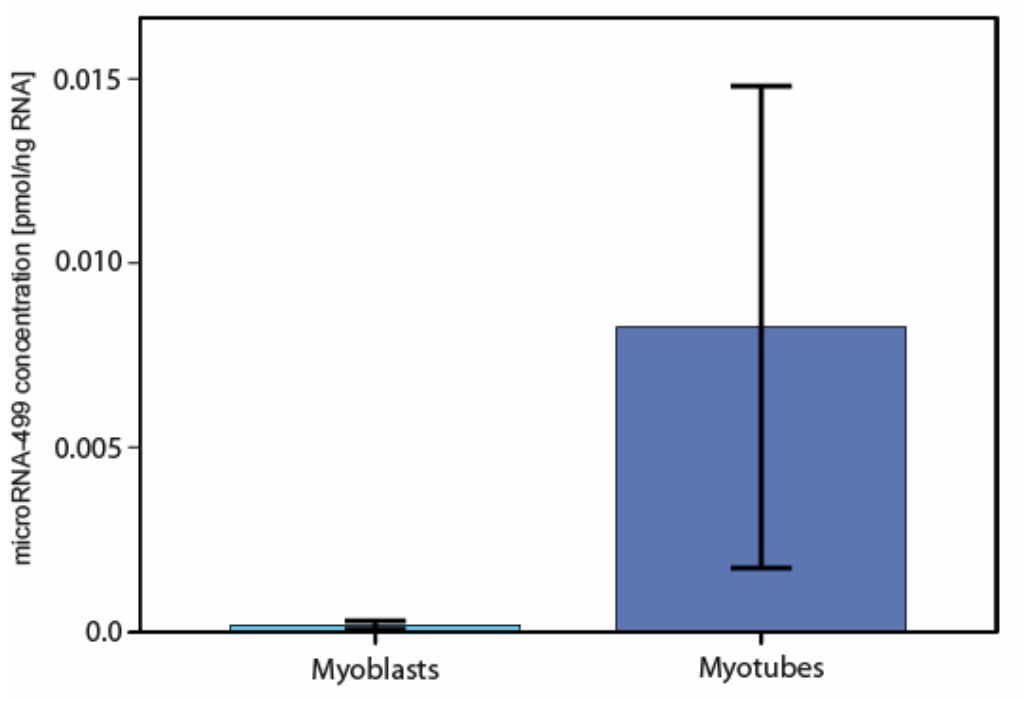

Figure 4-11: Expression of miRNA-499.

The absolute amount of miRNA-499 in the concentration of pmol / ng is shown in Fig. 4-11. Data are shown as mean ± SD (n=3). We detected a tendency for upregulation for miRNA-499 during differentiation, however, due to the high standard deviation and the small sample size, the change in expression level was not significant.

4.1.3.2 Immune-related miRNA

As it was proven that miRNA-155 is up-regulated in response to LPS (Tili et al., 2007) it may also be involved in inflammation-induced muscle changes which is the focus of the second set of our experiments. However, miRNA-155 should not change during differentiation.

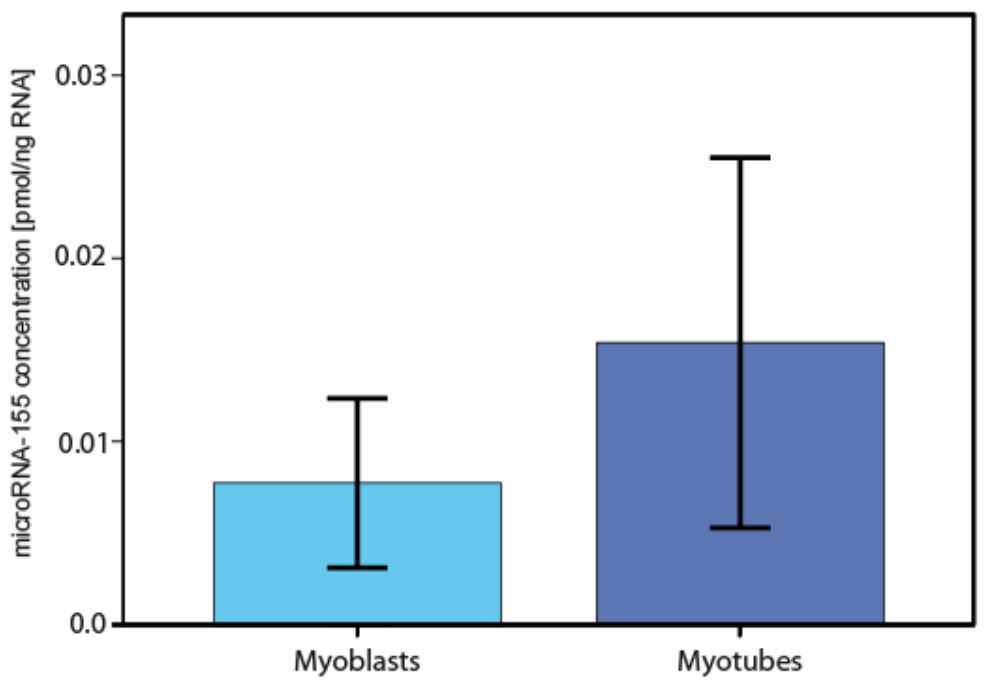

Figure 4-12: Expression of miRNA-155.

Fig. 4-12 shows the absolute amount of miRNA-155 in the concentration of pmol / ng. Data are shown as mean ± SD (n=3). As expected miRNA-155 levels did not change due to differentiation.

4.2 Myotube stimulation with inflammatory substances

Cells were seeded at a density of 0.05 x 10^5 cells / cm². They were allowed to settle for three days and then differentiated through serum deprivation. After four days in DM, the fully differentiated cells were stimulated either with Lipopolysaccharid (LPS), TNF-α or IL-6. PBS -/- was used as a vehicle as described in chapter 3.1.6.

Time kinetics were performed and analyzes took place 1h, 3h, 6h, 12h, 24h and 48h after stimulation. Measurements of all parameters were done via real time PCR and miRNA-specific PCR, respectively.

4.2.1 Myogenic marker gene expression

4.2.1.1 MyoD

Statistical analysis of MyoD mRNA levels revealed a significant time effect ($p=0.000$) but neither a group effect ($p=0.738$) nor a time x group interaction ($p=0.664$) (Fig. 4-13).

MyoD expression was down-regulated significantly after 1h to 70.2 ± 9.3% ($p<0.05$) for the control, to 69.0 ± 7.9% ($p<0.01$) for IL-6, and to 72.1 ± 6.2% ($p<0.01$) for TNF-α. LPS treatment also seems to down-regulate MyoD at this time-point (74.3 ± 12.1%), however the change in expression level was not significant ($p=0.199$). Thereafter, expression levels of MyoD returned to baseline levels in all experimental groups with the exception of treatment with TNF-α which resulted in an additional decrease after 12 hours of incubation. At this time point TNF-α leads to a drop of MyoD expression to 61.3 ± 6.2 % ($p<0.001$) staying at a low level until the end of the kinetic at 48h.

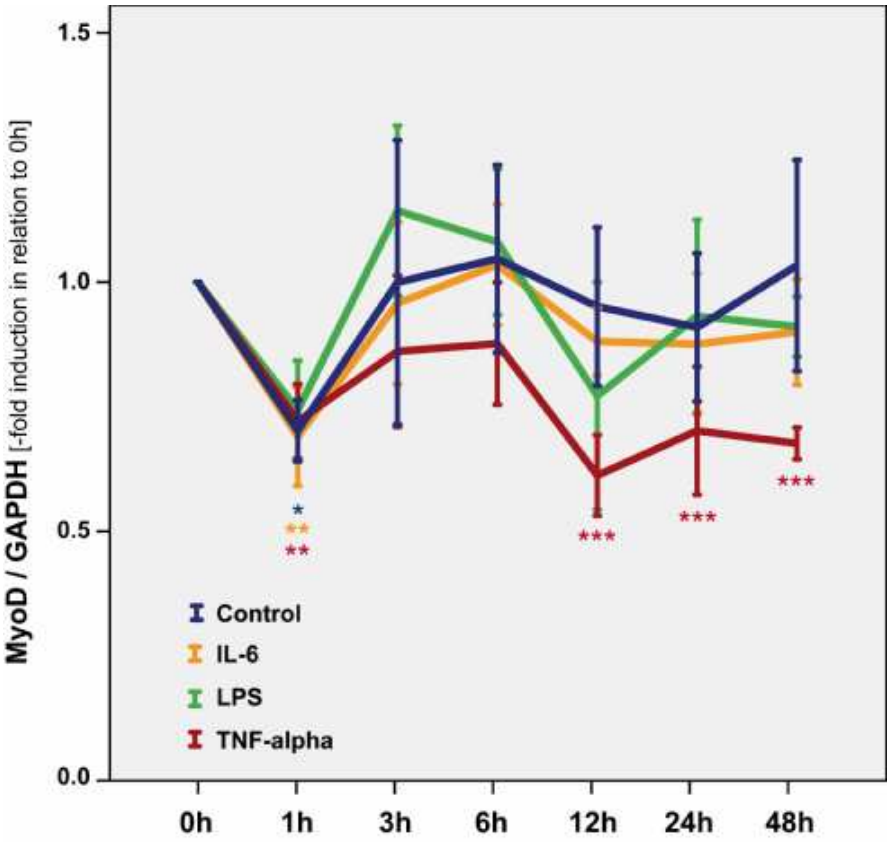

Figure 4-13: MyoD mRNA expression

Fig. 4-13 shows the MyoD mRNA expression after stimulation with vehicle (blue), 10ng/ml IL-6 (yellow), 1µg/ml LPS (green), and 10ng/ml TNF-α (red) for up to 48 hours. The ratios of MyoD/GAPDH normalized to 0h are shown as mean ± SD (* $p<0.05$, ** $p<0.01$ and *** $p<0.001$ vs. 0h, n=4).

4.2.1.2 Myogenin

Statistical analysis of myogenin mRNA levels revealed a significant time effect ($p=0.000$). The time x group interaction ($p=0.767$) and the group effect ($p=0.506$) were not significant (Fig. 4-14).

Time-kinetics of myogenin mRNA expression showed a general reduction of the expression levels of all experimental groups when compared to d4. The reduction in myogenin expression reached significance 6h after TNF-α stimulation, when it dropped to 65.4 ± 15.3% ($p<0.05$). The significantly low level was kept also after 12h, 24h and 48h when it decreased to 39.2 ± 15.3% ($p<0.01$), 46.0 ± 15.3% ($p<0.01$) and 43.6 ± 15.3% ($p<0.01$), respectively.

Interestingly, also the control decreased to 57.3 ± 11.7% ($p<0.01$) after 12h and to 54.3 ± 11.7% ($p<0.01$) after 24h. However, 48h after the start of the stimulation experiment myogenin levels of the control cells tend to normalize.

Myogenin level did not decrease significantly due to IL-6 or LPS treatment.

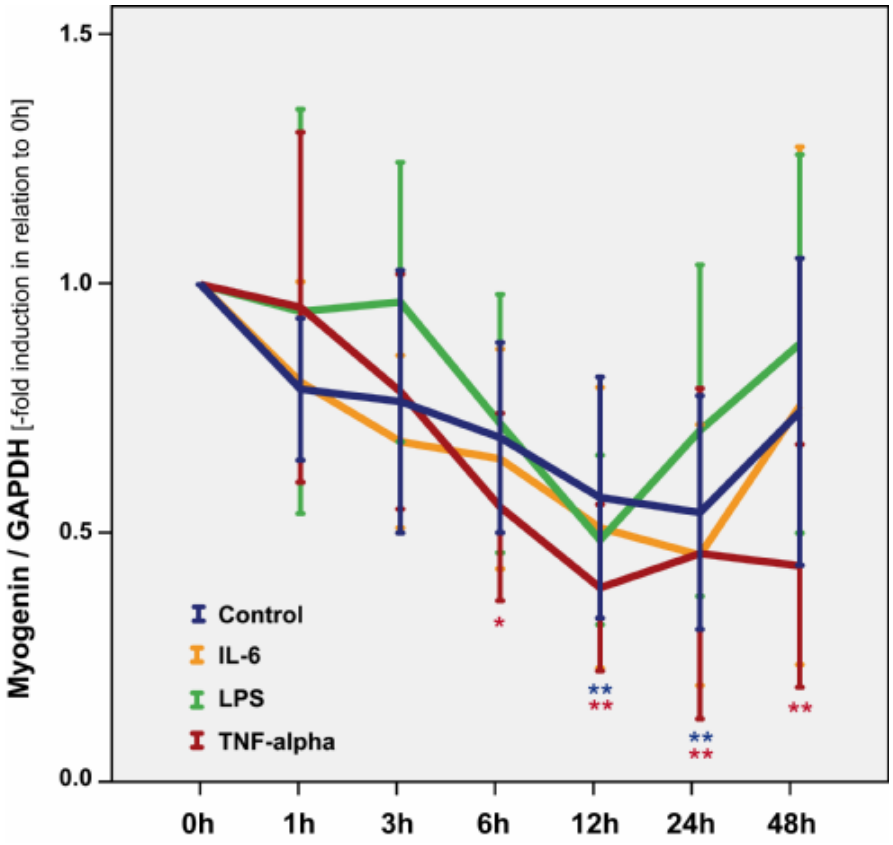

Figure 4-14: Myogenin mRNA expression

Fig. 4-14 shows the myogenin mRNA expression after stimulation with vehicle (blue), 10ng/ml IL-6 (yellow), 1µg/ml LPS (green), and 10ng/ml TNF-α for up to 48 hours. The ratios of myogenin/GAPDH normalized to 0h are shown as mean ± SD (* $p<0.05$ and ** $p<0.01$ vs. 0h, n=4).

4.2.2 IGF-1 splicing variants

Statistical analysis if **IGF-1Ea mRNA** levels revealed a significant time effect (p=0.000) and time x group interaction (p=0.000), whereas the group effect was not significant (p=0.236) (Fig. 4-15).

The reduction of IGF-1Ea mRNA, compared to the control at 0h, could already be observed 6h after TNF-α stimulation, when it dropped to 67.1 ± 11.3% (p<0.01). After 12h of TNF-α stimulation the IGF-1Ea expression level decreased to 34.3 ± 11.3 % (p<0.001). The expression level remained low at 41.0 ± 11.3% (p<0.001) after 24h and at 65.6 ± 11.3% (p<0.01) after 48h of TNF-α stimulation.

An increase of mRNA expression could be detected for the control as well as after stimulation with LPS or IL-6, starting 12h after incubation and reaching a significant maximum of 65.0% ±17.0% (p<0.01) after 48h for LPS-incubated cells as well as of 72.0 ± 13.9% (p<0.001) for the control.

IL-6 stimulation did not affect IGF-1Ea expression level.

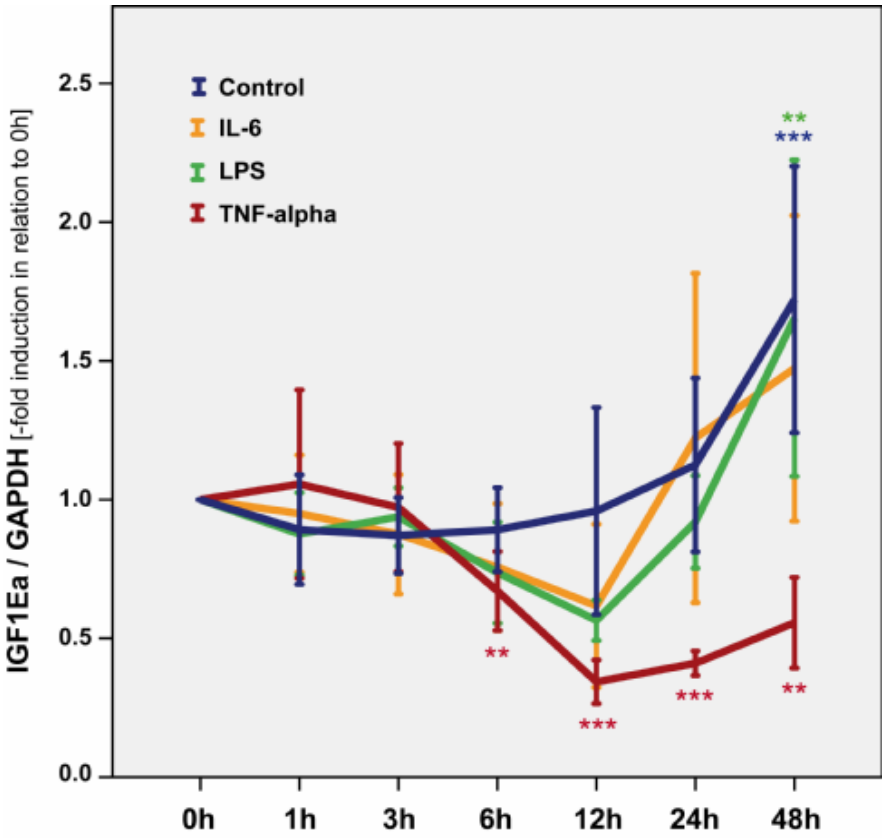

Figure 4-15: IGF-1Ea mRNA expression

Fig. 4-15 shows the IGF-1Ea mRNA expression after stimulation with vehicle (blue), 10ng/ml IL-6 (yellow), 1µg/ml LPS (green), and 10ng/ml TNF-α for up to 48 hours. The ratios of IGF1Ea/GAPDH normalized to 0h are shown as mean ± SD (** p<0.01 and *** p<0.001 vs. 0h, n=4).

Statistical analysis of **IGF-1Eb mRNA** levels revealed a significant time effect (p=0.000) but not a significant time x group interaction (p=0.809) and group effect (p=0.236), respectively.

Fig. 4-16 shows the reduction of IGF-1Eb compared to the control at the time point 0h. We could observe a significant down-regulation of IGF-1Eb expression to 69.9 ± 10.1% (p<0.05), to 65.4 ± 10.1% (p<0.05) after 6h, to 61.0 ± 10.1% (p<0.01) after 12h, and to 62.4 ± 10.1% (p<0.01) after 24h of IL-6 stimulation.

Neither LPS nor TNF-α incubation had a detectable effect on the IGF-1Eb expression level.

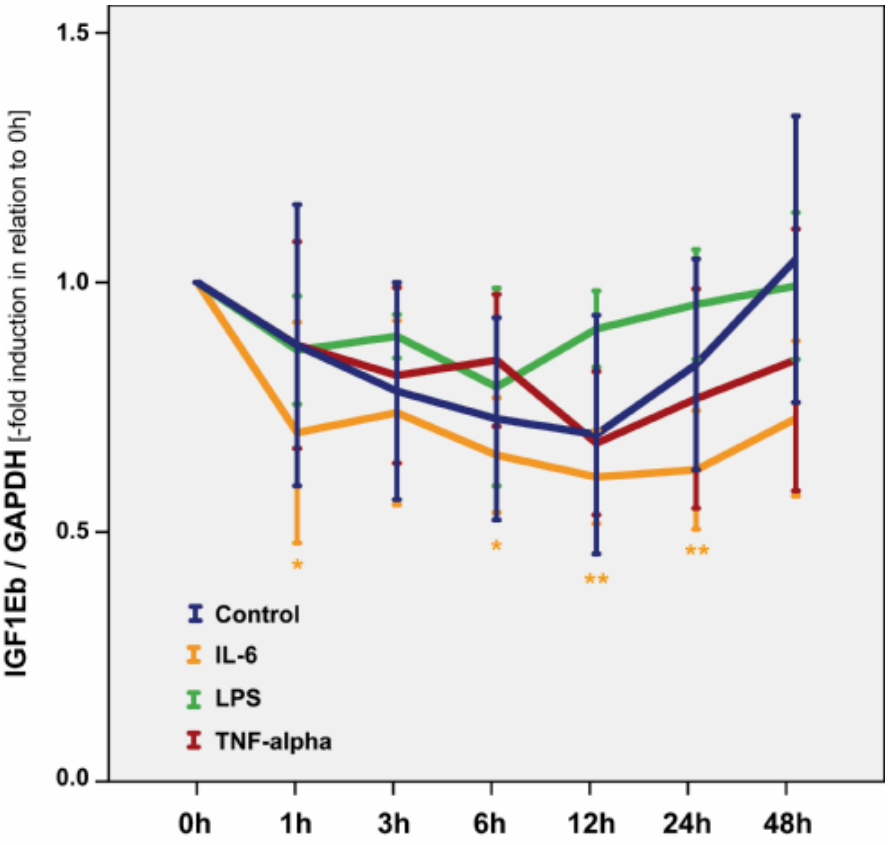

Figure 4-16: IGF-1Eb mRNA expression

Fig. 4-16 shows the IGF-1Eb expression after stimulation with vehicle (blue), 10ng/ml IL-6 (yellow), 1µg/ml LPS (green), and 10ng/ml TNF-α for up to 48 hours. The ratios of MyoD/GAPDH normalized to 0h are shown as mean ± SD (* $p<0.05$ and ** $p<0.01$ vs. 0h, n=4).

Statistical analysis of **MGF mRNA** levels revealed a significant time effect ($p=0.000$). The time x group interaction ($p=0.662$) and the group effect ($p=0.397$) were not significant.

Compared to the control at the time point 0h, MGF mRNA was down-regulated significantly already 6h after TNF-α treatment to 61.7 ± 11.4% ($p<0.05$) reaching a minimum of 32.3 ± 11.4 % ($p<0.001$) 12h after stimulation. The expression level of MGF stayed low at 51.2 ± 11.4% ($p<0.01$) also for the time point 24h and at 63.0 ± 11.4% ($p<0.05$) for the time point 48h.

LPS stimulation caused a significant decrease of MGF levels to 58.4 ± 12.5% ($p<0.05$) after 12h. However, 48 hours of LPS incubation caused a significant increase of 45.0 ± 12.5% ($p<0.01$) of MGF expression, correlating with a general increase of 59.2 ± 14.1% ($p<0.001$) also for the control. No detectable effect of IL-6 stimulation on MGF expression level could be observed.

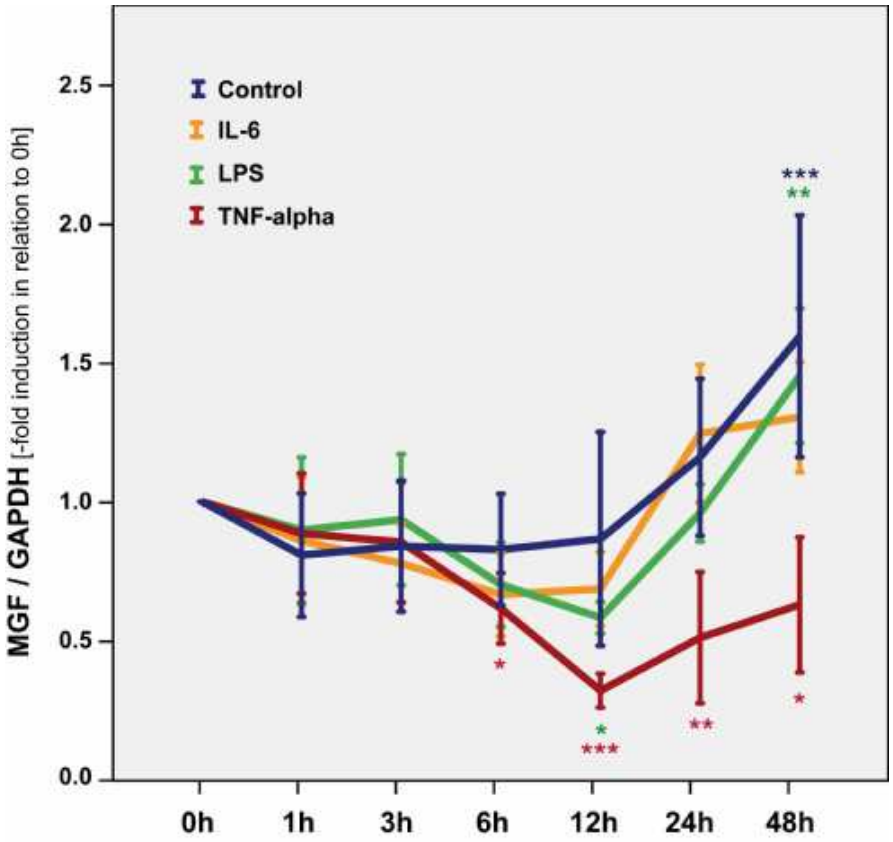

Figure 4-17: MGF mRNA expression

Fig. 4-17 shows the MGF mRNA expression after stimulation with vehicle (blue), 10ng/ml IL-6 (yellow), 1µg/ml LPS (green), and 10ng/ml TNF-α for up to 48 hours. The ratios of MGF/GAPDH normalized to 0h are shown as mean ± SD (* $p<0.05$, ** $p<0.01$ and *** $p<0.001$ vs. 0h, n=4).

4.2.1 miRNA expression

For miRNA analyzes the differentiated cells were stimulated with either 10 ng / ml of TNF-α or with 1 µg / ml of LPS. PBS $^{-/-}$ was used as a vehicle. IL-6 stimulation was omitted as we did not detect any changes in myogenic markers or the IGF-1 system due to stimulation with IL-6.

Under the influence of the inflammatory stimuli, the miRNA expression level of the muscle specific miRNAs -1, -206, -133a, -133b and 499 and of the immuno-specific miRNA-155 was measured via miRNA-specific PCR as described in chapter 3.2.3. MiRNAs were measured over absolute quantification, using a reference panel with known equimolar concentrations of different miRNAs as a standard.

4.2.1.1 Muscle-specific miRNAs

None of the here examined muscle-specific miRNAs showed a significant change of the expression level after stimulation with either LPS or TNF-α (see Figures 4-18, 4-19, 4-20, 4-21, and 4-22).

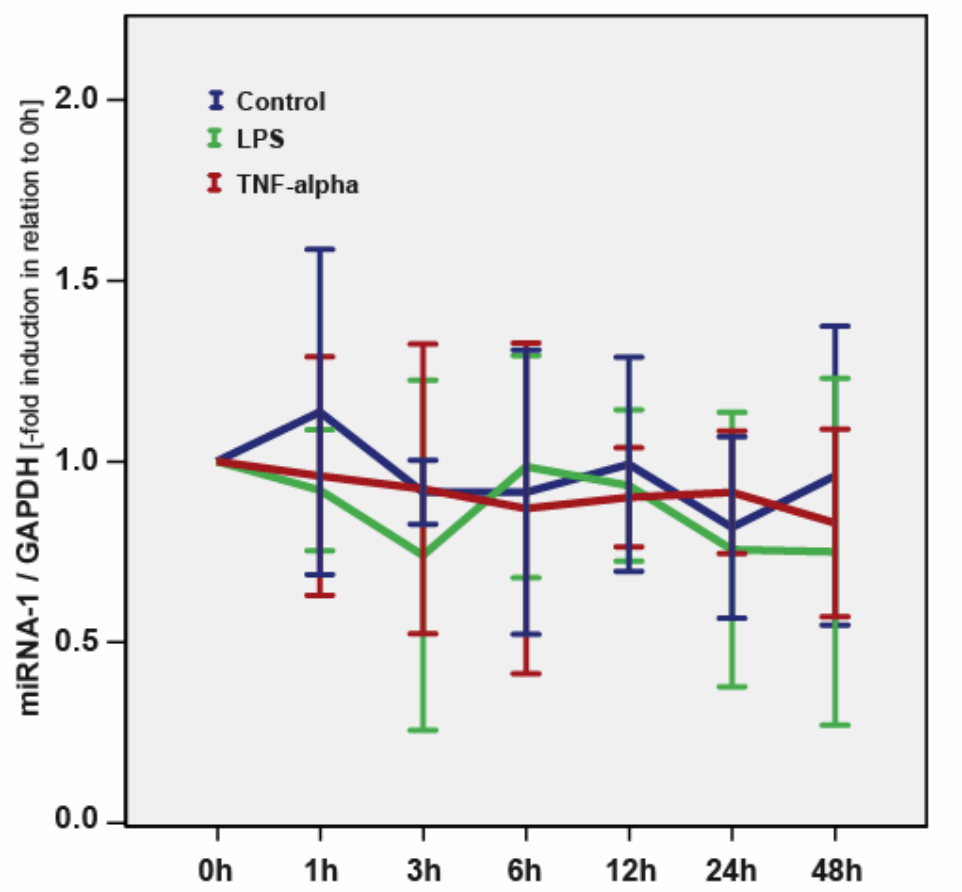

Figure 4-18: miRNA-1 expression

Fig. 4-18 shows miRNA-1 expression after stimulation with vehicle (blue), 1µg/ml LPS (green), and 10ng/ml TNF-α (yellow) for up to 48 hours. The amount of miRNA-1 was measured as absolute quantification with reference panel as a standard and is shown here as the x-fold change in relation to 0h. Data are expressed as mean ± SD, n=4.

Statistical analysis of miRNA-1 levels did not reveal any significant time effect (p=0.559), group effect (p=0.878) or time x group interaction (p=0.989).

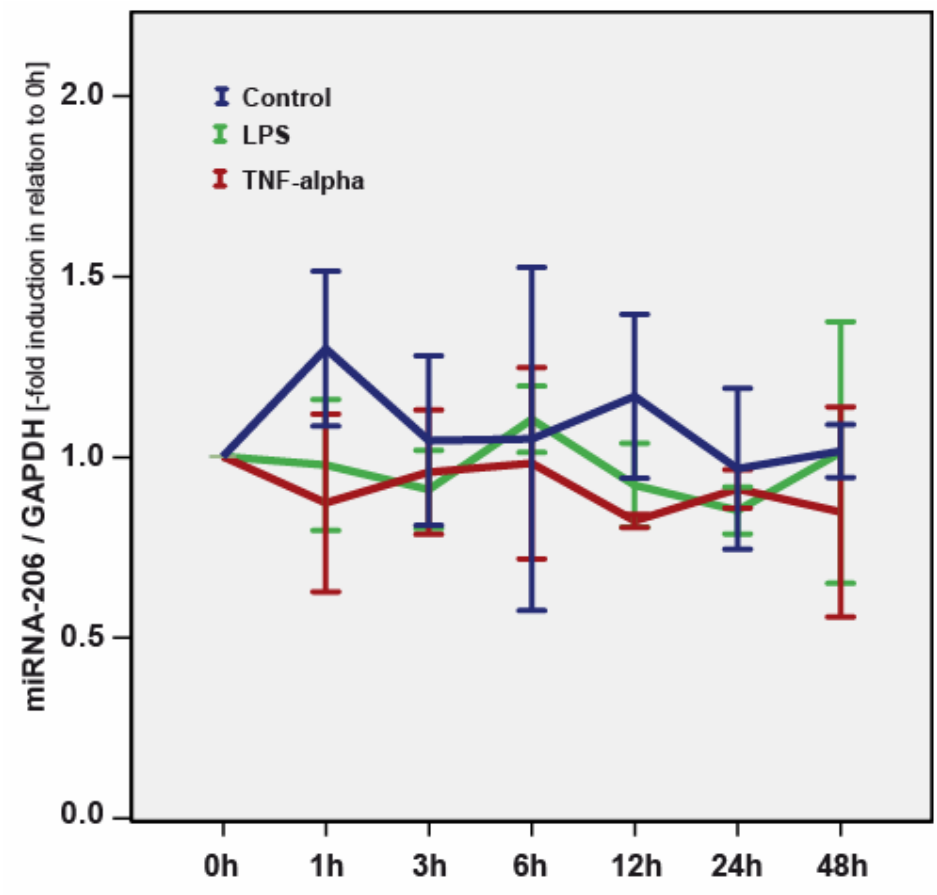

Figure 4-19: miRNA-206 expression

Figure 4-19 shows miRNA-206 expression after stimulation with vehicle (blue), 1µg/ml LPS (green), and 10ng/ml TNF-α (yellow) for up to 48 hours. The amount of miRNA-1 was measured as absolute quantification with reference panel as a standard and is shown here as the x-fold change in relation to 0h. Data are shown as mean ± SD, n=4.

Statistical analysis of miRNA-206 levels did not show any significant time effect (p=0.714), group effect (p=0.235) or time x group interaction (p=0.705).

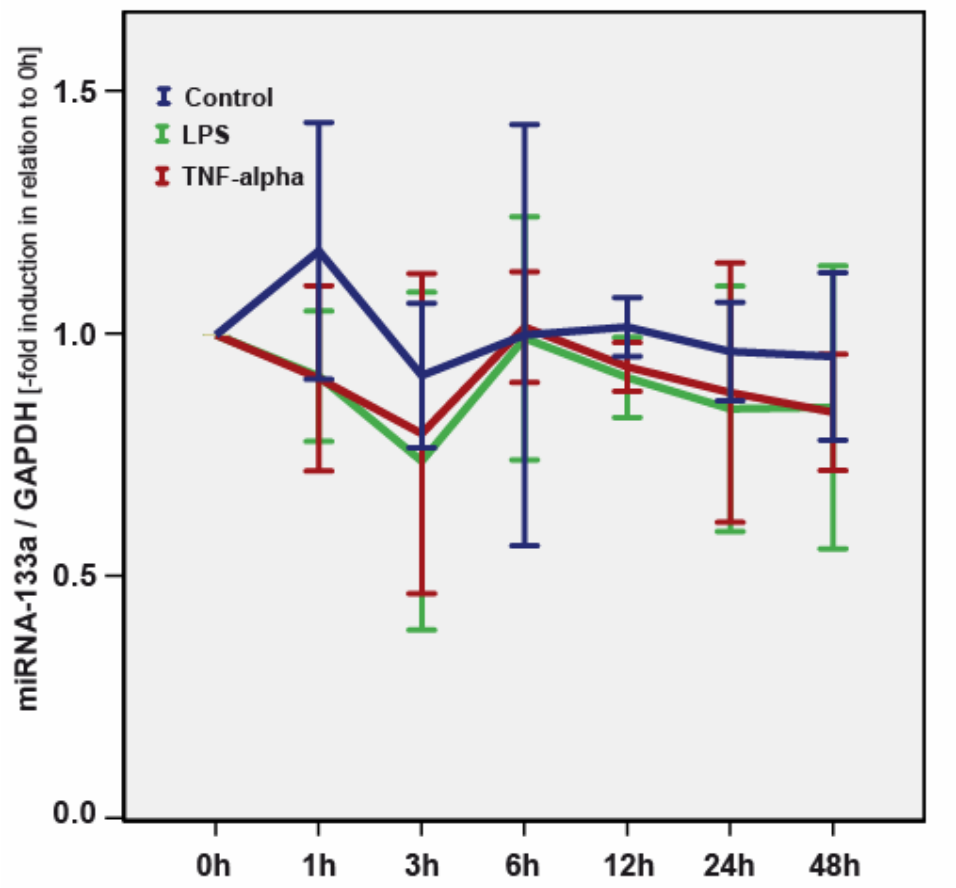

Figure 4-20: miRNA-133a expression

Fig. 4-20 shows the miRNA-133a expression after stimulation with vehicle (blue), 1µg/ml LPS (green), and 10ng/ml TNF-α (yellow) for up to 48 hours. The amount of miRNA-1 was measured as absolute quantification with reference panel as a standard and is shown here as the x-fold change in relation to 0h. Data are shown as mean ± SD, n=4.

Statistical analysis of miRNA-133a levels did not reveal any significant time effect (p=0.093), group effect (p=0.665) or time x group interaction (p=0.994).

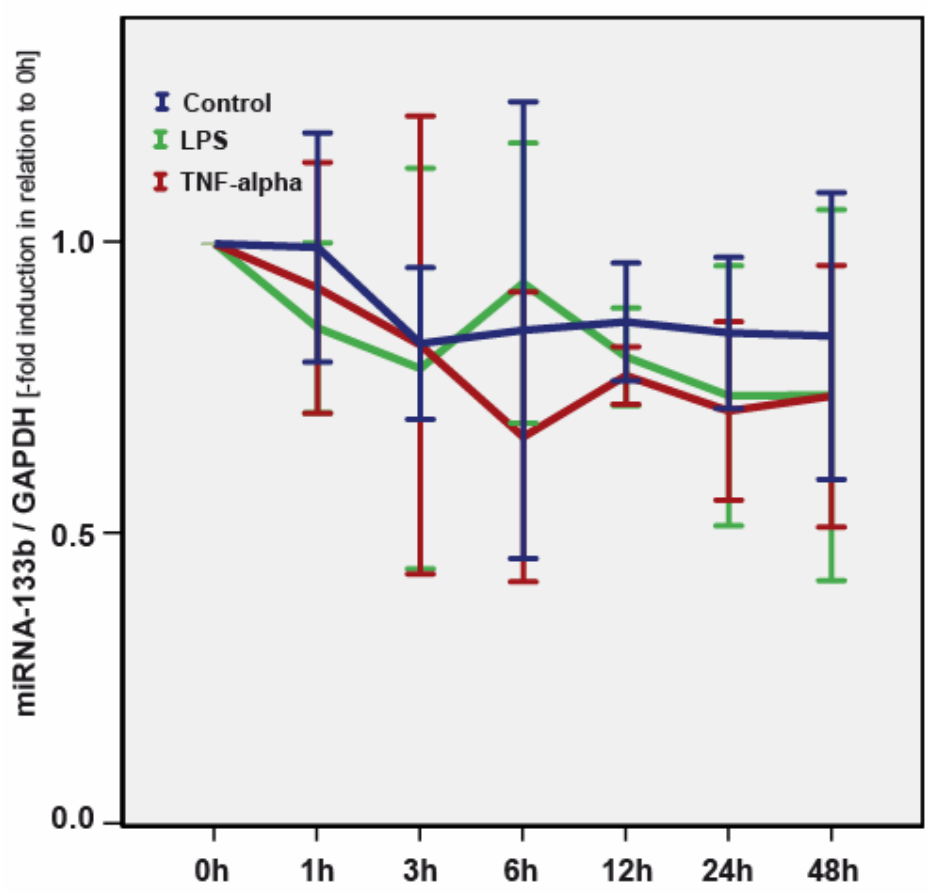

Figure 4-21: miRNA-133b expression

Fig. 4-21 shows miRNA-133b expression after stimulation with vehicle (blue), 1µg/ml LPS (green), and 10ng/ml TNF-α (yellow) for up to 48 hours. The amount of miRNA-1 was measured as absolute quantification with reference panel as a standard and is shown here as the x-fold change in relation to 0h. Data are shown as mean ± SD, n=4.

Statistical analysis of miRNA-133b levels revealed a significant time effect ($p = 0.047$) whereas the time x group interaction ($p=0.956$) and the group effect ($p=0.665$) were not significant.

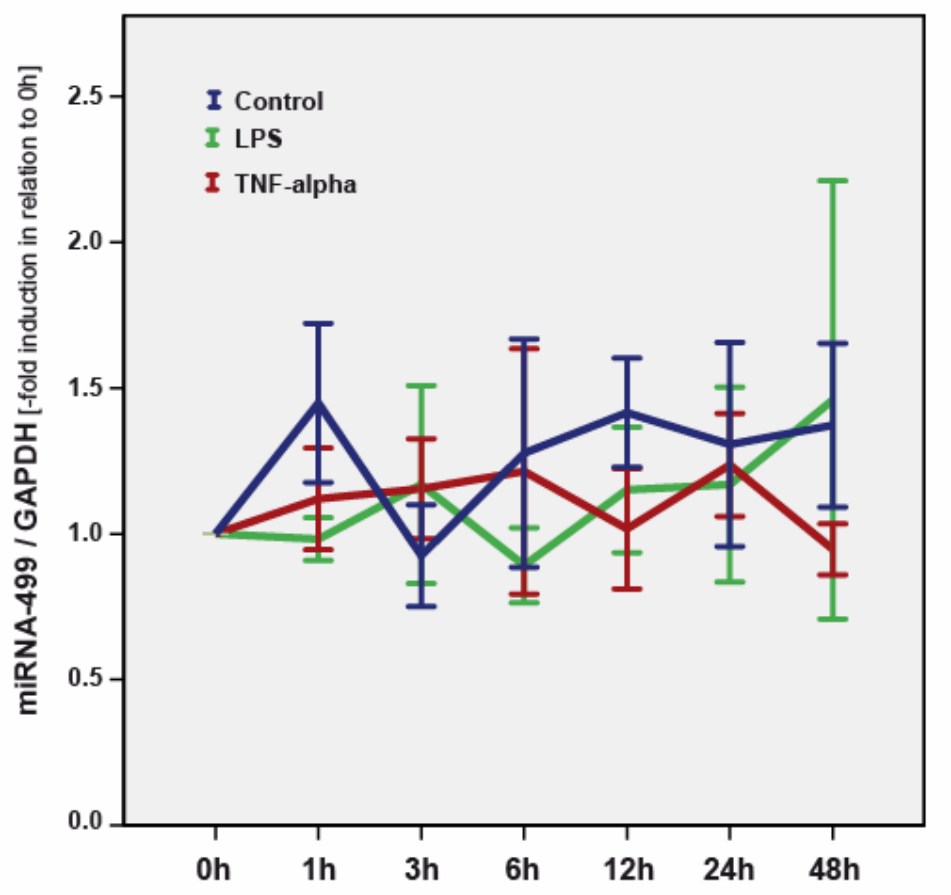

Figure 4-22: miRNA-499 expression

Fig. 4-22 shows miRNA-499 expression after stimulation with vehicle (blue), 1µg/ml LPS (green), and 10ng/ml TNF-α (yellow) for up to 48 hours. The amount of miRNA-1 was measured as absolute quantification with reference panel as a standard and is shown here as the x-fold change in relation to 0h. Data are shown as mean ± SD, n=4.

Statistical analysis of miRNA-499 levels did not reveal any significant time effect (p=0.465), time x group interaction (p=0.298) and group effect (p=0.280).

4.2.1.2 Immune-related miRNAs

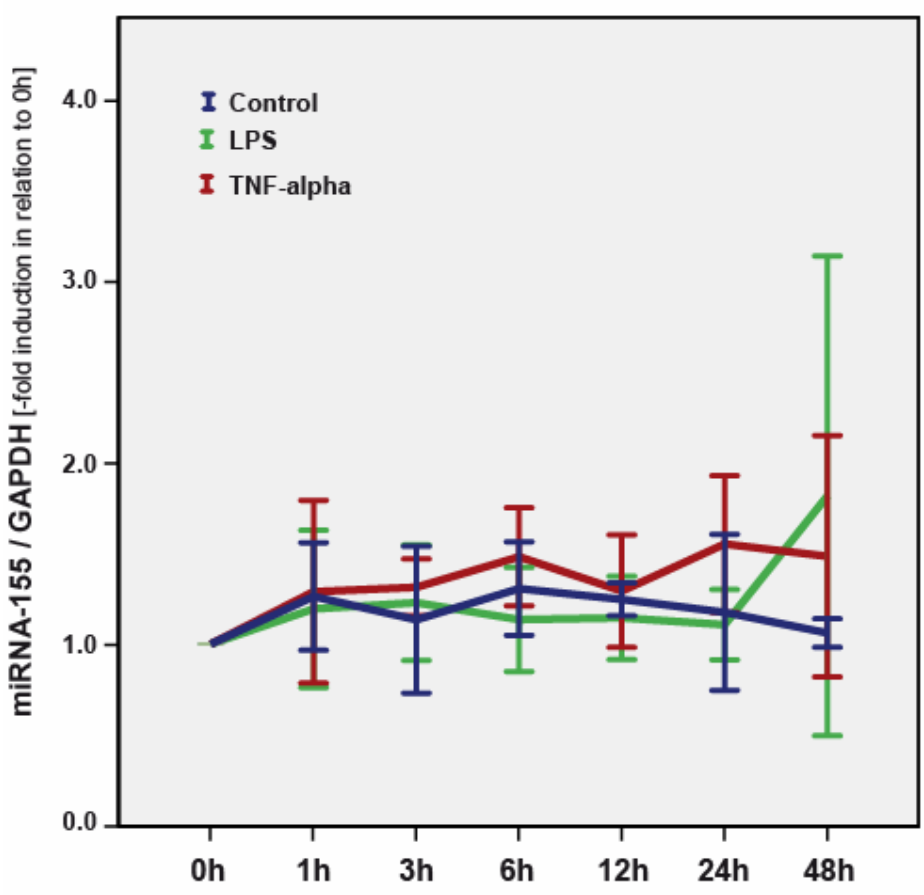

Figure 4-23: miRNA-155 expression

Fig. 4-23 shows miRNA-155 expression after stimulation with vehicle (blue), 1µg/ml LPS (green), and 10ng/ml TNF-α (yellow) for up to 48 hours. The amount of miRNA-1 was measured as absolute quantification with reference panel as a standard and is shown here as the x-fold expression in relation to 0h. Data are shown as mean ± SD, n=4.

Statistical analysis of miRNA-155 levels revealed no significant time effect (p=0.327), time x group interaction (p=0.738) and group effect (p=0.700).

4.3 IGF-1, IL-6, and TNF-α concentration in cell culture supernatants

ELISAS were used to determine the content of total IGF1 protein before and during stimulation as an additional indicator for possible translational inhibition and a comparison to IGF-1 mRNA levels. TNF- α and IL-6 protein was analyzed to test the stability of the used stimuli as well as for a suggested induced expression of these cytokines after stimulation with inflammatory stimuli.

4.3.1 Determination of IGF-1

The concentration of the IGF-1 protein in the cell culture supernatants was analyzed after 0h, 1h, 3h, 6h, 12h, 24h and 48h of incubation with LPS, TNF-α and IL-6, respectively via ELISA.

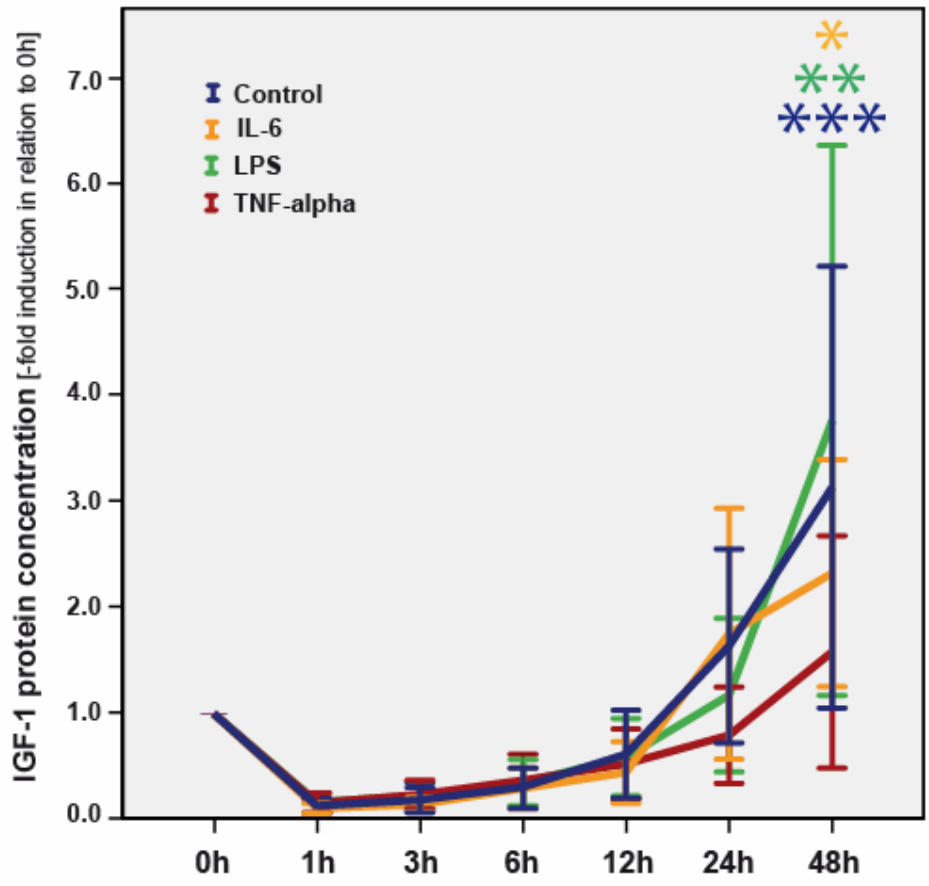

Figure 4-24: IGF-1 protein concentration

Fig. 4-24 shows IGF-1 protein concentration after stimulation with vehicle (blue), 1µg/ml LPS (green), 10ng/ml TNF-α (yellow) and 10ng / ml IL-6 (pink) for up to 48 hours. IGF concentrations in supernatants are shown as the x-fold change in relation to 0h. Data are shown as mean ± SD (* $p<0.05$, ** $p<0.01$ and *** $p<0.001$, vs. 0h, n=3).

Statistical analysis of IGF-1 ELISA revealed a significant time effect (p=0.000) and group effect (p=0.000), whereas the time x group interaction was not significant (p=0.212).

Compared to the IGF-1 concentration at 0h the level increased significantly 2.2-fold after 48h in the control (p<001), 2.8-fold after LPS incubation ($p<0.01$) and 1.4-fold after IL-6 incubation ($p<0.05$). No significant change of IGF-1 concentration after TNF-α stimulation could be detected.

4.3.1 Determination of TNF-a

The concentration of the TNF-α protein in the cell culture supernatants was analyzed after 0h, 1h, 3h, 6h, 12h, 24h and 48h of incubation with LPS, TNF-α and IL-6, respectively via ELISA.

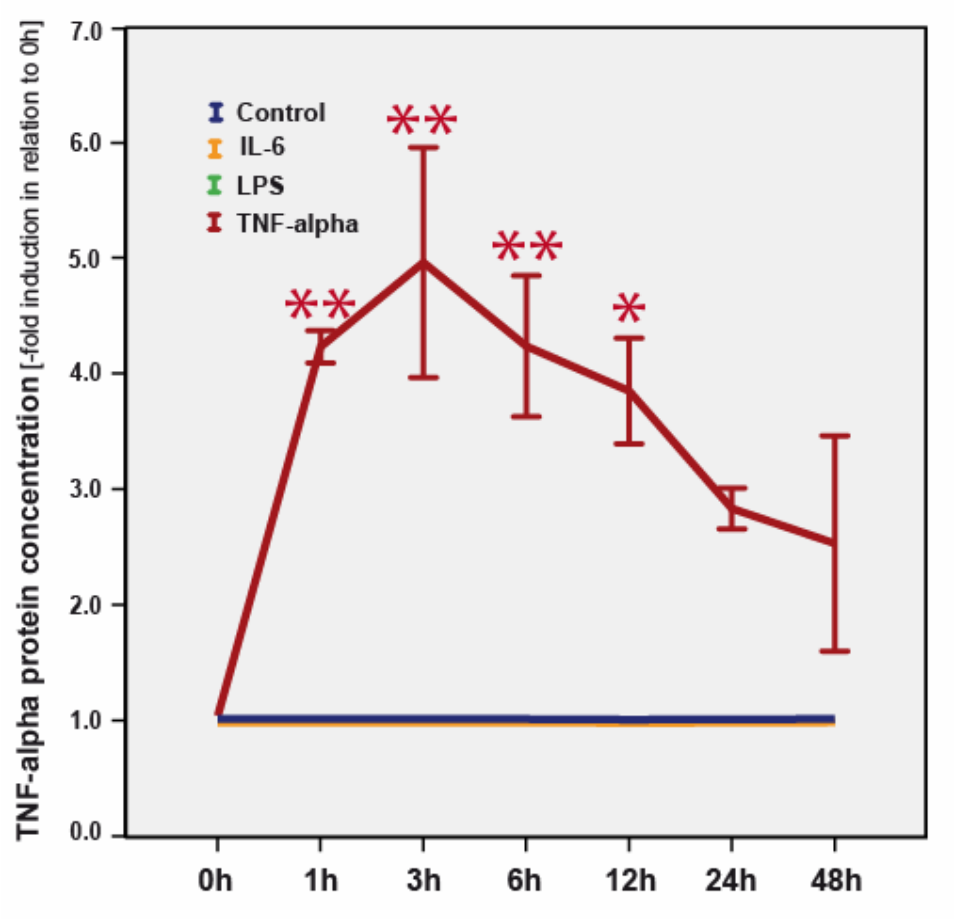

Figure 4-25: TNF-α protein concentration

Fig. 4-25 show TNF-α protein concentration in the supernatants after stimulation with vehicle (blue), 1µg/ml LPS (green), 10ng/ml TNF-α (yellow) and 10ng / ml IL-6 (pink) for up to 48 hours. IGF concentrations in supernatants are shown as the x-fold change in relation to 0h. Data are shown as mean ± SD (* $p<0.05$ and ** $p<0.01$, vs. 0h, n=3).

As expected TNF-α concentration in the supernatant increased after its addition 25-fold after 1h ($p<0.01$), 31-fold after 3h ($p<0.01$), 25-fold after 6h ($p<0.01$), and 22-fold after 12h ($p<0.05$), respectively. After 24h and 48h TNF-α levels tended to normalize.

TNF-α concentration was sparely detectable in control cells as well as after LPS and IL-6 stimulation.

4.3.2 Determination of IL-6

The concentration of the IL-6 protein in the cell culture supernatants was analyzed after 0h, 12h, 24h and 48h of incubation with LPS, TNF-α and IL-6, respectively via ELISA.

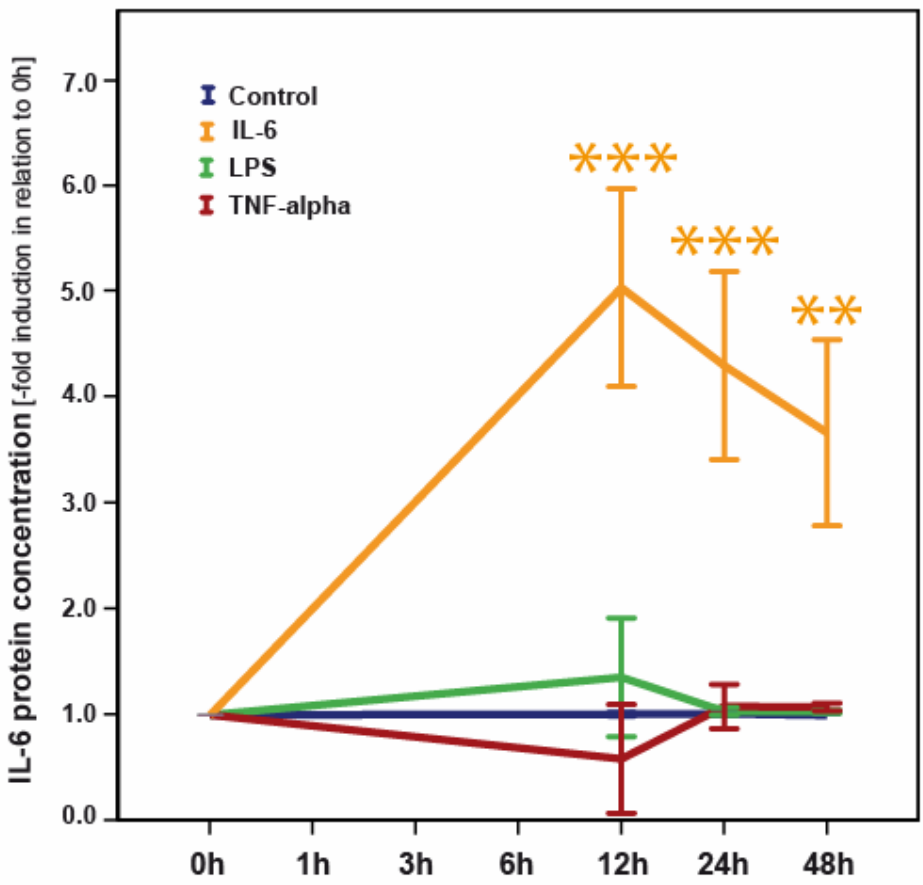

Figure 4-26: IL-6 protein concentration

Fig. 4-26 shows IL-6 protein concentration in the supernatants after stimulation with vehicle (blue), 1µg/ml LPS (green), 10ng/ml TNF-α (yellow) and 10ng / ml IL-6 (pink) for up to 48 hours. IGF concentrations in supernatants are shown as the x-fold change in relation to 0h. Data are shown as mean ± SD (** $p<0.01$ and *** $p<0.001$ vs. 0h, n=4).

After adding IL-6, the concentration is high after 12h, 24h and 48h of incubation, showing a slight but not significant tendency to drop.

IL-6 concentration was not changed in the control group as well as after LPS and TNF-α incubation.

5 DISCUSSION

5.1 Gene expression during differentiation

During the development of myotubes out of myoblasts, the expression levels of the myogenic marker genes MyoD and Myogenin are indicators for the quality of the cell culture model, as it determines the grade of the myoblast differentiation.

In our trials, the observation of the myogenic marker gene expression levels showed the expected results. Due to the developmental state of the undifferentiated myoblasts, the transcription level of MyoD was already at a high range, showing almost the same expression level before and after differentiation. The myogenin expression increased in a later cell determination phase, so in the myoblasts we were able to detect it only in very small amounts, whereas after differentiation the myogenin level increases. These results correlate with earlier findings concerning differentiation-dependent expression of skeletal muscle marker genes, where MyoD is described to be already at a high level in myoblasts, whereas myogenin expression increases significantly during differentiation (Rudnicki and Jaenisch, 1995) (Tapscott, 2005).

According to the MyoD/myogenin marker gene expression levels the C2C12 cells can be allocated to a certain differentiation state and serve therefore as a verification of our cell culture model indicating that the cells are in the desired differentiation state.

As it is already described in literature, a high IGF-1 expression correlates with an increase in muscle load (Goldspink, 2006). In our trials, we examined the different splicing variants of IGF-1 before and after differentiation. We were able to report a significant up regulation of IGF-1Ea and MGF expression levels. An in vivo study of the expression of IGF-1 splicing variants following acute muscle damage showed similar results in the muscle regeneration phase. They suggest a role for MGF in the activation / proliferation phase marked by an up-regulation of MyoD. IGF-1Ea and -Eb seem to be related to the myogenic differentiation program marked by an increase in myogenin (McKay et al., 2008). The results after a transfection of a muscle cell line with MGF or IGF-1Ea supported these suggestions (Philippou et al., 2007).

IGF-1Ea was shown in literature to promote terminal differentiation and myotube formation (Yang and Goldspink, 2002) (Hill and Goldspink, 2003). The findings concerning MGF and IGF-1Ea correlate with our results, however we were not able to determine a time-point-related difference of MGF and IGF-1Ea expression. Also the correlation between MGF and MyoD could not be detected. This difference might be cell culture-related, as due to our knowledge this is the first study analyzing the different IGF-1 splicing variants in C2C12 cells.

IGF-1Eb is the IGF-1 splicing variant with the most unknown function. It is mentioned only a few times in literature in connection with skeletal muscle differentiation. Taking our results, in contrast to IGF-1Ea and MGF, this splicing variant interestingly seems to be expressed already in the proliferating myoblasts and its expression level doesn't change during differentiation. Therefore we suggest that IGF-1Eb could be an earlier regulator in muscle cell differentiation. However, our results differ from the findings mentioned above, where IGF-1Eb is described to be up-regulated together with IGF-1Ea in connection with myogenic differentiation (McKay et al., 2008). This might be an in vitro – in vivo or cell culture model related difference, as due to our knowledge an up-regulation of IGF-1Eb during differentiation is not described for C2C12 cells so far.

Muscle specific miRNA are, as their name says, expected to be expressed in muscle cells. For all muscle specific miRNAs we analyzed, except miRNA-499, we detected a significant increase during differentiation.

The muscle specific miRNAs showed an impacting up regulation for up to more than 400 fold for miRNA-1 and miRNA-133a. These two miRNAs are proven to be encoded in one transcriptional locus which means that they are transcribed together (Chen et al., 2006), (Zhao et al., 2005). This theory is underlined with our results, as the level of up regulation of miRNA-1 and miRNA-133a tend to be almost the same.

The expression level of miRNA-133b and -206 increased during differentiation significantly, but with a lower extent. This is a consequence of the higher expression rate of these miRNAs already in the myoblasts, so that the x-fold up regulation is lower.

A significant increase of miRNA-133, -1 and -206 during differentiation was already described in literature (Rao et al., 2006) (Kim et al., 2006) (McCarthy and Esser, 2007).

Recent findings describe a significant up-regulation of miRNA-499 during differentiation (McCarthy et al., 2009). In our trials this miRNA shows the

tendency to increase during differentiation; however the up-regulation is not significant, due to the very high standard deviation, which might be a result of the low general expression level we detected for this miRNA. The acting of miRNA-499 in skeletal muscle remains to be discovered.

In fact, with our results we can underline the importance of all our analyzed muscle specific miRNAs for muscle development. Their up-regulation during the differentiation phase is an indicator for their crucial role in skeletal muscle cell development and muscle cell differentiation.

The expression level of the immuno-related miRNA-155 showed the tendency to increase during differentiation, however this change wasn't significant. A slight increase might be the reason of cell treatment during differentiation. Serum deprivation is accompanied by stress conditions which might force the cells to react over the up-regulation of the immune response.

5.2 Influence of inflammatory stimuli on differentiated myotubes

The stimulation of the fully differentiated myotubes with either TNF-α, LPS or IL-6 was our in vitro model for simulating an inflammatory state in a muscle tissue. Our findings concerning the myogenic marker gene MyoD correspond with earlier results, where especially TNF-α was shown to down-regulate the expression of MyoD in C2C12 cells (Langen et al., 2004) (Guttridge et al., 2000).

A decrease of MyoD after TNF-α / LPS treatment to nearly half of the control level proofs a strong effect of inflammation on this muscle specific gene. If the down-regulation of this important marker gene can be seen as a partial dedifferentiation or more as an arrest of certain muscular gene expression due to energy conservation under stress conditions, remains to be discovered. The assumption, concerning a MyoD mediated up-regulation of miRNA-133, does not go confirm with our findings, as MyoD is expressed already in the proliferating myoblast. Of course there might be a non direct influence including other signals. Also the initially high expression level of miRNA-133b seems to correlate with this thesis. Nevertheless the inflammation induced down-regulation of MyoD after TNF- α / LPS stimulation, respectively had no impact neither on the expression level of miR-133a nor on miRNA-133b. In contrast, we would support a positive regulatory effect between MyoD and UCP assumed by the author, as in the

context of inflammation, concerning our results, an inflammation induced drop in MyoD expression this way would directly influence the fatty acid and energy metabolism (Chen et al., 2009).

We were not able to measure any effect of inflammation on the expression of myogenin. In contrast to our findings, a differentially TNF-a induced inhibition of myogenin expression was described in C2C12 cells (Layne and Farmer, 1999) and a drop of myogenin level in muscle wasting of human cachexia (Ramamoorthy et al., 2009). Due to the general down-regulation of myogenin expression occurring in our trials after 0h, a possible decrease after TNF-α / LPS / IL-6 treatment might be overlaid and therefore not detectable. We suggest that the negative effect on myogenin expression after 0h might be primarily a result of a stress reaction after the media switch directly before stimulation. As for the other genes we could not observe such a long lasting reaction, we suppose that myogenin is especially sensitive to environmental signals. This theory is also supported by findings showing that myogenin, but not MyoD expression, is negatively regulated in C2C12 cells when they are exposed to low temperatures (Shima and Matsuda, 2008). While after LPS and IL-6 incubation as well as for the control myogenin expression returned to basic levels 48h after stimulation, TNF-α treated cells showed a significant drop in myogenin expression until the end of the time kinetics. This might be an indicator for a possible negative influence of TNF-α to the recovery mechanisms of skeletal muscle tissue.

As for MyoD, we also could detect an impacting decrease of mRNA expression levels of the two splicing variants IGF-1Ea and MGF to almost a third compared to the control. Both of them showed a similar down regulation curve after TNF-α incubation. As the importance of IGF-1 for muscle metabolism lies in increasing protein synthesis and inhibition of protein proteolysis, its down-regulation in stress conditions as inflammation seems to be necessary for the conservation of energy. Down-regulation of IGF-1 after TNF-α treatment was already described in literature. TNF-α is known to inhibit IGF-1 gene and protein expression (Fernandez-Celemin et al., 2002). We also detected a reduced increase of IGF-1 protein expression after 48h of TNF-α incubation. The drop of the IGF-1 gene-expression level seems to be JNK-dependent (Frost and Lang, 2007). Frost et al. described in experiments with C2C12 myocytes that LPS stimulates NF-kB activity, the activation of JNK signalling transduction, as well as the increase of NO-synthase 2 (NOS2) in these cells (Frost et al., 2006). Nf-kB is thought to promote cell proliferation over stimulation of Cyclin D1, which is suggested to inhibit MyoD (Muscat and Dressel, 2000). As LPS stimulates TNF-

α expression, the down-regulation of MyoD and IGF-1 we detected after TNF- α treatment might therefore be a result of the parallel activation of JNK and NfkB signalling.

The specific reactions of the different IGF-1 splicing variants on TNF- α / LPS are not described for skeletal muscle so far. However, an over-expression of IGF-1Ea was proven to reduce myofibre necrosis in mdx mice (Grounds et al., 2008).

The IGF-1Eb expression level is, in contrast to IGF-1Ea and MGF not influenced by LPS and TNF-α. Surprisingly, it is the only of our analyzed parameters which showed a significant down-regulation after IL-6 treatment almost throughout the whole time kinetics. Up to our knowledge, this is not described in literature so far. Due to these findings we assume a possible role for IGF-1Eb in negatively regulating muscle mass maintenance in response to inflammation and we suppose this regulation is mediated by the cytokine IL-6.

Due to our knowledge, the effect of TNF-α / LPS or IL-6 on the expression level of the here analyzed miRNAs has not been tested so far. In our trials, none of the measured miRNA expression levels changed significantly after incubation with TNF-α / LPS or IL-6. Therefore we suggest, that there is no direct connection between the here analyzed skeletal muscle specific miRNAs and the inflammatory stimuli used in our study. Of course there might be a connection to inflammation induced muscle atrophy over other cytokines or not yet discovered parameters. Meltzer et.al. observed for example a decreased expression of miRNA-1 / -206 and -133a during C2C12 differentiation after TNF-α / IFN-γ stimulation (Meltzer et al.). Compared to our data, these findings let us assume an influence of inflammation on the initial differentiation steps in myogenesis over slowing down the expression rate of muscle specific miRNAs. As we were not able to detect a miRNA down-regulation in TNF-α / LPS or IL-6 treated myotubes, we suggest that the influence of inflammation on these miRNAs is a non-direct one and includes other factors. That suggests a role for the inflammation – muscle specific miRNA network in inhibiting de novo protein synthesis more than in protein breakdown. Our findings concerning a constant expression of miRNA-1 and -133a also after stimulation are of great interest when being compared with the studies of McCarthy et al. They also describe no change in the expression rate of these miRNAs after 7 days of hindlimb suspension. Therefore we support their thesis that these miRNAs might be very stable concerning external conditions as inflammation or immobility which might also give them a certain role in buffering stress conditions and counteracting the dedifferentiation of the muscle cell (McCarthy and Esser, 2007).

In contrast to miRNA-1 and -133a, a study of Allen et al. describes a decline of miRNA-206 after skeletal muscle atrophy occurring 12 days after spaceflight (Allen et al., 2009). This let us assume that a possible regulation of this miRNA might also occur after inflammation but only after a time period longer than 48h.

The recently discovered muscle specific miRNA-208b and -499 are thought to play a role in fibre-type transition. In our trials, the amount of miRNA-208b was beyond the detection level at all time points. This may be a reason for the in general low expression level of miRNA-499 in our trials, due to earlier findings where miRNA-208b is described as an up-regulator of miRNA-499 (McCarthy et al., 2009). For miRNA-499 we observed a slight tendency to decrease after 48h of TNF-α stimulation, but this down-regulation was not at a significant level. Therefore we suggest once more, that the time period of measurement might have been too short.

As for the muscle specific miRNAs we couldn't observe any change in the expression for the immuno-related miRNA-155 after stimulation. Therefore the TNF-α mediated expression of miRNA-155 already shown in literature, could not be repeated in C2C12 cells (Kutty et al., 2011).

5.3 Effectiveness of inflammatory stimuli on C2C12 cells

In summary, the effects of the here used inflammatory stimuli differ in their effectiveness influencing muscular gene expression when being compared.

Concerning our trials, TNF-α showed the greatest influence on down regulating MyoD as well as IGF-1Ea and MGF. The drop of gene expression levels of these genes after LPS stimulation was similar to that of TNF-α, however the intensity of down regulation was not as strong. Our findings showed clear that in C2C12 myotubes, when exposed to the dose with the maximum effect on muscular gene expression, the TNF-α stimulation has a more severe influence on genes related to muscle wasting than LPS stimulation. It is known that LPS induces TNF-α expression in C2C12 cells (Frost et al., 2006), and as far as the results are similar, we assume that TNF-α plays the key role in regulation also after LPS incubation. However the switch on of TNF-α transcription and translation by LPS is a complex mechanism involving not only LPS but also a lot of other factors. Frost et al. described a short lived response of TNF-α mRNA

after LPS stimulation. Due to the LPS induced expression of IkB-s, which is an NF-kB inhibitor, they suggest that this would have a limiting effect on TNF-α mRNA expression. Beside the transcriptional inhibition they also hypothesize the involvement of the translational silencer TIA-1 (intracytoplasmic antigen 1), acting over binding to the AU-rich elements of the TNF-α mRNA preventing its translation. Correlating to our results, no TNF-α protein could be observed in their study after LPS stimulation (Frost and Lang, 2008). Both, the suggested transcriptional and the translational inhibitory mechanisms, correspond to our data and might be the reason for a reduced and controlled LPS induced expression of TNF-α and therefore a reduced regulatory effect on its targets.

Although IL-6 induced muscle wasting is often described in literature, we couldn't detect an influence of IL-6 incubation on any of the here measured parameters, accept IGF-1Eb. A performed IL-6 concentration analyzes (data not shown) didn't show an effect either. As the concentration is not the problem, it may be the time period of the measurement. We assume that 48h of IL-6 stimulation may be too short to get a measurable reaction of the cells.

However, beside the experimental design there might be another reason for the constant expression level. Earlier studies as well didn't find an influence of IL-6 on protein breakdown rates (Williams et al., 1998). Haddad et al. in contrary observed a significant increase in IGF-1 mRNA after IL-6 injection into a rat muscle. They suggest this as a compensatory response to the IL-6 induced decline in S6K1 phosphorylation they discovered (Bodell et al., 2009). A recent study unrolled the importance of IL-6 for the initial growth response during the recovery from atrophy (Washington et al.). Taken together, these results show a very disperse picture of IL-6 signalling. It seems like IL-6 plays an important role in skeletal muscle atrophy / hypertrophy, but the detailed signalling mechanism of this pro-inflammatory cytokine remains to be discovered.

6 FUTURE ASPECTS

Skeletal muscle tissue is one of the most essential tissues of the human body and the attempt of this diploma thesis was to contribute to unroll the mechanisms how muscle related genes, inflammation and miRNAs play together in the process of muscle wasting.

In our study we clearly showed, that there is an influence of inflammatory conditions, provided by TNF-α and LPS, on muscle specific and growth related genes. Although the murine cell culture line C2C12 was used for basic research in our trials, we strongly assume, that not only myoblast cell culture cells but also muscle tissue is sensitive to these signals and that inflammation might therefore be a strong contributor to skeletal muscle atrophy.

Secondly we proofed that the expression levels of the muscle specific miRNAs are almost not affected by the here used inflammatory stimuli within a period of 2 days. This indicates that these miRNAs are not involved in atrophy processes directly related to the inflammation induced down-regulation of MyoD and IGF-1 splicing variants.

It needs to be further investigated, if and in which way other miRNAs play a role in skeletal muscle atrophy and in which context the down-regulation of MyoD and IGF-1 influences the decrease of skeletal muscle mass.

Another interesting attempt for further investigations could be over the observation of miRNA expression in connection with a broader spectrum of cytokines and prolonged time kinetics.

To summarize our results we can say that there is a direct influence of inflammation on muscle specific and growth related genes which, so far, seem to be independent from the here analyzed miRNAs.

7 ANNEXES

7.1 TE buffer preparation

Materials:

$Na_2EDTA2H_20$, Tris, NaOH and HCl (all purchased by Merck, Darmstadt, Germany), 0.2µl filter (Nalgene Nunc International, Rochester, NY), deionized water (Milli-Q Ultra Pure Water System, Millipore GmbH, Billerica, MA)

0.1M EDTA:

Add 3.72g disodium ethylenediaminetetraacetic acid dihydrate (Na2EDTA

2H2O) to 80ml of deionized water; and stir vigorously until dissolved

Adjust the pH to 8.0 (+/-0.2) at room temperature with 1N NaOH

Fill up to 100ml with deionized water and mix

The solution has to be filter through a 0.2µm Nalgene filter or autoclaved

Discard after 6 months

0.1M Tris-HCl:

Dissolve 12,11g Tris base in 800ml deionized water

Adjust the pH to 8.0 (+/-0.2) at room temperature with 1N HCl

Fill up to one liter with deionized water and mix

The solution has to be filtered through a 0.2µm filter or autoclaved

Discard after 6 months

TE Buffer

Mix 100ml of 0.1M Tris-HCl (pH 8.0), 10ml of 0.1M EDTA and 800ml of

deionized water.

Adjust to one liter with deionized water and mix

Autoclave or filter (0,2µm filter), store it in 100ml aliquots and discard after 6 months

7.2 List of abbreviations

AMPK = Adenosin monophosphate kinase

Cdks = cyclin-dependent kinases

COPD = chronic obstructive lung disease

4E-BP1 = 4E-binding protein

FOXO1 = forkhead box protein 1

Fstl1 = follistatin-related protein 1

IGF-1 = insulin-like growth factor 1

LPS = Lipopolysaccharide

MHC = Myosin heavy chain

MRF = myogenic regulatory factors

MGF = mechanical growth factor

mTOR = mammalian target of Rapamycin

MuRF1 = muscle ringfinger 1

MAFbx = Atrogin

NFAT = nuclear factor of cativated T-cells

Nf-kB = nuclear factor 'kappa-light-chain-enhancer' of activated B-cells

PDK4 = pyruvate dehydrogenase kinase 4

PGC-1alpha = peroxisome proliferators-activated receptor-gamma coactivator 1alpha

PI3K = phosphoinositid 3 kinase

PPARdelta = peroxisome proliferators-activated receptor delta

Pur-beta = Purine-rich element-binding protein B

Rb = Retinoblastoma protein

Rheb = Ras homolog enriched in brain

RISC = RNA-induced scilencing complex

Sox6 = SRY (sex determining region Y)-box 6

Thrap1 = Thyroid Hormone Receptor Associated Protein 1

TIA-1 = intracytoplasmic antigen 1

TNF-a = Tumor necrosis factor alpha

TSC1 / TSC2 = tuberous sclerosis complex -1 and -2

UCPs = uncoupling proteins

Utrn = utrophin

8 REFERENCES

Allen, D.L., E.R. Bandstra, B.C. Harrison, S. Thorng, L.S. Stodieck, P.J. Kostenuik, S. Morony, D.L. Lacey, T.G. Hammond, L.L. Leinwand, W.S. Argraves, T.A. Bateman, and J.L. Barth. 2009. Effects of spaceflight on murine skeletal muscle gene expression. *J Appl Physiol*. 106:582-95.

Alvarez, B., L.S. Quinn, S. Busquets, F.J. Lopez-Soriano, and J.M. Argiles. 2002. TNF-alpha modulates cytokine and cytokine receptors in C2C12 myotubes. *Cancer Lett*. 175:181-5.

Ambion. 2010. TaqMan® MicroRNA Assay Mechanism. http://www.ambion.com/catalog/workflows/miRNA/figs/fig2.gif. Last access on 21.8.2010.

Ambros, V. 2004. The functions of animal microRNAs. *Nature*. 431:350-5.

Anderson, J.E. 2000. A role for nitric oxide in muscle repair: nitric oxide-mediated activation of muscle satellite cells. *Mol Biol Cell*. 11:1859-74.

Applied_Biosystems. 2008. TaqMan PCR schematic
http://www.appliedbiosystems.com/etc/medialib/appliedbio-media-library/images/.html. Last access on

Barber, R.D., D.W. Harmer, R.A. Coleman, and B.J. Clark. 2005. GAPDH as a housekeeping gene: analysis of GAPDH mRNA expression in a panel of 72 human tissues. *Physiol Genomics*. 21:389-95.

Binoux, M. 1995. The IGF system in metabolism regulation. *Diabete Metab*. 21:330-7.

Biosystemdevelopment. 2006. Sandwich ELISA schematic. http://thefutureofthings.com/upload/image/articles/2006/biopen/biopen-elisa-schematic.jpg. Last access on 21.8.2010.

Bischoff, R. 1989. Analysis of muscle regeneration using single myofibers in culture. *Med Sci Sports Exerc*. 21:S164-72.

Bodell, P.W., E. Kodesh, F. Haddad, F.P. Zaldivar, D.M. Cooper, and G.R. Adams. 2009. Skeletal muscle growth in young rats is inhibited by chronic exposure to IL-6 but preserved by concurrent voluntary endurance exercise. *J Appl Physiol*. 106:443-53.

Bodine, S.C., E. Latres, S. Baumhueter, V.K. Lai, L. Nunez, B.A. Clarke, W.T. Poueymirou, F.J. Panaro, E. Na, K. Dharmarajan, Z.Q. Pan, D.M. Valenzuela, T.M. DeChiara, T.N. Stitt, G.D. Yancopoulos, and D.J. Glass. 2001. Identification of ubiquitin ligases required for skeletal muscle atrophy. *Science*. 294:1704-8.

Bruunsgaard, H., and B.K. Pedersen. 2003. Age-related inflammatory cytokines and disease. *Immunol Allergy Clin North Am*. 23:15-39.

Buckingham, M. 2001. Skeletal muscle formation in vertebrates. *Curr Opin Genet Dev*. 11:440-8.

Callahan, L.A., and G.S. Supinski. 2009. Sepsis-induced myopathy. *Crit Care Med*. 37:S354-67.

Callis, T.E., Z. Deng, J.F. Chen, and D.Z. Wang. 2008. Muscling through the microRNA world. *Exp Biol Med (Maywood)*. 233:131-8.

Campell. 2000. Biologie. *Spectrum, Academischer Verlag GmbH*.

Chambers, R.L., and J.C. McDermott. 1996. Molecular basis of skeletal muscle regeneration. *Can J Appl Physiol*. 21:155-84.

Chandran, R., T.J. Knobloch, M. Anghelina, and S. Agarwal. 2007. Biomechanical signals upregulate myogenic gene induction in the presence or absence of inflammation. *Am J Physiol Cell Physiol*. 293:C267-76.

Chen, C., D.A. Ridzon, A.J. Broomer, Z. Zhou, D.H. Lee, J.T. Nguyen, M. Barbisin, N.L. Xu, V.R. Mahuvakar, M.R. Andersen, K.Q. Lao, K.J. Livak, and K.J. Guegler. 2005. Real-time quantification of microRNAs by stem-loop RT-PCR. *Nucleic Acids Res*. 33:e179.

Chen, J.F., E.M. Mandel, J.M. Thomson, Q. Wu, T.E. Callis, S.M. Hammond, F.L. Conlon, and D.Z. Wang. 2006. The role of microRNA-1 and microRNA-133 in skeletal muscle proliferation and differentiation. *Nat Genet*. 38:228-33.

Chen, W., Q. Yang, and R.G. Roeder. 2009. Dynamic interactions and cooperative functions of PGC-1alpha and MED1 in TRalpha-mediated activation of the brown-fat-specific UCP-1 gene. *Mol Cell*. 35:755-68.

Coller, H.A. 2007. What's taking so long? S-phase entry from quiescence versus proliferation. *Nat Rev Mol Cell Biol*. 8:667-70.

Collins, S., W. Cao, K.W. Daniel, T.M. Dixon, A.V. Medvedev, H. Onuma, and R. Surwit. 2001. Adrenoceptors, uncoupling proteins, and energy expenditure. *Exp Biol Med (Maywood)*. 226:982-90.

Degens, H. 2011. The role of systemic inflammation in age-related muscle weakness and wasting. *Scand J Med Sci Sports*. 20:28-38.

Diao, J., Y. Zhang, J.M. Huibregtse, D. Zhou, and J. Chen. 2008. Crystal structure of SopA, a Salmonella effector protein mimicking a eukaryotic ubiquitin ligase. *Nat Struct Mol Biol*. 15:65-70.

Endo, I., D. Inoue, T. Mitsui, Y. Umaki, M. Akaike, T. Yoshizawa, S. Kato, and T. Matsumoto. 2003. Deletion of vitamin D receptor gene in mice results in abnormal skeletal muscle development with deregulated expression of myoregulatory transcription factors. *Endocrinology*. 144:5138-44.

Fernandez-Celemin, L., N. Pasko, V. Blomart, and J.P. Thissen. 2002. Inhibition of muscle insulin-like growth factor I expression by tumor necrosis factor-alpha. *Am J Physiol Endocrinol Metab*. 283:E1279-90.

Frost, R.A., and C.H. Lang. 2007. Protein kinase B/Akt: a nexus of growth factor and cytokine signaling in determining muscle mass. *J Appl Physiol*. 103:378-87.

Frost, R.A., and C.H. Lang. 2008. Regulation of muscle growth by pathogen-associated molecules. *J Anim Sci*. 86:E84-93.

Frost, R.A., G.J. Nystrom, and C.H. Lang. 2003. Lipopolysaccharide and proinflammatory cytokines stimulate interleukin-6 expression in C2C12 myoblasts: role of the Jun NH2-terminal kinase. *Am J Physiol Regul Integr Comp Physiol*. 285:R1153-64.

Frost, R.A., G.J. Nystrom, and C.H. Lang. 2004. Lipopolysaccharide stimulates nitric oxide synthase-2 expression in murine skeletal muscle and C(2)C(12) myoblasts via Toll-like receptor-4 and c-Jun NH(2)-terminal kinase pathways. *Am J Physiol Cell Physiol*. 287:C1605-15.

Frost, R.A., G.J. Nystrom, and C.H. Lang. 2006. Multiple Toll-like receptor ligands induce an IL-6 transcriptional response in skeletal myocytes. *Am J Physiol Regul Integr Comp Physiol*. 290:R773-84.

Furuyama, T., K. Kitayama, H. Yamashita, and N. Mori. 2003. Forkhead transcription factor FOXO1 (FKHR)-dependent induction of PDK4 gene expression in skeletal muscle during energy deprivation. *Biochem J*. 375:365-71.

Gallagher, S. 2001. Quantitation of nucleic acids with absorption spectroscopy. *Curr Protoc Protein Sci*. Appendix 4:Appendix 4K.

Glass, D.J. 2005. Skeletal muscle hypertrophy and atrophy signaling pathways. *Int J Biochem Cell Biol*. 37:1974-84.

Goldspink, G. 2003. Gene expression in muscle in response to exercise. *J Muscle Res Cell Motil*. 24:121-6.

Goldspink, G. 2004. Age-related loss of skeletal muscle function; impairment of gene expression. *J Musculoskelet Neuronal Interact*. 4:143-7.

Goldspink, G. 2006. Impairment of IGF-I gene splicing and MGF expression associated with muscle wasting. *Int J Biochem Cell Biol*. 38:481-9.

Goldspink, G., B. Wessner, and N. Bachl. 2008. Growth factors, muscle function and doping. *Curr Opin Pharmacol*. 8:352-7.

Grounds, M.D., H.G. Radley, B.L. Gebski, M.A. Bogoyevitch, and T. Shavlakadze. 2008. Implications of cross-talk between tumour necrosis factor and insulin-like growth factor-1 signalling in skeletal muscle. *Clin Exp Pharmacol Physiol*. 35:846-51.

Guttridge, D.C., C. Albanese, J.Y. Reuther, R.G. Pestell, and A.S. Baldwin, Jr. 1999. NF-kappaB controls cell growth and differentiation through transcriptional regulation of cyclin D1. *Mol Cell Biol*. 19:5785-99.

Guttridge, D.C., M.W. Mayo, L.V. Madrid, C.Y. Wang, and A.S. Baldwin, Jr. 2000. NF-kappaB-induced loss of MyoD messenger RNA: possible role in muscle decay and cachexia. *Science*. 289:2363-6.

Halevy, O., B.G. Novitch, D.B. Spicer, S.X. Skapek, J. Rhee, G.J. Hannon, D. Beach, and A.B. Lassar. 1995. Correlation of terminal cell cycle arrest of skeletal muscle with induction of p21 by MyoD. *Science*. 267:1018-21.

Harridge, S.D. 2003. Ageing and local growth factors in muscle. *Scand J Med Sci Sports*. 13:34-9.

Heidt, A.B., A. Rojas, I.S. Harris, and B.L. Black. 2007. Determinants of myogenic specificity within MyoD are required for noncanonical E box binding. *Mol Cell Biol*. 27:5910-20.

Hill, M., and G. Goldspink. 2003. Expression and splicing of the insulin-like growth factor gene in rodent muscle is associated with muscle satellite (stem) cell activation following local tissue damage. *J Physiol*. 549:409-18.

Hirano, S., R. Hirako, N. Kajita, and M. Norita. 1995. Morphological analysis of the role of the neural tube and notochord in the development of somites. *Anat Embryol (Berl)*. 192:445-57.

Hornberger, T.A., and S. Chien. 2006. Mechanical stimuli and nutrients regulate rapamycin-sensitive signaling through distinct mechanisms in skeletal muscle. *J Cell Biochem*. 97:1207-16.

Jacinto, E., and M.N. Hall. 2003. Tor signalling in bugs, brain and brawn. *Nat Rev Mol Cell Biol*. 4:117-26.

Jackman, R.W., and S.C. Kandarian. 2004. The molecular basis of skeletal muscle atrophy. *Am J Physiol Cell Physiol*. 287:C834-43.

Jespersen, J., M. Kjaer, and P. Schjerling. 2006. The possible role of myostatin in skeletal muscle atrophy and cachexia. *Scand J Med Sci Sports*. 16:74-82.

Keller, C., A. Steensberg, H. Pilegaard, T. Osada, B. Saltin, B.K. Pedersen, and P.D. Neufer. 2001. Transcriptional activation of the IL-6 gene in human contracting skeletal muscle: influence of muscle glycogen content. *Faseb J*. 15:2748-50.

Kim, H.K., Y.S. Lee, U. Sivaprasad, A. Malhotra, and A. Dutta. 2006. Muscle-specific microRNA miR-206 promotes muscle differentiation. *J Cell Biol*. 174:677-87.

Kimball, S.R., and L.S. Jefferson. 2004. Molecular mechanisms through which amino acids mediate signaling through the mammalian target of rapamycin. *Curr Opin Clin Nutr Metab Care*. 7:39-44.

Kitzmann, M., and A. Fernandez. 2001. Crosstalk between cell cycle regulators and the myogenic factor MyoD in skeletal myoblasts. *Cell Mol Life Sci*. 58:571-9.

Kumar, A., Y. Takada, A.M. Boriek, and B.B. Aggarwal. 2004. Nuclear factor-kappaB: its role in health and disease. *J Mol Med (Berl)*. 82:434-48.

Kutty, R.K., C.N. Nagineni, W. Samuel, C. Vijayasarathy, J.J. Hooks, and T.M. Redmond. 2011. Inflammatory cytokines regulate microRNA-155 expression in human retinal pigment epithelial cells by activating JAK/STAT pathway. *Biochem Biophys Res Commun*. 402:390-5.

Langen, R.C., J.L. Van Der Velden, A.M. Schols, M.C. Kelders, E.F. Wouters, and Y.M. Janssen-Heininger. 2004. Tumor necrosis factor-alpha inhibits myogenic differentiation through MyoD protein destabilization. *Faseb J*. 18:227-37.

Larsen, A.E., D. Cameron-Smith, and T.C. Crowe. 2008. Conjugated linoleic acid suppresses myogenic gene expression in a model of human muscle cell inflammation. *J Nutr*. 138:12-6.

Layne, M.D., and S.R. Farmer. 1999. Tumor necrosis factor-alpha and basic fibroblast growth factor differentially inhibit the insulin-like growth factor-I induced expression of myogenin in C2C12 myoblasts. *Exp Cell Res*. 249:177-87.

Lee, C.E., A. McArdle, and R.D. Griffiths. 2007. The role of hormones, cytokines and heat shock proteins during age-related muscle loss. *Clin Nutr*. 26:524-34.

Li, W., J.S. Moylan, M.A. Chambers, J. Smith, and M.B. Reid. 2009. Interleukin-1 stimulates catabolism in C2C12 myotubes. *Am J Physiol Cell Physiol*. 297:C706-14.

LO-Laboroptik. 1999. Counting chamber. www.zaehlkammer.de. Last access on 7.8.2010.

Mack, G.S. 2007. MicroRNA gets down to business. *Nat Biotechnol*. 25:631-8.

Majer, M., K.M. Popov, R.A. Harris, C. Bogardus, and M. Prochazka. 1998. Insulin downregulates pyruvate dehydrogenase kinase (PDK) mRNA: potential mechanism contributing to increased lipid oxidation in insulin-resistant subjects. *Mol Genet Metab*. 65:181-6.

Matsakas, A., and K. Patel. 2009. Intracellular signalling pathways regulating the adaptation of skeletal muscle to exercise and nutritional changes. *Histol Histopathol*. 24:209-22.

McCarthy, J.J., and K.A. Esser. 2007. MicroRNA-1 and microRNA-133a expression are decreased during skeletal muscle hypertrophy. *J Appl Physiol*. 102:306-13.

McCarthy, J.J., K.A. Esser, C.A. Peterson, and E.E. Dupont-Versteegden. 2009. Evidence of MyomiR network regulation of beta-myosin heavy chain gene expression during skeletal muscle atrophy. *Physiol Genomics*. 39:219-26.

McKay, B.R., C.E. O'Reilly, S.M. Phillips, M.A. Tarnopolsky, and G. Parise. 2008. Co-expression of IGF-1 family members with myogenic regulatory factors following acute damaging muscle-lengthening contractions in humans. *J Physiol*. 586:5549-60.

Meltzer, M., K. Long, Y. Nie, M. Gupta, J. Yang, and M. Montano. The RNA editor gene ADAR1 is induced in myoblasts by inflammatory ligands and buffers stress response. *Clin Transl Sci*. 3:73-80.

Moylan, J.S., J.D. Smith, M.A. Chambers, T.J. McLoughlin, and M.B. Reid. 2008. TNF induction of atrogin-1/MAFbx mRNA depends on Foxo4 expression but not AKT-Foxo1/3 signaling. *Am J Physiol Cell Physiol*. 295:C986-93.

Muscat, G.E., and U. Dressel. 2000. Not a minute to waste. *Nat Med*. 6:1216-7.

Narkar, V.A., M. Downes, R.T. Yu, E. Embler, Y.X. Wang, E. Banayo, M.M. Mihaylova, M.C. Nelson, Y. Zou, H. Juguilon, H. Kang, R.J. Shaw, and R.M. Evans. 2008. AMPK and PPARdelta agonists are exercise mimetics. *Cell*. 134:405-15.

National_Institutes_of_Health, U.S. 2000. Structure of Skeletal Muscle. Last access on 10.5.2010.

National_Institutes_of_Health, U.S. 2010. Structure of Skeletal Muscle. Last access on

Philippou, A., M. Maridaki, A. Halapas, and M. Koutsilieris. 2007. The role of the insulin-like growth factor 1 (IGF-1) in skeletal muscle physiology. *In Vivo*. 21:45-54.

Philippou, A., E. Papageorgiou, G. Bogdanis, A. Halapas, A. Sourla, M. Maridaki, N. Pissimissis, and M. Koutsilieris. 2009. Expression of IGF-1 isoforms after exercise-induced muscle damage in humans: characterization of the MGF E peptide actions in vitro. *In Vivo*. 23:567-75.

Pillai, R.S., C.G. Artus, and W. Filipowicz. 2004. Tethering of human Ago proteins to mRNA mimics the miRNA-mediated repression of protein synthesis. *Rna*. 10:1518-25.

Porter, M.M., A.A. Vandervoort, and J. Lexell. 1995. Aging of human muscle: structure, function and adaptability. *Scand J Med Sci Sports*. 5:129-42.

Rabinovich, R.A., and J. Vilaro. 2011. Structural and functional changes of peripheral muscles in chronic obstructive pulmonary disease patients. *Curr Opin Pulm Med*. 16:123-33.

Ramamoorthy, S., M. Donohue, and M. Buck. 2009. Decreased Jun-D and myogenin expression in muscle wasting of human cachexia. *Am J Physiol Endocrinol Metab*. 297:E392-401.

Rao, P.K., R.M. Kumar, M. Farkhondeh, S. Baskerville, and H.F. Lodish. 2006. Myogenic factors that regulate expression of muscle-specific microRNAs. *Proc Natl Acad Sci U S A*. 103:8721-6.

Remels, A.H., R.C. Langen, H.R. Gosker, A.P. Russell, F. Spaapen, J.W. Voncken, P. Schrauwen, and A.M. Schols. 2009. PPARgamma inhibits NF-kappaB-dependent transcriptional activation in skeletal muscle. *Am J Physiol Endocrinol Metab*. 297:E174-83.

Riquet, F.B., M. Rodriguez, N. Guigal, S. Dromaint, I. Naime, J.A. Boutin, and J.P. Galizzi. 2003. In vivo characterisation of the human UCP3 gene minimal promoter in mice tibialis anterior muscles. *Biochem Biophys Res Commun*. 311:583-91.

Rockl, K.S., C.A. Witczak, and L.J. Goodyear. 2008. Signaling mechanisms in skeletal muscle: acute responses and chronic adaptations to exercise. *IUBMB Life*. 60:145-53.

Rosenberg, M.I., S.A. Georges, A. Asawachaicharn, E. Analau, and S.J. Tapscott. 2006. MyoD inhibits Fstl1 and Utrn expression by inducing transcription of miR-206. *J Cell Biol*. 175:77-85.

Roth, S.M., J.M. Zmuda, J.A. Cauley, P.R. Shea, and R.E. Ferrell. 2004. Vitamin D receptor genotype is associated with fat-free mass and sarcopenia in elderly men. *J Gerontol A Biol Sci Med Sci*. 59:10-5.

Roubenoff, R. 2003. Catabolism of aging: is it an inflammatory process? *Curr Opin Clin Nutr Metab Care*. 6:295-9.

Rudnicki, M.A., and R. Jaenisch. 1995. The MyoD family of transcription factors and skeletal myogenesis. *Bioessays*. 17:203-9.

SanDiego_State_University. 2005. Regulation of the NfkB signalling. Last access on 18.5.2010.

Sesmilo, G., K.K. Miller, D. Hayden, and A. Klibanski. 2001. Inflammatory cardiovascular risk markers in women with hypopituitarism. *J Clin Endocrinol Metab*. 86:5774-81.

Shima, A., and R. Matsuda. 2008. The expression of myogenin, but not of MyoD, is temperature-sensitive in mouse skeletal muscle cells. *Zoolog Sci*. 25:1066-74.

Strasser, E.M., B. Wessner, and E. Roth. 2007. [Cellular regulation of anabolism and catabolism in skeletal muscle during immobilisation, aging and critical illness]. *Wien Klin Wochenschr*. 119:337-48.

Talmadge, R.J., and R.R. Roy. 1993. Electrophoretic separation of rat skeletal muscle myosin heavy-chain isoforms. *J Appl Physiol*. 75:2337-40.

Tang, K., P.D. Wagner, and E.C. Breen. 2010. TNF-alpha-mediated reduction in PGC-1alpha may impair skeletal muscle function after cigarette smoke exposure. *J Cell Physiol*. 222:320-7.

Tapscott, S.J. 2005. The circuitry of a master switch: Myod and the regulation of skeletal muscle gene transcription. *Development*. 132:2685-95.

Taulli, R., F. Bersani, V. Foglizzo, A. Linari, E. Vigna, M. Ladanyi, T. Tuschl, and C. Ponzetto. 2009. The muscle-specific microRNA miR-206 blocks human rhabdomyosarcoma growth in xenotransplanted mice by promoting myogenic differentiation. *J Clin Invest*. 119:2366-78.

Tili, E., J.J. Michaille, A. Cimino, S. Costinean, C.D. Dumitru, B. Adair, M. Fabbri, H. Alder, C.G. Liu, G.A. Calin, and C.M. Croce. 2007. Modulation of miR-155

and miR-125b levels following lipopolysaccharide/TNF-alpha stimulation and their possible roles in regulating the response to endotoxin shock. *J Immunol*. 179:5082-9.

Tothova, J., B. Blaauw, G. Pallafacchina, R. Rudolf, C. Argentini, C. Reggiani, and S. Schiaffino. 2006. NFATc1 nucleocytoplasmic shuttling is controlled by nerve activity in skeletal muscle. *J Cell Sci*. 119:1604-11.

Trappe, S., D. Costill, P. Gallagher, A. Creer, J.R. Peters, H. Evans, D.A. Riley, and R.H. Fitts. 2009. Exercise in space: human skeletal muscle after 6 months aboard the International Space Station. *J Appl Physiol*. 106:1159-68.

Tsujinaka, T., C. Ebisui, J. Fujita, M. Kishibuchi, T. Morimoto, A. Ogawa, A. Katsume, Y. Ohsugi, E. Kominami, and M. Monden. 1995. Muscle undergoes atrophy in association with increase of lysosomal cathepsin activity in interleukin-6 transgenic mouse. *Biochem Biophys Res Commun*. 207:168-74.

Wang, D.Z. 2006. Micro or mega: how important are microRNAs in muscle? *Cell Cycle*. 5:1015-6.

Wang, Y.X., C.L. Zhang, R.T. Yu, H.K. Cho, M.C. Nelson, C.R. Bayuga-Ocampo, J. Ham, H. Kang, and R.M. Evans. 2004. Regulation of muscle fiber type and running endurance by PPARdelta. *PLoS Biol*. 2:e294.

Washington, T.A., J.P. White, J.M. Davis, L.B. Wilson, L.L. Lowe, S. Sato, and J.A. Carson. Skeletal muscle mass recovery from atrophy in IL-6 knockout mice. *Acta Physiol (Oxf)*. 202:657-69.

Wasserman, W.W., and J.W. Fickett. 1998. Identification of regulatory regions which confer muscle-specific gene expression. *J Mol Biol*. 278:167-81.

Williams, A., J.J. Wang, L. Wang, X. Sun, J.E. Fischer, and P.O. Hasselgren. 1998. Sepsis in mice stimulates muscle proteolysis in the absence of IL-6. *Am J Physiol*. 275:R1983-91.

Wolfe, R.R. 2006. The underappreciated role of muscle in health and disease. *Am J Clin Nutr*. 84:475-82.

Wullschleger, S., R. Loewith, and M.N. Hall. 2006. TOR signaling in growth and metabolism. *Cell*. 124:471-84.

Yang, S.Y., and G. Goldspink. 2002. Different roles of the IGF-I Ec peptide (MGF) and mature IGF-I in myoblast proliferation and differentiation. *FEBS Lett*. 522:156-60.

Zhao, Y., E. Samal, and D. Srivastava. 2005. Serum response factor regulates a muscle-specific microRNA that targets Hand2 during cardiogenesis. *Nature*. 436:214-20.

Figures:

9 CURRICULUM VITAE

Personal information

Name: Gryadunov-Masutti Laura
Date of birth: 12.01.1981
Nationality: Austrian
Family status: married to DI Gryadunov-Masutti Sergey

Address: Aspettenstraße 30 / 5 / 1
2380 Perchtoldsdorf
Mob: 0664 340 9998
E-mail: lauramasuttiat@yahoo.com

Education

1987 - 1991 Primary school Gleisdorf
1991 - 1996 Grammar school Gleisdorf (AHS)
1996 - 2000 Grammar school Feldbach (BORG)
9.2000-7.2001 Language courses English (USA), Chinese (Beijing), Russian (St. Petersburg), EF International Language Schools
2001 - 2002 Study of Ecology-Systemscience, Karl-Franzens-University Graz
2002 - 2011 Study of Biology, Mikrobiology and Genetics, University of Vienna

Work experience:

7. 2003: Ecological internship (WWF)
2006-2009: Research assistant (Medical University Vienna)
2009-2011: Research assistant (University of Vienna, institute of sports science)

10 ACKNOWLEDGEMENT

I want to say “Thank you”:

To Georg Weitzer, for being my supervisor and giving me the opportunity to write my diploma thesis.

To Erich Roth, for help and advices and for giving me the possibility to do the practical work for my diploma thesis in the Surgical Research Laboratories of the General Hospital Vienna.

To Barbara Wessner, for support in my practical work and for guiding me through the scientific jungle.

To family, friends and colleagues for support and help in any possible and impossible situation.